Develop Small Molecule Regulators of GTPase-activating Proteins of ADP-ribosylation Factors (ARFGAPs)

Wei Sun

A dissertation submitted to the faculty of the University of North Carolina at Chapel Hill in partial fulfillment of the requirements for the degree of Doctor of Philosophy in the UNC Eshelman School of Pharmacy (Division of Chemical Biology and Medicinal Chemistry).

Chapel Hill
2012

Approved by:

Qisheng Zhang, Ph.D.

Jian Liu, Ph.D.

David Lawrence, Ph.D.

John Sondek, Ph.D.

Stephen Frye, Ph.D.

Abstract

**WEI SUN: Develop Small Molecule Regulators of GTPase-activating Proteins of
ADP-ribosylation Factors (ARFGAPs)
(Under the direction of Qisheng Zhang)**

GTPase-activating proteins of ADP-ribosylation factors (ARFGAPs) play essential roles in cell growth and migration, tumor invasion and neuronal development. Increasing evidence also implicates that ARFGAPs are involved in cancer, Alzheimer's disease, and autism. However, the precise mechanisms whereby ARFGAPs regulate different diseases are yet to be elucidated. Consequently, direct and efficient regulators of ARFGAPs are urgently needed. In this thesis, I describe our efforts in developing small molecule ARFGAP inhibitors.

It has been reported that a small molecule, QS11, potentially inhibits multiple ARFGAPs and is able to activate the Wnt/β-catenin signaling pathway. However, the mechanism of how QS11 inhibits different ARFGAPs is not well known. To define the molecular basis of the regulation of ARFGAP1 by QS11, we demonstrate that QS11 binds to the lipid packing sensor (ALPS) motifs of ARFGAP1 instead of its GAP domain. This interaction also contributes to the inhibition of ARFGAP1 by QS11 ($IC_{50} = 4.0$ μM). Further studies suggest that QS11 inhibits ARFGAP1 activity in a non-competitive manner. Next, we have synthesized a small library of 31 analogs of QS11 to improve its potency and solubility. The binding affinities of these analogs to ARFGAP1 and their capacities to inhibit the GAP activity of ARFGAP1 are measured to establish a preliminary structure-activity relationship (SAR).

iii

To identify novel small molecule inhibitors of the catalytic GAP domain of ARFGAPs, a fluorescence polarization-based ARFGAP assay has been developed. The Z' factor of the assay is 0.75 in 384-well format. When applied to a pilot screen of the LOPAC library of 1,280 compounds, the assay demonstrated high reproducibility, reasonable hit rates, high tolerance with DMSO, and suitability for automation. Compared to the traditional assays for ARFGAP activity, this new assay is more user and environmentally friendly, and represents the first assay of ARFGAP enzymatic activity that allows the large-scale screening of compound libraries to identify inhibitors of ARFGAPs.

The illustration of the mechanism by which QS11 interacts with ARFGAP1 also prompts us to engineer myristoylated ADP-ribosylation factor 1 (ARF1) for novel functions. Myristoylation is a pervasive co- and post-translational modification of proteins through the irreversible covalent bond formation with myristic acid at the N-terminal glycine. Myristoylated proteins are involved in many signalling pathways, oncogenesis and viral replication. We have designed and synthesized six modified myristic acids and incorporated them into ARF1 through metabolic interference. The resulting new ARF1 proteins can be loaded with GTP and the bound GTP is as efficiently hydrolyzed in the presence of ARFGAP1 as the native ARF1, but with the added potential functions of dye labeling, responding to redox changes or light illumiation, or selective separation.

Dedication

I dedicate this work to my parents Mr. Shouming Sun and Ms. Yuzheng Cao, and my wife Ms. Chia-wen Hsu, who are always there to support and inspire me through the course of this dissertation and my life.

Acknowledgements

Preface

Chapter 2 and Chapter 4 represent unpublished research. Part of Chapter 3 was published previous to writing this dissertation with the following citation:

Sun W, Vanhooke JL, Sondek J, Zhang Q. High-throughput Fluorescence Polarization Assay for the Enzymatic Activity of GTPase-activating Protein of ADP-ribosylation Factor (ARFGAP). *J Biomol Screen*. **2011** Aug; 16(7):717-23.

Permission to include the article in its entirety in a Ph.D dissertation was retained from Society for Laboratory Automation and Screening as explained at

http://s100.copyright.com/AppDispatchServlet

All copyrighted material included in this dissertation is used with permission from the relevant copyright holders.

Table of Contents

List of Tables

List of Schemes

List of Figures

List of Abbreviations

ARFGAP – ADP-ribosylation factors directed GTPase activating proteins

ALPS – ARFGAP1 lipid packing sensor

SAR – Structure-activity relationship

ARF – ADP-ribosylation factor

GEF – Guanine nucleotide-exchange factor

GAP – GTPase-activating protein

ER – Endoplasmic reticulum

CHA – Common hydrophobic area

CB – Calm binding Domain

CALM – Clathrin-box

FG – Phenylalanine-glycine repeats

SHD – Spa-homology domain

CC – coiled-coil

PBS – Paxillin binding sites

BAR – Bin/Amphiphysin/Rvs

PH – Pleckstrin homology

ANK – Ankyrin repeat

PxxP – Proline-rich

D/ELPPKP – Tandem Proline rich

SH3 – Src homology 3

GLD – GTP-binding protein-like domain

SAM – Sterile α-motif

RA – Ras association motif

COPI – Coat protein complex I

TfR – Transferrin receptor

PLC-γ – Phospholipase C gamma

PIP_2 – Phosphatidylinositol 4,5-bisphosphate

IP_3 – Inositol 1,4,5-trisphosphate

PI3K – Phosphatidylinositol 3-kinases

SHIP2 – Phosphatidylinositol 5-phosphatase

PAK – P21-activated kinase

PIX – PAK-interacting exchange factor

GPCR – G-protein-coupled receptor

FA – Focal adhesion

MHC – Histocompatibility complex

DAG – Diacylglycerol

PIP_3 – Phosphatidylinositol 3,4,5-trisphosphate

PE – Phosphatidylethanolamine

PS – Phosphatidylserine

PI – Phosphatidylinositol

PC – Phosphatidylcholine

ITC – Isothermal Titration Calorimetry

SPR – Surface plasmon resonance

CD – Circular Dichroism

HTS – High throughput screening

FP – Fluorescence polarization

SD – Standard deviation

LOPAC – Library of Pharmacologically-Active Compounds

SMAP2 – Stromal membrane-associated GTPase-activating protein 2

NMT – N-myristoyl transferase

NIP71 – NMT inhibitor protein 71

LC-MS/MS – Liquid chromatography-tandem mass spectrometry

PBS – Phosphate buffered saline

SDS-PAGE – Sodium dodecyl sulfate polyacrylamide gel electrophoresis

DMF – Dimethylformamide

RFU – Relative fluorescence units

DIAD – Diisopropyl azodicarboxylate

NMR – Nuclear magnetic resonance

Log P – The logarithm of the ratio of the concentrations of the un-ionized solute in the solvents

MALDI-TOF – Matrix-assisted laser desorption/ionization

Chapter 1.

GTPase-activating Protein of ADP-ribosylation Factor (ARFGAP)

1.1 Introduction to ARFGAP

1.1.1 ARF family proteins ARF family proteins are small GTPases that regulate membrane traffic and organelle structures.(1,2) They function through cycling between active GTP-bound forms and inactive GDP-bound forms (**Fig. 1.1**).(3) The activation of ARF-GDP is promoted by guanine nucleotide-exchange factors (GEFs) whereas the hydrolysis of ARF-GTP is catalyzed by GTPase-activating proteins (GAP). (1,4-6) Unlike other GTPases within the Ras super family, the nucleotide exchange rates and the intrinsic GTP hydrolysis rates for ARFs are slow. (7-10) Consequently, ARFGEFs and ARFGAPs are essential for the regulation of ARF activity.
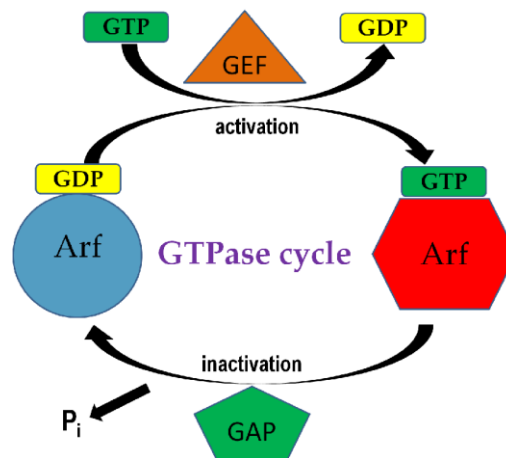
Figure 1.1. General regulation of ARF activation and inactivation. A GDP-bound, inactive form of ARF is converted to a GTP-bound, active form through GDP-GTP

exchange catalyzed by a GEF. The GTP molecule bound to ARF is then hydrolyzed to GDP with the aid of a GAP.

Six conserved members of ARFs have been identified in mammalian cells. They are classified into three subfamilies based on structure similarities: Class I (ARF1, ARF2 and ARF3), Class II (ARF4 and ARF5) and Class III (ARF6). ARFs localize both on the lipid membranes and in the cytosol.(11) ARF1 and ARF3 bind to the plasma membrane when in GTP-bound form and are released to cytosol when in GDP-bound form. ARF4, ARF5 and ARF6 bind to the plasma membrane when in either GTP- or GDP-bound form.(12,13) The N-terminal amphipathic helix of ARFs and the myristoylation at the N-terminus are critical elements for their membrane binding (**Fig. 1.2**).(10,14)

ARF1 and ARF6 have been extensively studied among the six ARFs. ARF1 regulates vesicle trafficking from endoplasmic reticulum (ER) to Golgi, as well as function and morphology of Golgi.(15) ARF6 is involved in endocytosis, phagocytosis, receptor recycling and actin-cytoskeletal remodeling.(14,16) Importantly, overexpression of ARF6 has been found in multiple invasive breast cancer cells.(17-19) Knock-down of the level of ARF6 effectively reduced tumor invasion in these breast cancer cells. (17)
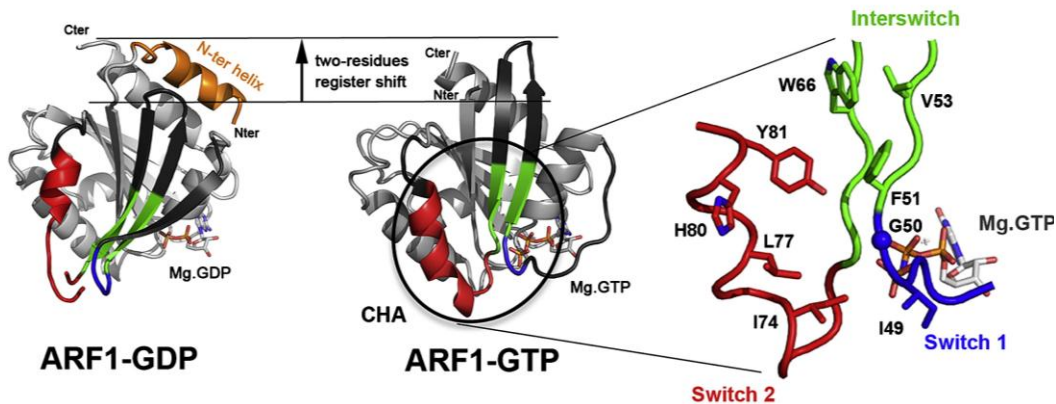
Figure 1.2. The common hydrophobic area of the ARF family proteins. Cartoon representation of ARF1-GDP (left) and ARF1-GTP (center) are shown and compared. The switch regions are indicated in dark gray while the common hydrophobic area (CHA)

2

region in colors (switch 1 part, in blue; interswitch part, in green; switch 2 part, in red). A detailed view (right) of the CHA region is shown in ribbons, with the residues forming this region indicated in sticks. (This figure was reprinted from (4). Chavrier, P., and Ménétrey, J. (2010) *Structure* **18**, 1552-1558 © 2010 Elsevier Science, used with permission).

In humans, 15 ARFGEFs have been discovered and they share a conserved catalytic Sec7 domain of approximately 200 amino acids,(5) while 31 discovered human ARFGAPs are categorized into 10 subfamilies based on the sequence similarity of GAP and other functional domains (**Fig 1.3**).(20) All ARFGAPs share a catalytic GAP domain of approximately 130 amino acids in which a characteristic zinc finger motif $(CX_2CX_{16}CX_2CX_4R)$ and an arginine residue are highly conserved.(21)

1.1.2 ARFGAP family proteins The ARFGAP activity was initially discovered in 1994.(8) It was shown that a crude extract from bovine brain could stimulate GTP hydrolysis catalyzed by mammalian ARF1. Both soluble (20-40%) and particulate fractions (60-40%) of the brain extract have GTPase activating activity. Enrichment of this activity was observed by extraction with 0.75 M NaCl. Heating or trypsin treatment will reduce more than 90% of this activity. This activity was then defined as the property of ARF-GTPase activating protein (ARFGAP). A few months later, ARFGAP1 was cloned and purified as the first member of the ARFGAP family.(22) A zinc finger motif near the N-terminus of ARFGAP1 was identified as the key requirement for its catalytic activity. The majority of active ARFGAP1 was localized to the Golgi complex, while inactive ARFGAP1 diffused to cytosol after the inactivation of ARF.(7,15,23-26) Since then, 30 other ARFGAPs have been identified in the mammalian systems. Further study suggested that the GAP domain is ancient and conserved in *R. norvegicus, C. elegans, D. melanogaster, A. thaliana*, *S. cerevisiae* and *Gallus gallus*.(21)

1.1.3 Domain structures of ARFGAP family proteins ARFGAP1 is the first member of the ARFGAP family proteins, with a molecular weight of 45 kD. The GAP domain of ARFGAP1 is located at the N-terminus and the remaining region contains two ARFGAP1 lipid-packing sensors (ALPS) motifs (**Fig 1.3**).(20) The ARFGAP2 subfamily lacks the ALPS motifs and shares little sequence similarity with ARFGAP1 except the GAP domain. ADAP subfamily is composed of a GAP domain and two PH domains. SMAP subfamily only shares 47% sequence similarity: SMAP2 has a calm BD domain (CB) and a clathrin-box (CALM) while SMAP1 does not have a CB domain. AGFG subfamily contains a GAP domain and 10 phenylalanine-glycine repeats (FG). GIT subfamily shares a GAP domain, three ankyrin repeats (27), a Spa-homology domain (SHD), coiled-coil (CC) and Paxillin binding sites (PBS). The typical ASAP subfamily has a Bin/Amphiphysin/Rvs (BAR) domain, a pleckstrin homology (PH) domain (28), a GAP domain, three ankyrin repeats (ANK), a cluster of three Proline-rich (PxxP) motif (Pro(PxxP)3), eight tandem Proline rich (D/ELPPKP) motifs, and a Src homology 3 domain (SH3). ACAP subfamily contains a Bar domain, a PH domain, a GAP domain and ANK. AGAP subfamily consists of a GTP-binding protein-like domain (GLD), a PH domain, a GAP domain and ANK. The ARAP subfamily has a sterile α-motif (SAM), two PH domains, a GAP domain, ANK, another two PH domains, a RhoGAP domain, a Ras association motif (RA) and another PH domain.
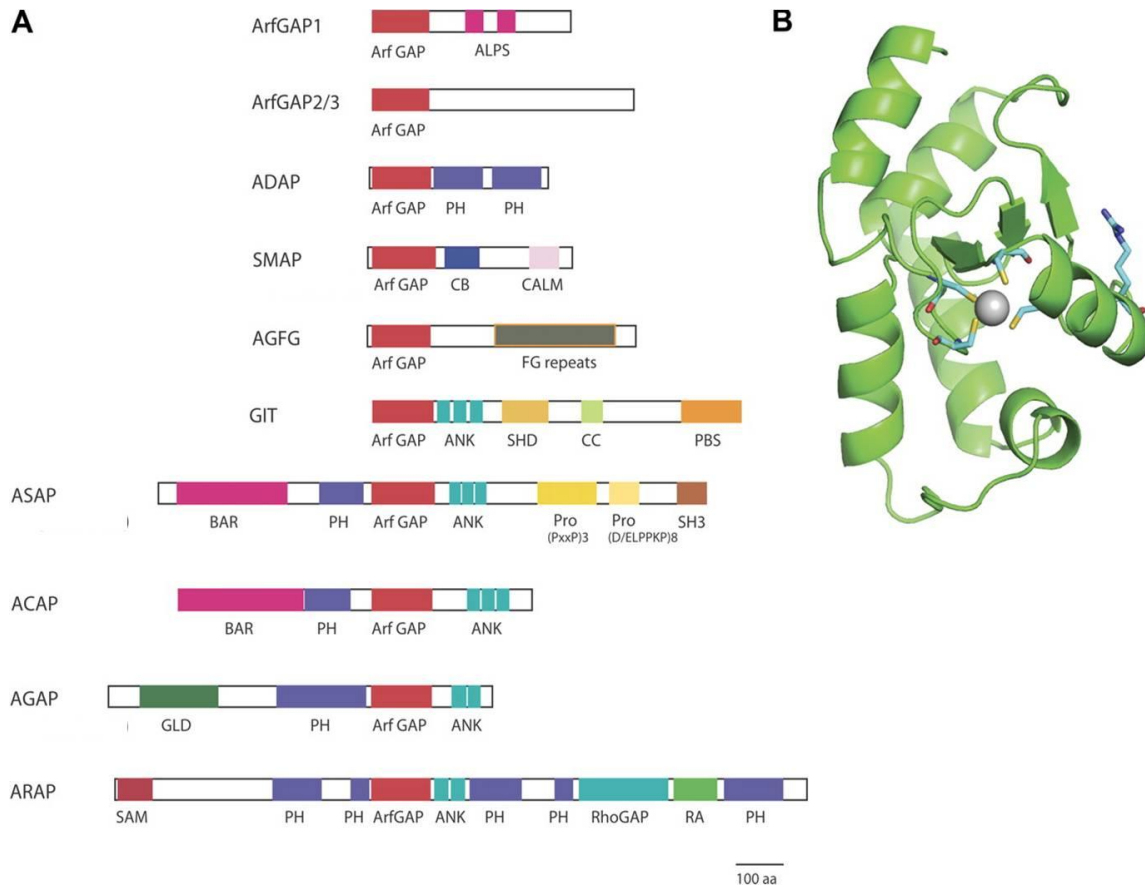
Figure 1.3 Domain organization of human ARFGAP subfamilies and structure of GAP domain of ARFGAP1 (This figure was adapted from (20). Kahn, R. A., Bruford, E., Inoue, H., Logsdon, J. M., Nie, Z., Premont, R. T., Randazzo, P. A., Satake, M., Theibert, A. B., Zapp, M. L., and Cassel, D. (2008) *J Cell Biol* **182**, 1039-1044)

1.2 Roles of ARFGAPs in Cellular Processes

ARFGAPs are primarily considered as negative regulators of ARFs before numerous studies have shown that most ARFGAPs also served as effectors for other proteins and lipids due to their multi-domain structures.(1,2,4,29-32) ARFGAPs containing catalytic domains other than ARFGAP could also regulate other protein family through their enzymatic activity. For instance, ARAPs containing Rho GAP domains catalyze the hydrolysis of GTP that bind to the RhoA GTPase. (28)

ARFGAPs have a variety of interacting partners due to their multi-domain structures. The functions of interacting proteins dictate the roles of ARFGAPs for membrane traffic, cellular signaling and cytoskeleton reorganization (**Fig 1.4**).
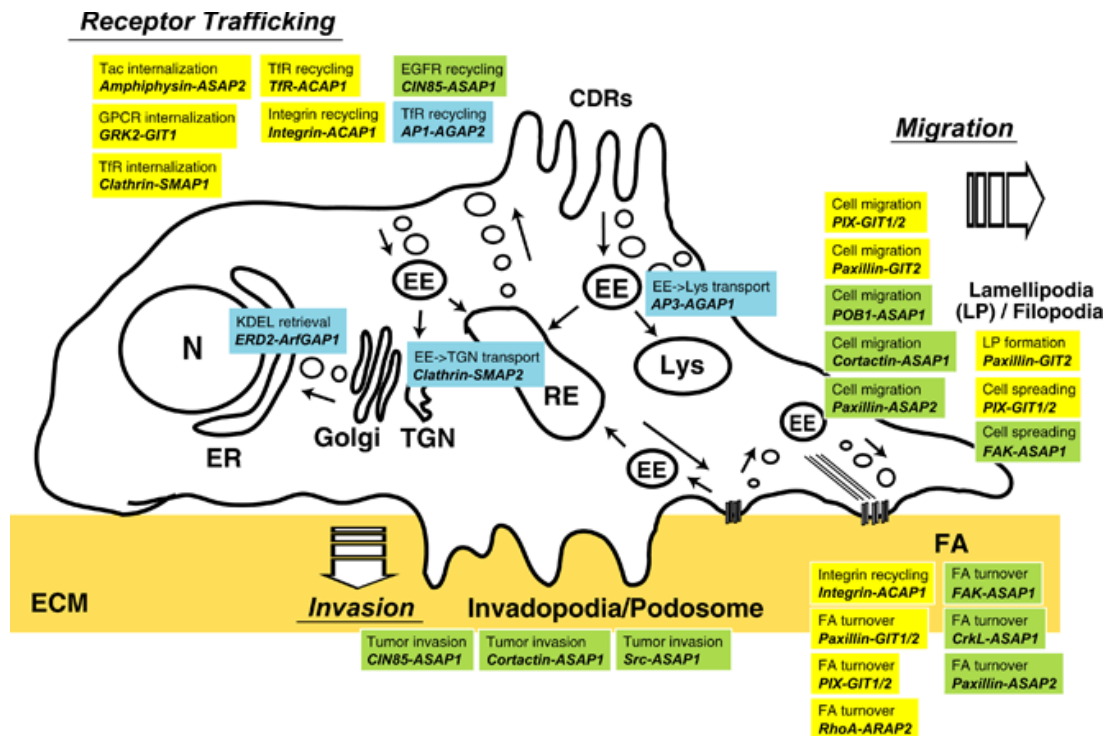
Figure 1.4 Selected ARFGAPs protein complexes involved in receptor trafficking, cell migration and invasion. Several ARFGAPs related to receptor trafficking, focal adhesion turnover, cell migration/spreading or tumor invasion are illustrated with their interacting proteins and the corresponding ARF substrates . The GAPs that use ARF1 or ARF6 as a substrate are colored in blue or yellow, respectively. The GAPs whose substrate specificity is controversial or those that may use ARF5 as the substrate are

colored in green. (This figure was reprinted from from (33). Inoue, H., and Randazzo, P. A. (2007) *Traffic* **8**, 1465-1475. © 2007 Blackwell Publishing Ltd, used with permission)

1.2.1 Membrane traffic Several ARFGAPs are involved in regulating membrane traffic. For example, ERD2 is a transmembrane receptor that mediates retrograde transport of ER-resident proteins from the Golgi to the ER. ARFGAP1 binds to p24 cargo proteins and to ERD2 to regulate cargo sorting.(34-36) ARFGAP1 was also indicated to bind to coatomer and clathrin AP1 to control membrane traffic.(37,38) The binding to the coatmer was reported to stimulate the activity of ARFGAP1 by 10-1,000 fold. (21) (39)Another ARFGAP, ACAP1, binds to transferrin receptor (TfR), cellubrevin, and integrin-β1 to serve as novel coat or adaptor protein in the recycling compartments.(40,41) In addition, SMAP proteins interact with clathrin to drive the formation of transport intermediates from both the plasma membrane and the trans Golgi network.(42,43) Furthermore, AGAP1 and AGAP2 interact with clathrin adaptor proteins, AP3 and AP1, respectively, to regulate the endocytic compartments.(34) Finally, ASAP1 interacts with CIN85 to accelerate the recycling of EGF and EGFR,(44) and also coordinates with POB1 and RalBP to regulate actin cytoskeleton and membrane traffic.(45,46) ASAP2 has also been shown to bind to the SH3 domain of amphiphysin IIm to function in synaptic vesicle endocytosis.(47) It was suggested that the ARFGAPs function as a subunit of a vesicle coat protein similar to the role of Sec23 in ER to Golgi transport mediated by COPII vesicle coats.(48)

1.2.2 Cellular signaling GIT1, AGAP2 and ARAP3 interact with related enzymes to control the levels of important phosphoinositol lipids in cellular signaling. GIT1 binds to phospholipase C gamma (PLC-γ), which catalyzes the hydrolysis of PIP_2 to IP_3.(46) The interaction between AGAP2 and phosphatidylinositol 3-kinases (PI3K)

could prevent neuronal apoptosis.(47,49,50) ARAP3 binds to phosphatidylinositol 5-phosphatase (SHIP2) to negatively regulate PI3K signaling.(51) In addition, GIT1 interacts with Rac1, Cdc42, p21-activated kinase (PAK), PAK-interacting exchange factor (PIX), MEK1, and paxillin.(52) The interaction between GIT1 and PAK are shown to regulate cytoskeletal dynamics by inhibiting Rac1 and Cdc42. GRK2 recruits and binds to both GIT1 and GIT2 to mediate internalization of the G-protein-coupled receptor (GPCR).(52,53) Fyn, a Src family kinase, phosphorylates AGAP2 and prevents degradation of AGAP2 during programmed cell death in the anti-apoptotic signaling pathway.(54) The interaction between AGAP2 and Akt is essential to this pathway as well.(55,56) ASAP1 binds to focal adhesion kinase (FAK) to mediate the localization of paxillin and affect cell motility.(57) Src and Pyk2 bind to and phosphorylate ASAP1 to inhibit the GAP activity of ASAP1.(58) ARAP1, ARAP2 and ARAP3 containing Rho GAP domains interact with RhoA, a Rho GTPase to regulate actin and actin-associated structures.(51,59) ARAP3 also regulates peripheral actin ruffles by binding to Rap1 GTPase.(51)

1.2.3 Cytoskeleton reorganization GIT1 interacts with paxillin to regulate focal adhesion (FA) dynamics and ultimately affect cell adhesion, spreading and migration.(60) ASAP1 binds to cortactin to regulate actin cytoskeleton(18,61,62) and the ASAP1/cortactin complex uncovers the crosstalk between the highly tubulated membranes and polymerized/branched actin.(26,51) GIT2 and ASAP2 also interact with paxillin and related proteins to regulate FAs.(45,55) ACAPs bind to bacteria-derived intracellular peptidoglycan sensor proteins, NOD1 and NOD2, and vaccinia virus protein KILT that are associated with changes in actin or membranes.(55,62,63)

8

1.3 Models of ARFGAP Functions in Cell Signaling

ARFGAP1 and ARFGAP2/3 are the simplest ARFGAPs in domain structures and studies on them form the basis for many models of the ARFGAP functions. Initially, ARFGAPs were proposed to only function as negative regulators of ARF signaling. In the prevailing model, the cycle of active ARF1 and inactive ARF1 is linked to coat association and dissociation from membranes.(2,34,64-67) Although a variety of modifications to this model have been proposed, the central hypothesis is that active ARF1-GTP is critical for recruiting coat proteins on the membrane while its hydrolysis would release the coat proteins from the membranes. In this model, the function of ARFGAP1 is to catalyze hydrolysis of ARF1-GTP to induce coat dissociation. The GTP hydrolysis is also dependent on the assembling of coat promoters into a vesicle coat.

1.3.1 Membrane curvature sensing The cellular functions of ARFGAPs have been proposed in several conflicting models.(21,68-70) The hydrolysis of GTP on ARF1 requires the recruitment of ARFGAP to the membrane, where the active myristoylated ARF1 is localized. Previous studies have emerged into two regulatory mechanisms for ARFGAP1. In one model, GAP activity is stimulated by coat protein-coatomer and is inhibited by cargo proteins.(25,64,71,72) The second and more extensively studied model involves membrane curvature sensing of ARFGAP1 (**Fig 1.5**).(30,73-77) In this model, ARFGAP1 is able to sense membrane curvature through the ARFGAP1 lipid-packing sensor (ALPS) motifs. The ALPS motif associates with the exposed hydrophobic interior of the bilayer to force bending of the membrane.(73) During this process, the two ALPS motifs will transform from random coils into amphipathic helix structures.(74) The activity of ARFGAP1 increases with the decreasing size of the curved surface.
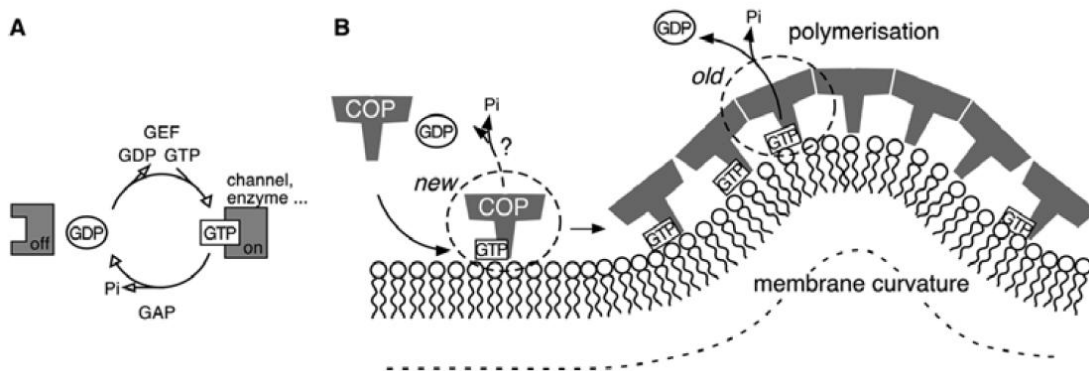
Figure 1.5 GTP hydrolysis and COP dynamics: a complex issue (A) The typical G-protein activation cycle. The GEF and GAP regulate the functions of the G protein. (B) The assembly–disassembly cycle of the protein coats is not necessarily in phase with the GTPase cycle. The first coatbuilding unit is a recently formed 1:1 complex between Arf-GTP and a COP complex wandering at the membrane surface by lateral diffusion. The second is an older unit, which has been incorporated in the coat lattice. (This figure was reprinted from (67), Antonny, B., Bigay, J., Casella, J. F., Drin, G., Mesmin, B., and Gounon, P. (2005) *Biochem Soc Trans* **33**, 619-622. © 2005 Biochemical Society, used with permission)

The model of membrane curvature sensing is attractive and has been extensively demonstrated in numerous experiments.(67,75,77-79) However, the model has its own limitations. First, although multiple ARFGAPs are involved in membrane traffic, the ALPS motifs are only present in ARFGAP1.(74) Therefore, expanding this model to other ARFGAPs is conceptually challenging, especially for other large ARFGAPs with additional domains. Second, ASAPs with BAR domains are not as sensitive as ARFGAP1 to curvature changing, although the primary role of BAR domain is reported to sense membrane curvature.(30,74,80,81) Third, cargo sorting is not involved in this model.(30)

1.3.2 Cargo sorting and coatomer In ARFGAP family proteins, at least one member of eight subclasses has confirmed GAP activity. However, ADAPs do not have detectable GAP activity *in vitro*.(72) Therefore, an additional model is proposed where ARFGAPs function as ARF effectors as well as terminators (**Fig 1.6**).(82) In yeast, four

10

ARFGAPs (Gcs1p, Glo3p, Age1p and Age2p) expressed from a high copy plasmid suppressed a loss-of-function allele of ARF1(2,83) suggesting that ARFGAPs function as downstream effectors of ARFs. Structure evidences suggested that both the yeast ARFGAP1 Gcs1p and the ARFGAP2/3 homologue Glo3p interact with SNARE proteins to induce the recruitment of ARF1p and coatomer to the SNAREs.(84-86) It is proposed that the formation of the primer complexes is required for vesicle transportation. In other studies, the most intriguing finding was that COPI vesicles only contain ARFGAP1 instead of complex of ARFs and ARFGAPs. *In vivo* data confirmed that COPI persists on membrane after the dissociation of ARF.(87) In addition, ARF was not detected in proteomic analysis of the COPI coated vesicles(66,88-91) further indicating that ARFGAP1 plays a critical role in this type of cargo sorting.
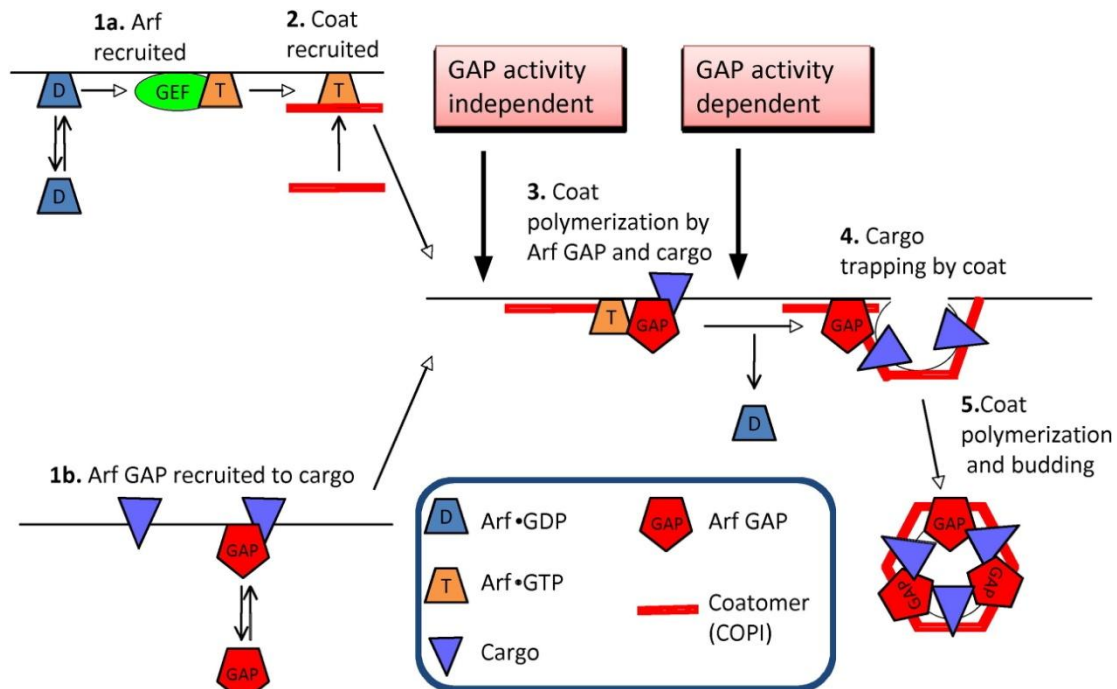
Figure 1.6. Scheme of the dual role of ARFGAPs. ARFGAPs have a role as ARF effectors in helping recruit cargo and play a vital part in transport vesicle formation. This role does not require GAP activity. The second and more established role is to function together with ARF as a heterodimeric GTPase, which promotes coat-cargo association and coat polymerization.(This figure was reprinted from (31) Spang, A., Shiba, Y., and

Randazzo, P. A. (2010) *FEBS Lett* **584**, 2646-2651. © 2010 Federation of European Biochemical Societies, used with permission)
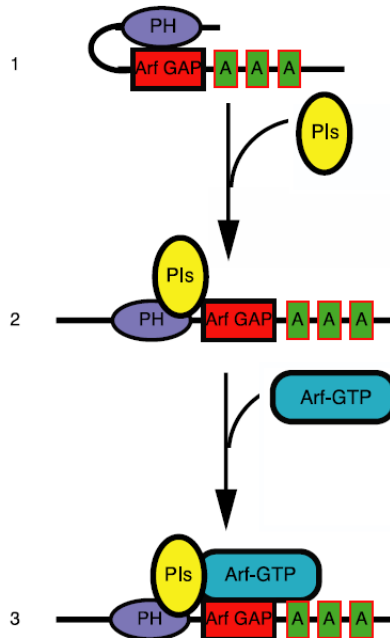
Figure. 1.7. Model for the role of the PH domain in autoinhibition of ASAP1 GAP activity. (1) The PH domain interacts with the GAP domain in the absence of PIP_2. (2) PIP_2 binds to the PH domain, leading to the exposure of the GAP domain. (3) The GAP domain interacts with ARF-GTP and catalyzes GTP hydrolysis. (This Figure was reprinted from (92), Randazzo, P. A., and Hirsch, D. S. (2004) *Cell Signal* **16**, 401-413. © 2003 Elsevier Inc, used with permission)

The function of ASAP1 has been examined extensively. PIP_2 and PA enhance GAP activity approximately 10,000 fold.(93,94) It is proposed that PIP_2 binds to the PH domain and induces a conformational change in the ARFGAP domain.(93) In this model, the PH domain binds to the catalytic GAP domain and blocks the interaction of ASAP1 with ARF-GTP (**Fig 1.7**).(95) The binding of PIP_2 to the PH domain releases the catalytic site and consequently stimulates GAP activity. However, more evidences are required to support this model.

1.4 Disease Relevance of ARFGAPs

ARFGAPs are involved in various diseases (**Fig 1.8**). For example, ASAP1 is amplified and overexpressed in uveal melanomas and in colorectal, prostate, and breast carcinomas.(16,96-99) Overexpression of ASAP1 causes increased cell motility in low-grade melanoma cells, while siRNAs against ASAP1 reduce cell migration in ASAP1-overexpessing cells.(16) Furthermore, overexpression of ASAP1 correlates with poor metastasis-free survival and prognosis in colorectal cancer patients. (100)
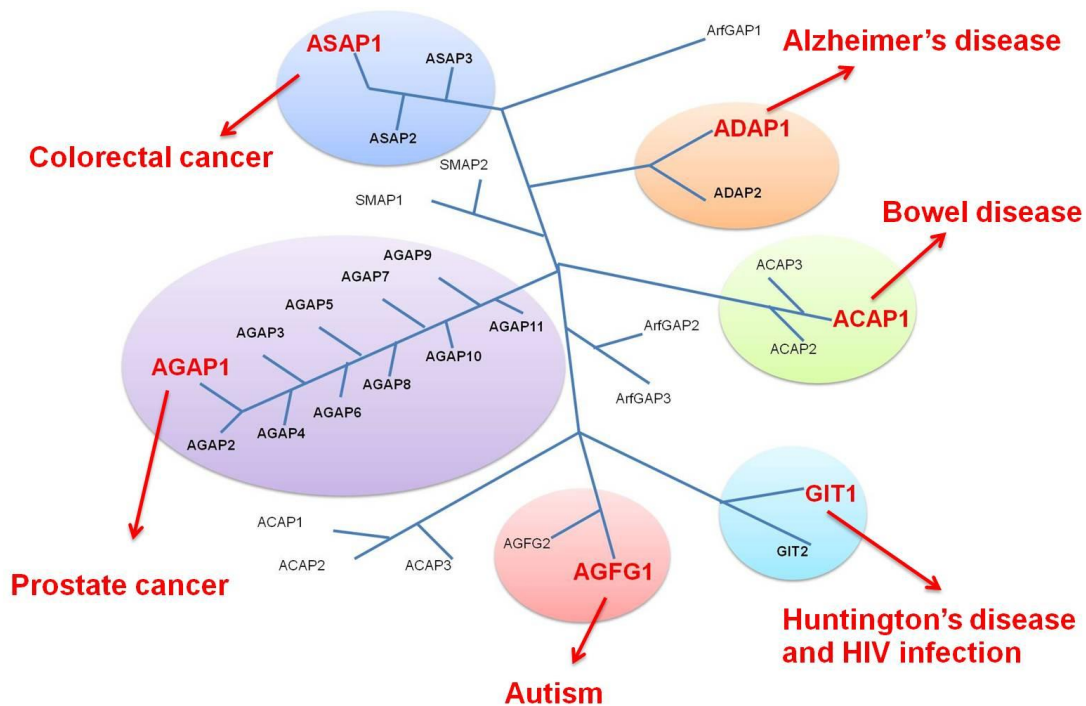
Figure 1.8. Disease relevance of ARFGAP family proteins

Another ARFGAP, GIT1, was involved in the altered membrane trafficking that contributes to Huntington's disease.(100,101) Aggregation of a huntington mutant protein is correlated with increased expression of a catalytic dead GIT1 mutant.(102) In neurons of patients with Huntington's disease, the mutations of GIT1 were observed, and these mutants may represent the catalytic dead GIT1.(102) GIT1 and GIT2 also bind to the presynaptic neuronal proteins to regulate release of presynaptic vesicles.(103,104)

GIT proteins were also involved in HIV infectivity. The inactivation of ARF6 by GITs are likely to mediate downregulation of major histocompatibility complex (MHC) class I on the host cell after infection by the viral protein Nef.(105)

ADAP1 is involved in Alzheimer's disease through its interaction with casein kinase I and nucleolin.(106-108) ACAP1 mRNA level is increased in the inflamed mucosa of patients with inflammatory bowel disease.(109,110) AGAP1 was found to be an intriguing candidate gene in autism.(111) Despite the implication of ARFGAPs in these diseases, the detailed mechanisms by which ARFGAPs contribute the disease development are not well known. Regulators of ARFGAPs would help better understand the roles of ARFGAPs in these diseases.

1.5 Regulation of ARFGAP Activity

The regulation mechanism of ARFGAP is not completely resolved. The catalytic mechanism of other GAPs, such as Ras and Rho, has been elucidated.(112,113) Both structural and biochemical studies lead to an "arginine finger" model for catalysis of GTP hydrolysis.(112-115) In this model, GAPs of Ras and Rho GTPases supply a critical arginine residue, which is missing in the GTPases. Mutation of the arginine residue caused a reduction of GAP activity. (112-115)

1.5.1 Crystal structures of ARFGAPs Currently, three crystal structures of ARF-ARFGAP pairs have been resolved.(21,116,117) In the crystal structure of ARF-GDP and ARFGAP1, the conserved arginine of ARFGAP1 was remote from the catalytic center.(21) In biochemical assays, coatomer accelerated the GTP hydrolysis by 1,000-fold.(21) This finding led the authors to propose that the catalytic arginine was provided by coatomer. In contrast, some other biochemical studies have demonstrated a critical catalytic role for the conserved arginine of ARFGAP1.(68,116) Structure and mutagenesis investigation of GA-PAPβ indicated that the conserved arginine residue plays an important role in ARFGAP activity.(68,116) In a recent crystal structure of ARF and ASAP3 in the transition state, the conserved arginine of ASAP3 is clarified to be the catalytic residue (**Fig 1.9**).(117) Mutation of the Arg469 to Ala abolished the GAP activity.(117) Furthermore, the authors discovered that calcium ions stimulated GAP activity of ASAPs, but not other members of ARFGAP family.

15
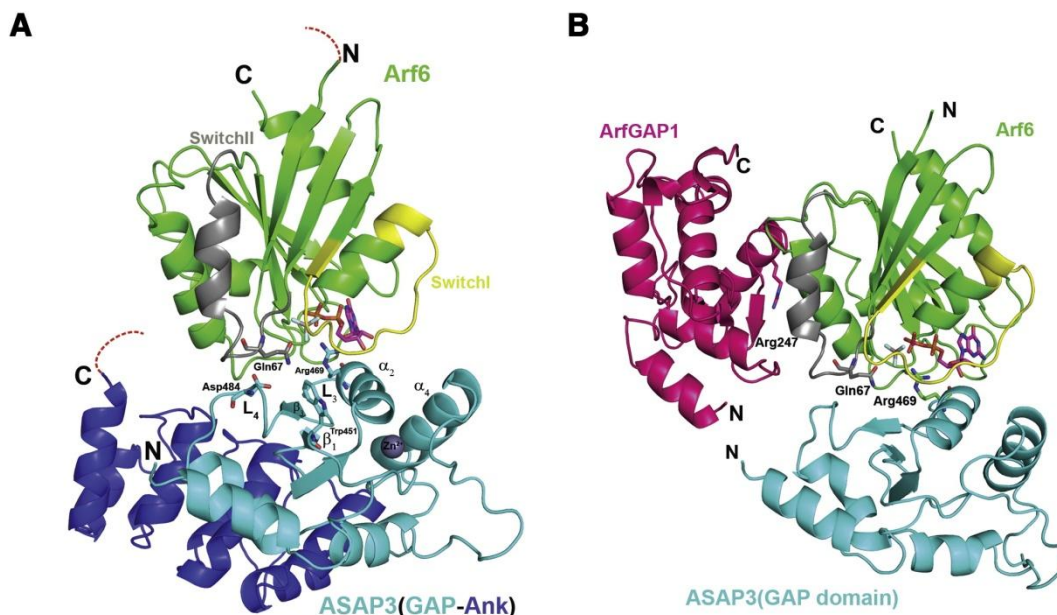
Figure 1.9. Overall structure and superimpositions. (A) Ribbon representation of the ARF6-GDPAlF$_3$ASAP3 structure, with the ASAP3 GAP domain in cyan, the ankyrin domain in blue, and ARF6 in green, and with its switch I in yellow and switch II in gray.(B) Comparison of ARF6-GDPAlFxASAP3 with ARF1-GDPARFGAP1 reported previously (118), obtained by superimposition of ARF1 with ARF6, with ARFGAP1 in dark pink, and ARF6GDP-AlF$_3$-ASAP3 as in Figure 1.9 A, leaving out the ankyrin repeats for clarity.(This Figure was reprinted from (117). Ismail, S. A., Vetter, I. R., Sot, B., and Wittinghofer, A. (2010) *Cell* **141**, 812-821. © 2010 Elsevier Inc, used with permission)

1.5.2 Biochemical studies Besides the structural studies on ARFGAPs, extensive biochemical experiments have been carried out to understand other lipid-based regulators of ARFGAP activity.(8,68,75,77,81,93,94,119,120) PIP$_2$ was shown to stimulate the ARFGAP1 activity by 30-fold.(8) In the presence of diacylglycerols (DAG), the rate of GTP hydrolysis was also accelerated by 10-fold.(119) Extensive experiments have been carried out to support that the activity of ARFGAP1 increases with the decreased size of curved membrane.(67,75,77,79) However, the detailed regulation mechanism of ARFGAPs is not well understood.

1.6 Peptide and Small Molecule Regulators of ARFGAPs

Currently, there are no effective small molecule inhibitors of ARFGAPs. Because cargo proteins bind to coatomer and ARFGAP to form a complex, peptides from the cytoplasmic tail of p24 cargo proteins were synthesized and found to inhibit the GAP activity of ARFGAP1 and ARFGAP2.(64,121) However, the inhibitory effect was nonspecific and coatomer independent. Later, peptides from several p24 family members p23 and p25 were also found to enhance GAP activity of ARFGAP1 and ARFGAP2.(68) These results are in conflict with the current regulator mechanism in which activation of ARFGAP occurs after vesicle assembly.

Understanding the molecular basis of how ARFGAPs interact with endogenous partners are helpful to understand the physiology and pathology of ARFGAPs. Small molecule regulators such as enzyme inhibitors and activators could bind to enzymes and alter their activities. Such molecules typically have molecular weight less than 800 Daltons, are cell permeable, and have been powerful tools in biochemistry, molecular biology, and pharmacology. Similarly, small molecule regulators of ARFGAPs would be useful tools to understand how ARFGAPs contribute to normal and aberrant development. In this thesis, I will describe our efforts in developing small molecule regulators of ARFGAPs to dissect their cell signaling.

Chapter 2.

Inhibition of ARFGAP1 Activity by QS11: Mechanism of Action and Analog Synthesis

2.1 Introduction

Small molecule regulators of ARFGAPs will be useful tools to study the functions of ARFGAPs in cellular processes, yet only a peptide inhibitor of ARFGAP1 have been characterized in biochemical assays. (122) Recently, a small molecule, QS11, has been shown to synergize with the Wnt proteins to activate the Wnt/β-catenin signaling pathway. (123) In the subsequent target identification process, ARFGAP1 was identified as one of the primary targets of QS11. In the presence of QS11, both ARF1-GTP and ARF6-GTP showed accumulated levels in NIH 3T3 cells indicating that the GAP activities in these cells were inhibited. In addition, in ASAP1-overexpressing MDA-MB-231 cells, QS11 inhibited cell migration in a dose-dependent manner. Overexpression of ARFGAP1 in HEK293 cells abolished synergistic effect of QS11. These results implicate that QS11 is an inhibitor of ARFGAPs *in vivo*. However, whether QS11 inhibits the activities of ARFGAPs in *in vitro* biochemical assays and what is the detailed mechanism of this inhibition are not well understood.

Preliminary structure-activity relationship studies of QS11 were also carried out.(123) One key finding was that the biphenyl substitution at the N9 position in QS11 is critical for its activity; Substitution of biphenyl group with either phenyl or (*p*-

trifluoromethyl)phenyl yields more than 10-fold decrease in activity. Replacement of the aryloxy group at the C2 position with amino groups also leads to reduced activity. Furthermore, the stereochemistry of the substituent at the C6 position is important as the enantiomer of QS11 does not show synergistic activation with the Wnt proteins.

In this chapter, I will describe our efforts to understand the molecular mechanism by which QS11 inhibits the GAP activity of ARFGAP1, and to further modify QS11 to generate more active and water-soluble analogs.

2.2 Results and Discussion

2.2.1 Generation of purified ARFGAP1 and ARF1 Human ARFGAP1 has 415 amino acid residues and contains the GAP domain and two ALPS motifs (**Fig 2.1A**). The WETF sequence in rat ARFGAP1 interacts strongly with clathrin adaptors AP1 and AP2 whereas the C-terminal peptide (^{405}AADEGWDNQNW) binds to coatmer(124). To map which region of ARFGAP1 is critical for its interaction with QS11, we generated six different ARFGAP1 proteins that include [1-136]ARFGAP1, [1-257]ARFGAP1, [1-257]ARFGAP1[L207D], [1-257]ARFGAP1[L207D/V279D], full-length ARFGAP1, and [1-415]ARFGAP1[R50K] (**Fig. 2.2**). The expression constructs for the first four proteins were kindly provided by Dr. Jonathan Goldberg (Memorial Sloan-Kettering Cancer Center) and Dr. Bruno Antonny (Institut de Pharmacologie Moleculaire et Cellulaire. The SF9 cell pellets of full-length ARFGAP1 and ARFGAP1[R50K] are from Dr. Richard Premont (Duke Univesity). The proteins were expressed and purified according to the literature protocols.(21,77,125)
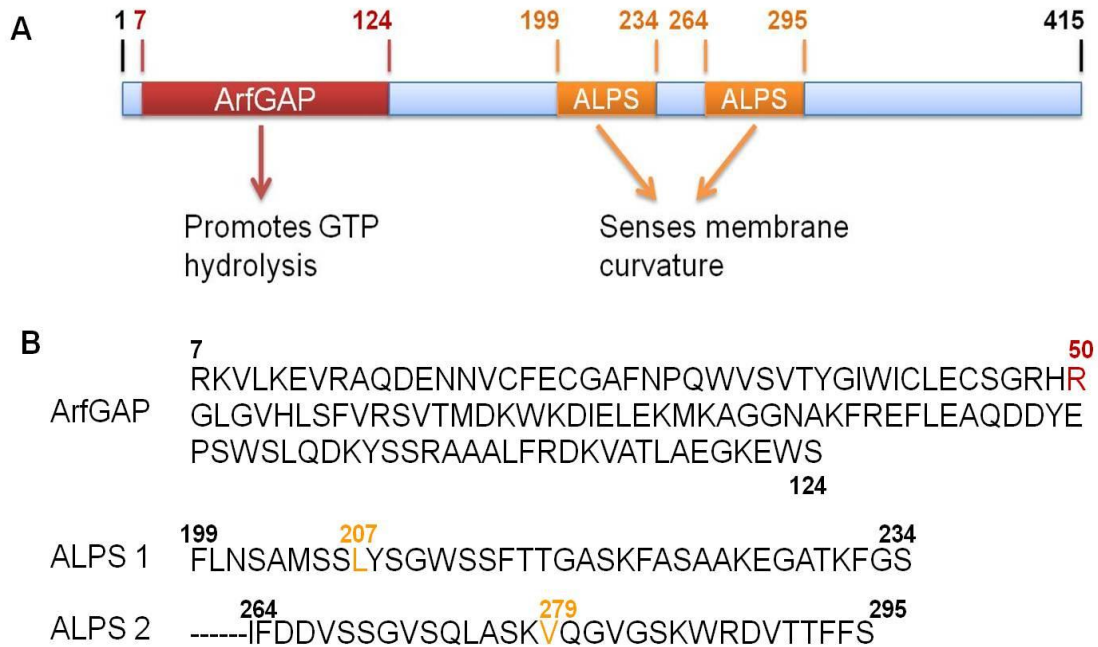
Figure 2.1. ARFGAP1 contains one GAP domain and two ALPS motifs. A. Location of the GAP domain and ALPS motifs in ARFGAP1. B. Three critical amino acids-R50, L207, and V279 are highlighted in sequences of the GAP domain and two ALPS motifs.

In **Fig 2.2**, [1-136]ARFGAP1 represents the minimal residues that are required for GAP activity (21) [1-257]ARFGAP1 containing a catalytic domain and an ALPS motif has sensitivity on liposome radius similar to that of the full-length ARFGAP1. The GAP activity of [1-257]ARFGAP1 increases slightly in the presence of liposome (75) while the introduction of mutation L207D decreases its binding affinity with liposome and GAP activity. (75,77) The full-length [1-415]ARFGAP1 has been shown to bind with QS11. (123) Its mutant [1-415]ARFGAP1[R50K] does not possess GAP activity due to the absence of the arginine finger.(29,68,120,126,127) The double mutations L207D/V279D decrease binding to liposome and the GAP activity in liposome with either small or large curvature.

Figure 2.2. Domain structures of various truncations and mutants of ARFGAP1.

We chose ARF1 as the substrate for ARFGAP1 because the crystal structure of ARF1 and GAP domain of ARFGAP1 has been solved and the detailed kinetic studies on ARFGAP1-catalyzed hydrolysis of ARF1-GTP have been carried out.(21,68) Under physiological conditions, ARF1 is myristoylated and localized at the Golgi membrane when it is GTP-bound. A truncated ARF1 with the N-terminal 17 amino acid residues deleted has also been widely used in enzymatic assays because it is soluble and technically less challenging to prepare in large quantities. Consequently, we have purified both mysritoylated ARF1 and [Δ17]ARF1.(21,122,128) The expression construct for myristoylated ARF1 was obtained from Dr. Paul Randazzo (National Cancer Institute) while that for soluble ARF1 was obtained from Dr. Jonathan Goldberg (Memorial Sloan-Kettering Cancer Center).

2.2.2 QS11 inhibits the activity of full-length ARFGAP1 but not that of [1-136]ARFGAP1 Varieties of phosphoinositol lipids stimulate GAP activity.(8,75,82,94,119) For instance, phosphatidylinositol 3,4,5-trisphosphate (PIP$_3$) enhances the GAP activity of ASAP1 while phosphatidylethanolamine (PE) and diacylglycerol (DAG) stimulate the GAP activity of full-length ARFGAP1.(82,119) To optimize the activity assay conditions, we first investigated how the lipisome system containing various lipids alters the GAP activity of ARFGAP1. Consistent with the

22

literature, we observed that DAG and PE significantly enhanced the hydrolysis of ARF1-GTP (**Fig 2.3**). We then tested QS11 in the ARFGAP reaction composed of myristoylated ARF1, full-length ARFGAP1 and DAG/PE-stimulated liposome system. When treated with 10 μM QS11, the GAP activity of ARFGAP1 was inhibited by approximately 80% compared to the control where either DMSO or an inactive analog, QS11-NC, was used (**Fig 2.4**). To further investigate how QS11 inhibits ARFGAP1, we employed the soluble [Δ17]ARF1 and the truncated [1-136]ARFGAP1 for the enzymatic reaction. It has been demonstrated that this system can still hydrolyze GTP, but at a much slower rate compared to the system containing myristoylated ARF1 and full-length ARFGAP1. More importantly, both the truncated ARFGAP1 and ARF1 are soluble, making the enzymatic reactions easier to handle. However, when treated with QS11, the GAP activity of [1-136]ARFGAP1 was not inhibited (**Fig 2.5**). We then measured the binding affinities between QS11 and [1-136]ARFGAP1 by isothermal titration calorimetry (ITC) (**Fig 2.6**); QS11 did not bind to the GAP domain.
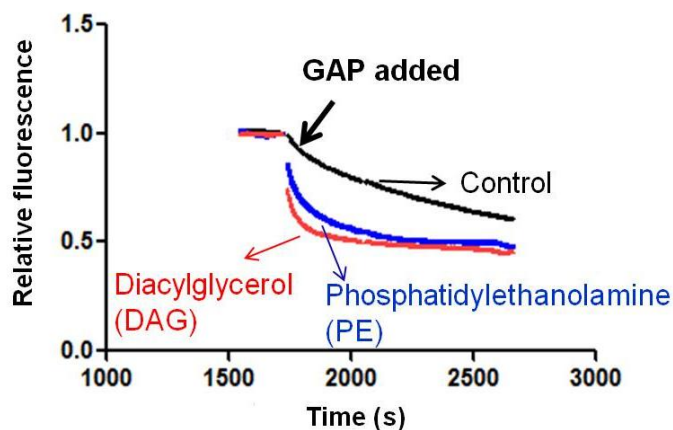
Figure 2.3. Stimulation of ARFGAP1 activity by DAG or PE. Time course of [1–415]ARFGAP1-catalyzed hydrolysis of ARF1-GTP with liposome containing phosphatidylserine (PS) (5%), phosphatidylinositol (PI) (10%), cholesterol (16%) and where indicated DAG (15%) or PE (19%). The remaining lipid is phosphatidylcholine (PC). Myristoylated ARF1-GDP (0.4 μM) was mixed with liposome (total lipid concentration, 400 μM) and exchanged to ARF1-GTP state by adding GTP (40 μM)and chelating free Mg^{2+} with EDTA. The concentration of Mg^{2+} was then adjusted to 3 mM and [1-415]ARFGAP1 (40 nM) was added to initiate the GTP hydrolysis on ARF.
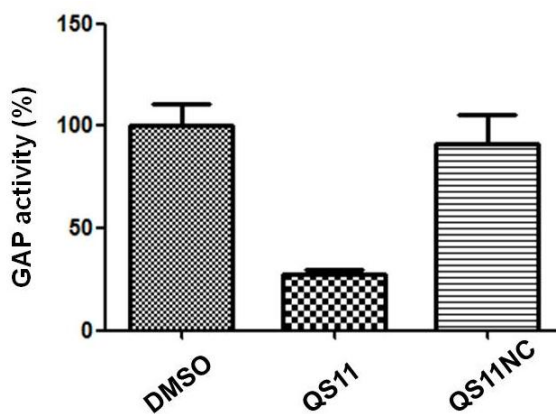
Figure 2.4. Inhibition of [1-415]ARFGAP1 by QS11. QS11 (20 μM), QS11NC (20 μM) or DMSO were incubated with [1-415]ARFGAP1 for 10 min. In the meantime, myristoylated ARF1 (0.8 μM) was exchanged with [γ^{32}P] GTP in the presence of liposome (400 μM) containing PC (35%), PS (5%), PI (10%), cholesterol (16%), DAG (15%) and PE (19%). The mixture containing compounds (20 μM) and [1-415]ARFGAP1 (16 nM) were then added to myristoylated ARF-[γ^{32}P] GTP (0.8 μM) as a ratio of 1:1. The reactions were stopped at fixed time, and the free GTP and hydrolyzed phosphate were removed. The membrane–bound radioactivity was measured using scintillation counting. The GAP activity in the presence of DMSO was normalized to 100%.
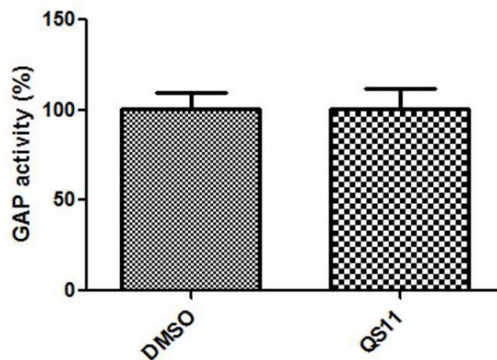
Figure 2.5. No inhibition of [1-136]ARFGAP1 by QS11. QS11 (20 μM) or DMSO were incubated with [1-136]ARFGAP1 for 10 min. [Δ17]ARF1 (10 μM) was exchanged with $[\gamma^{32}P]$ GTP This mixture containing compounds (20 μM) and [1-136]ARFGAP1 (5 μM) were then added into $[\Delta17]ARF-[\gamma^{32}P]$ GTP (10 μM) as a ratio of 1:1. The reactions were stopped, sperated and record. GAP activity in the presence of DMSO was normalized to 100%
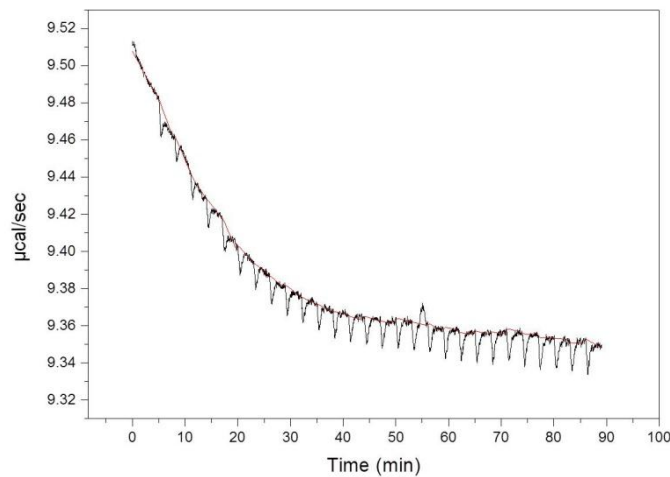
Figure 2.6. Binding affinity of [1-136]ARFGAP1 to QS11 as measured by isothermal titration calorimetry (ITC). Raw heat data obtained from injections of 100 μM GAP domain into the sample cell containing 10 μM QS11.

2.2.3 Characterization of binding affinities between QS11 and different forms of ARFGAP1 To understand the mechanism of action, we then studied the molecular basis of the interaction between ARFGAP1 and QS11. We have generated six truncated or mutated ARFGAP1 proteins and used them for the binding studies (**Figs 2.2 and 2.7**). Small molecule affinity pull-down and MS analysis were used to identify ARFGAP1 as the potential target of QS11 in the previous study. (123) This pull-down approach measures the relative levels of the QS11-bound proteins in cell lysates through the small molecule matrix. In analogy, we used this method to distinguish the relative binding affinities between QS11/QS11NC and different forms of ARFGAP1 (**Fig 2.7**). Compared with the traditional binding assays such as SPR analysis and ITC, this pull-down experiment is more efficient since multiple proteins and small molecules can be evaluated at the same time.

The affinity matrices were prepared according to the literature protocol.(123) The purified ARFGAP1 was then incubated with the packed affinity matrix at 4 ^{o}C for 2 h. Subsequently, the affinity matrix was extensively washed with binding buffer and eluted by boiling with Laemmli sample buffer. Samples were separated by SDS-PAGE and detected by coomassie blue staining and western blot against ARFGAP1. Full-length ARFGAP1 was efficiently enriched by the QS11, but not the QS11NC matrix (**Fig 2.7D**). This result is consistent with previous report that ARFGAP1 in the lysate of HEK 293 cells was selectively pulled down by the QS11 but not the QS11NC matrix . Interestingly, similar amounts of [1-415]ARFGAP1[R50K] proteins bound to the QS11 matrix, suggesting that QS11 does not bind this catalytic arginine residue. The catalytic domain of ARFGAP1 did not bind to the QS11 matrix at all, in agreement with the result that

R50K mutation does not affect the binding affinity between ARFGAP1 and QS11. These results indicated that QS11 does not bind to the active site of ARFGAP1. The double mutations [1-415]ARFGAP1[L207D/V279D], however, dramatically reduced the binding affinity of ARFGAP1 to the QS11 matrix, indicating that these two residues in the ALPS motifs play essential roles in the binding of ARFGAP1 to QS11. Along the same line, [1-257]ARFGAP1 showed much weaker binding affinity to QS11 when compared to the full-length ARFGAP1 suggesting that the second ALPS motif plays a more important role in binding to QS11. This was further confirmed by western blot analysis. [1-257]ARFGAP1[L207D] with a single mutation L207D in the first ALPS motif showed further reduced amount of ARFGAP1 that bound to the QS11 matrix which is possibly due to the partial disruption of the first ALPS motif. These data suggested that the first ALPS motif contribute to binding of ARFGAP1 to QS11 but to a less extent than the second ALPS motif. Taken together, the two ALPS motifs, especially the second ALPS motif, contribute to the interaction between ARFGAP1 and QS11.
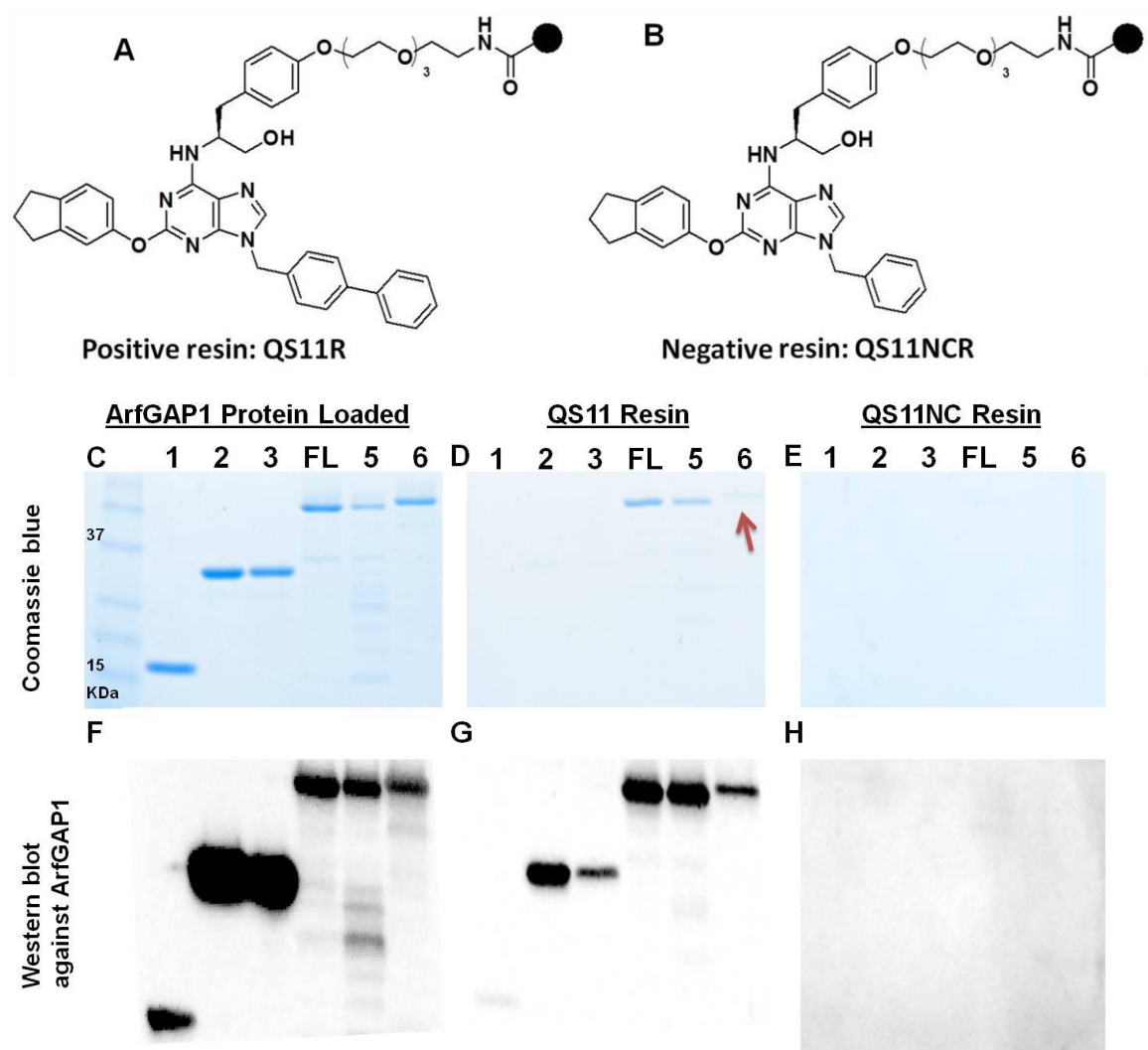
Figure 2.7. ARFGAP1 pull-down experiments with small molecule matrices. A and B. Chemical structures of QS11 (positive) and QS11NC (negative) based small molecule matrices (agarose gel). C-H. Pull-down results of six forms of ARFGAP1 by QS11 and QS11NC matrices. C. purified, recombinant ARFGAP1 proteins were visualized by coomassie blue staining. **1**: [1-136]ARFGAP1, **2**: [1-257]ARFGAP1, **3**: [1-257]ARFGAP1[L207D], **4**: full-length ARFGAP1, **5**: [1-415]ARFGAP1[R50K], **6**: [1-415]ARFGAP1[L207D/V279D]. F. the same amounts of samples were detected by antibody against ARFGAP1. D and G. Six ARFGAP1s were incubated with QS11 resin at 4℃ for 2 h, and then, bound proteins were washed, eluted and determined by coomassie blue staining and western blot. E and H. Six ARFGAP1s were treated with QS11NC resin in the same way.

28

We further validated this interaction in surface plasmon resonance (SPR) assays. Purified full-length ARFGAP1, ARFGAP1[R50K], [1-136]ARFGAP1, [1-257]ARFGAP1, [1-257]ARFGAP1[L207D] or [1-415]ARFGAP1[L207D/V279D] was covalently immobilized to a CM5 chip surface. The control channel was treated in the same way but without protein immobilization. Ethanolamine was subsequently injected to block the unreacted surface. QS11 was then injected for at increasing concentrations (0, 156, 312, 625, 1,250, 2,500, 5,000, 8,000 and 10,000 nM) in HBS-EP buffer and the dissociation of ARFGAP1-QS11 complex was followed for 10 min. SPR analysis afforded K_d values of 1.3 ±0.3 μM for both full-length ARFGAP1 and ARFGAP1[R50K] (**Fig 2.8**). This is consistent with the result that both full-length ARFGAP1 and ARFGAP1[R50K] can effectively bind to the QS11 matrix in the small molecule pull-down assays. The interaction of QS11 with [1-257]ARFGAP1 generated a weaker response in RU and did not reach plateau with QS11 at 10 μM (close to its maximal solubility). The single mutant [1-257]ARFGAP1[L207D] showed a further reduced response. The catalytic domain of ARFGAP1 showed no binding at all in the SPR assays, in consistent with the pull-down results. In addition, the double mutant [1-415]ARFGAP1[L207D/V279D] showed similar effects as the catalytic domain. We therefore concluded that QS11 binds to ARFGAP1 through the ALPS motifs.
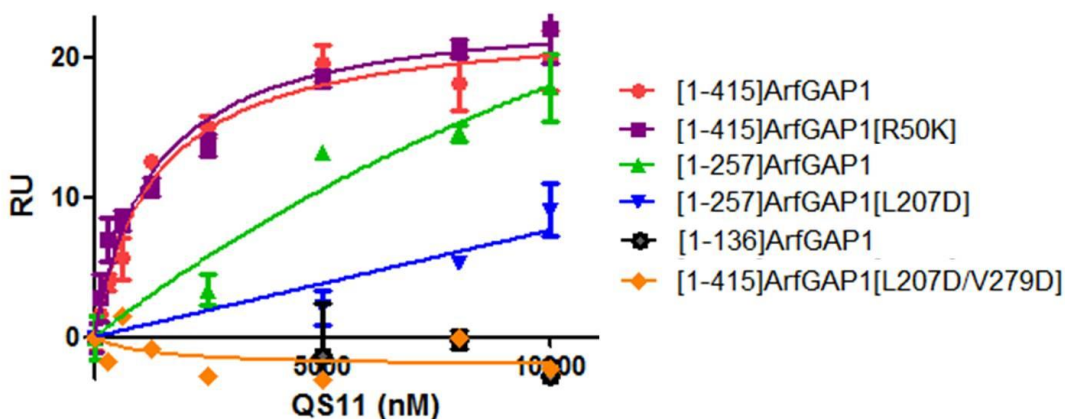
	1-415	1-415 [R50K]	1-415 [L207D/ V279D]	1-257	1-257 [L207D]	1-136
K_d (µM)	1.3 ± 0.3	1.3 ± 0.3	n.d.	> 10	> 10	n.d.

Figure 2.8. Binding affinities between different ARFGAP1 proteins and QS11 as measured by surface plasmon resonance (SPR). The proteins were immobilized on surfaces of CM5 chips. Equilibrium responses of the binding of QS11 to ARFGAP1 proteins were plotted against concentrations of QS11. The data were fitted using a 1:1 binding model to calculate the binding constant K_d.

2.2.4 QS11 inhibited GAP activity of ARFGAP1 To quantify the inhibition of GAP activity by QS11, we first compared the relative capacity of the six ARFGAP1 proteins as described in the binding experiments in catalyzing the hydrolysis of ARF1-GTP. We used $[\gamma^{32}P]$ GTP hydrolysis assay to detect the loss of $[\gamma^{32}P]$ GTP that was bound to myristoylated ARF1 in liposome, which can indirectly report the GAP activity. Myristoylated ARF1 was activated in the presence of GTP and $[\gamma^{32}P]$ GTP, EDTA and liposome. Then, MgCl$_2$ was added to stabilize myristoylated ARF-$[\gamma^{32}P]$ GTP. The GTP hydrolysis was initiated by adding ARFGAP1 (**Fig 2.9**). The full-length ARFGAP1 showed the best activity while the catalytic inactive ARFGAP1[R50K] remains inactive at the maximum concentration (29,68,126,127) The double mutant

ARFGAP1[L207D/V279D] dramatically reduced the GAP activity probably due to its poor affinity to the liposome, which was also observed in another reported intrinsic fluorescence ARF-GTP hydrolysis assay.(77) In addition, [1-257]ARFGAP1 showed a slightly reduced GAP activity compared to full-length ARFGAP1(77) while [1-257]ARFGAP1[L207D] dramatically reduced the GAP activity due to the reduced interactions with liposome. Finally, the catalytic domain of ARFGAP1 did not exhibit good activity under current reaction conditions, possibly due to its weak interaction with liposome.
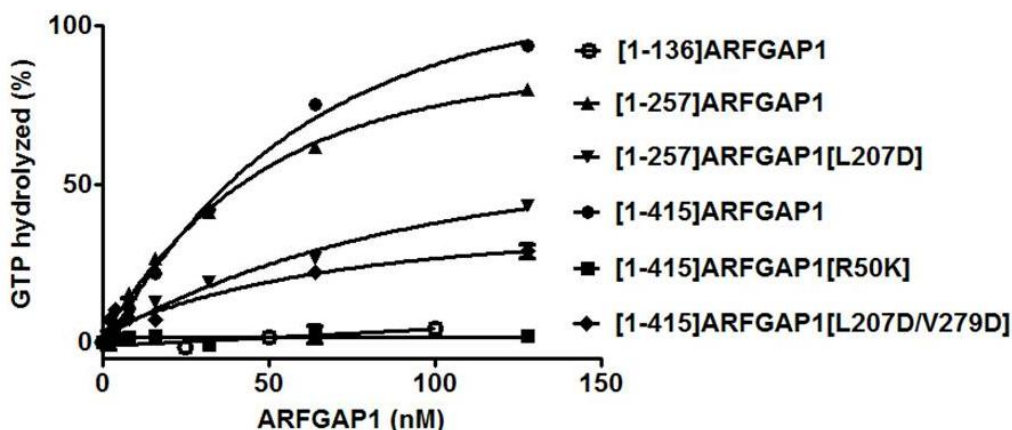
Figure 2.9. Activities of different forms of ARFGAP1. A. Determination of GAP activity of ARFGAP1 on GTP hydrolysis. ARFGAP1 was titrated into a reaction containing myristoylated ARF-$[\gamma^{32}P]$ GTP and measured as described under "Experimental Procedures"

Next, dose-dependent inhibition of the GAP activity of each ARFGAP1 was evaluated under conditions that the rate of GTP hydrolysis was within the linear range (**Fig. 2.10**). The IC_{50} for inhibiting the GAP activity of full-length ARFGAP1 by QS11 was 4.0 ± 0.5 μM. In contrast, none of the other ARFGAP1 proteins can be inhibited at 10 μM QS11 in the GTP hydrolysis assays. To investigate whether QS11 competitively inhibits ARFGAP1, the concentration of QS11 was fixed at the IC_{50} value but that of

ARF1-GTP varied. QS11 inhibited the GAP activity of full length ARFGAP1 across a

wide range of concentrations of ARF-GTP (**Fig 2.11**) indicating that QS11 likely

inhibited ARFGAP1 non-competitively with ARF1-GTP.
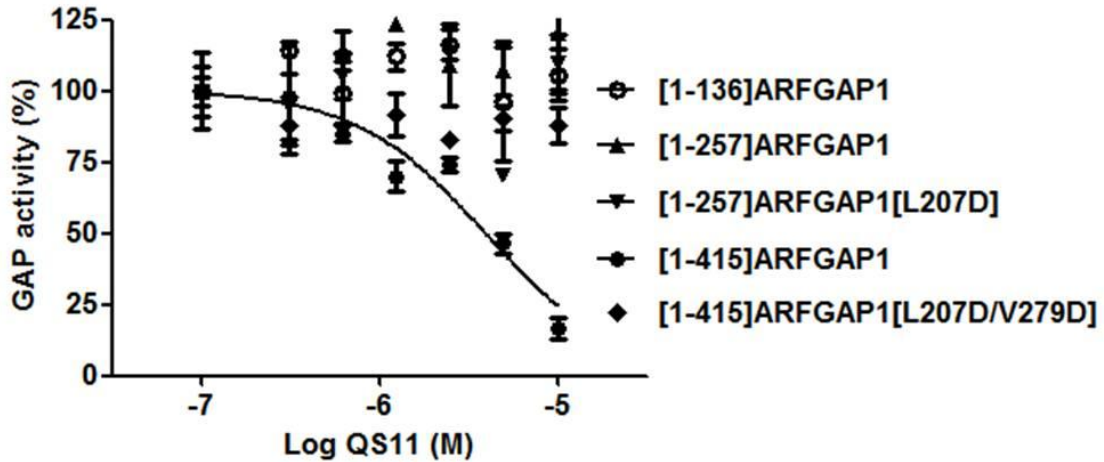
Figure 2.10. Inhibition of the GAP activity of different ARFGAP1 proteins by QS11.
QS11 was pre-incubated with ARFGAP1 for 10 min and the reaction was initiated by
adding myristoylated ARF1-[γ^{32}P] GTP (400 nm) with liposome (0.2 mM). The
percentage of remained GAP activity was calculated as the ratio of the GAP activity in
the presence of QS11 to that of DMSO treatment.
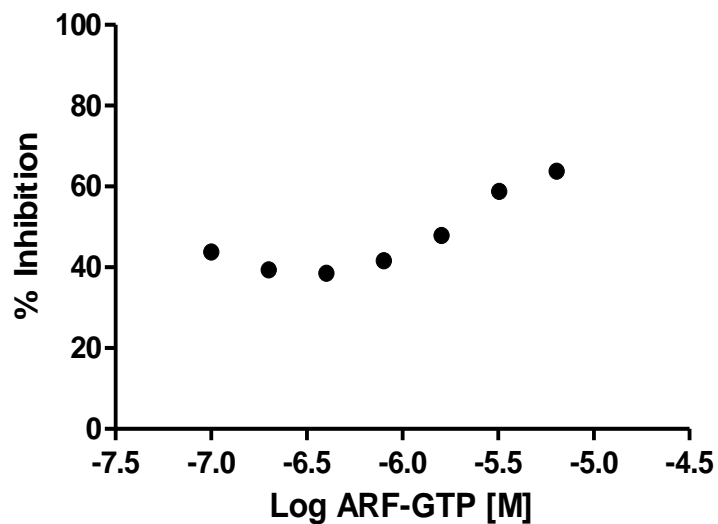
Figure 2.11. Non-competitive inhibition of ARFGAP1 by QS11 to ARF-GTP binding sites. QS11 was at the IC_{50} concentration (4.0 µM) while the concentrations of substrate ARF1-[γ^{32}P] GTP varied from 100 nM to 6.4 µM.

2.2.5 Investigation of secondary structures of ARFGAP1 The ALPS motifs in ARFGAP1 are random coils in solution and rearrange to α-helix structures when they interact with lipid membranes.(67,77,120) The Circular Dichroism (CD) spectra showed that adding liposome to the full length ARFGAP1 led to increased absorbance at 208 and 222 nm. More detailed analysis indicated that the major contribution of this increase in absorbance was from the ALPS motifs, especially the first ALPS motif.(77) Mutations in the ALPS motifs dramatically decreased or disrupted the increase of the α-helix structures.

We hypothesize that QS11 interacts with the non-structured ALPS motifs to prevent the interactions between ARFGAP1 and the lipid membranes. To test this hypothesis, we measured the changes of the secondary structures of ARFGAP1 in the presence of both QS11 and liposome (**Fig 2.12**). As expected, ARFGAP1 showed a slight increase of α-helix structures in the presence of liposome. When ARFGAP1 is treated with both QS11 and liposome, the increased secondary structures were disrupted due to reduced interaction between ARFGAP1 and the liposome. This data supports the notion that QS11 interacts with the ALPS motifs and disrupts the interactions between ARFGAP1 and membrane.
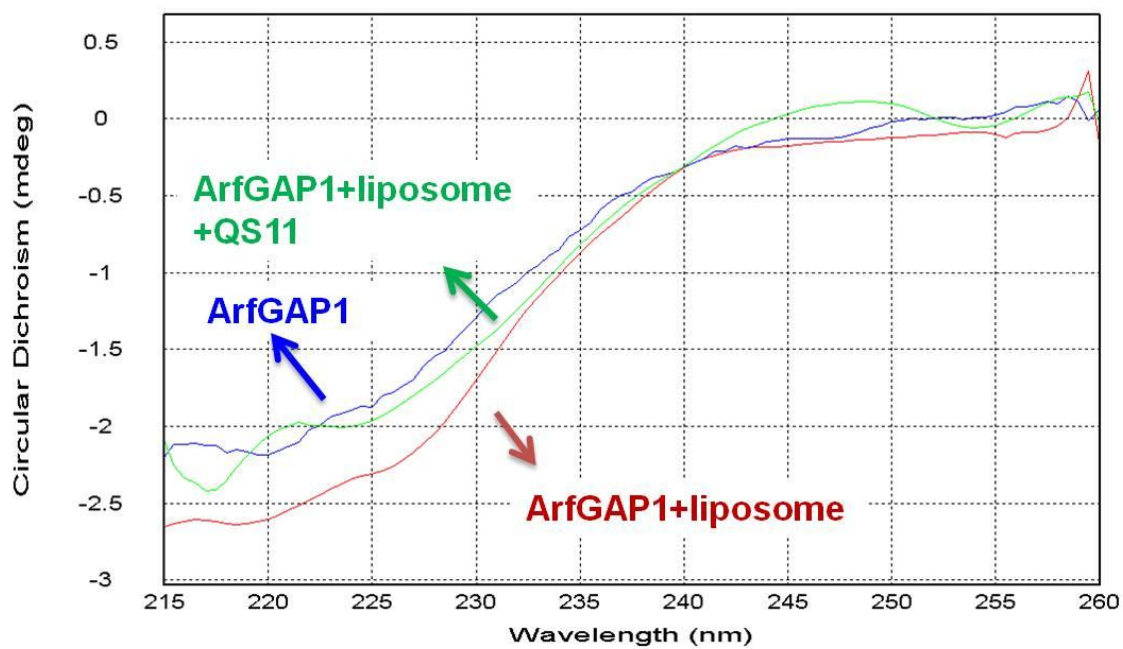
Figure 2.12. Far-UV CD spectra of [1-415]ARFGAP1 (1.4 μM) in solution, with PC/PS (70:30) liposome (0.5 mM), or with both PC/PS liposome (0.5 mM) and QS11 (10 μM).

2.2.6 Localization of ARFGAP1 in the presence of QS11 The ALPS motifs are required for proper localization of ARFGAP1 in Golgi membrane(77,129,130): ARFGAP1 majorly localize in Golgi membrane(76,129,130) while mutations in the ALPS motifs cause diffused localization of ARFGAP1.(77,129) Consequently, QS11 should disrupt the Golgi localization of ARFGAP1 to regulate its catalytic action on hydrolysis of ARF1-GTP. Dr. Juyoun Beak in our lab thus transfected NIH3T3 cells with YFP-ARFGAP1 and treated the resulting cells with QS11 or QS11NC. Preliminary data indeed suggested that the Golgi structures were disrupted upon QS11 treatment (**Fig 2.13**). We are optimizing the condition and testing the effects of QS11 in these cells.
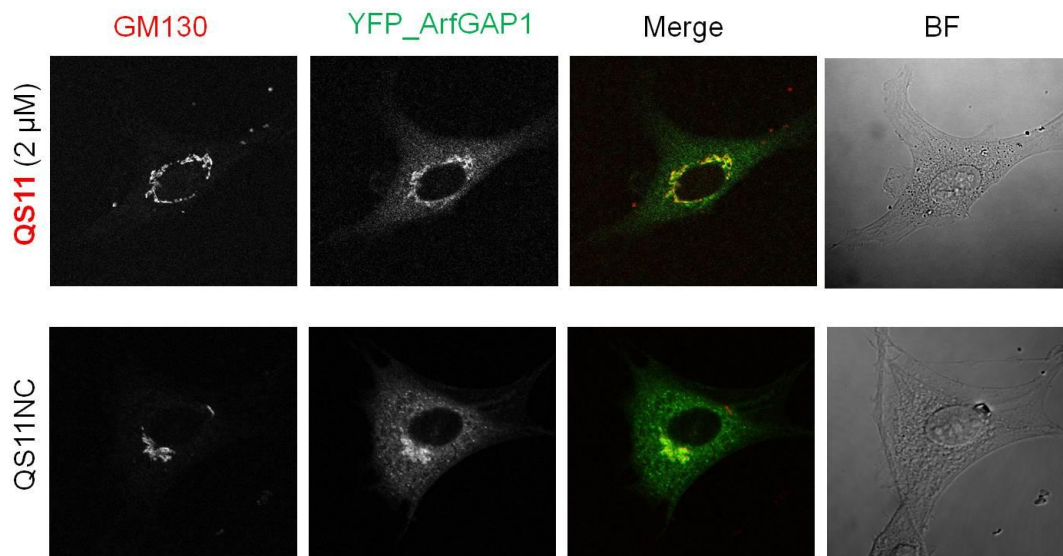
Figure 2.13. Effects of QS11 on localization of ARFGAP1. [1-415]ARFGAP1 fused to YFP was transiently expressed in NIH 3T3 cells. The cells were then treated with QS11 (2 μM) or QS11NC (2 μM) for 24 hours before immunostaining with antibody against GM130 and YFP. "BF" is defined as "bright field"

2.2.7 Working model on how QS11 inhibits the GAP activity of ARFGAP1

Based on our data, we propose a working model where QS11 regulates the activity of ARFGAP1 through hydrophobic interaction with the ALPS motifs which disrupts the Golgi localization of ARFGAP1 in the endogenous systems (**Scheme 2.1**). QS11 non competitively inhibits ARFGAP1 activity through the ALPS motifs. Consistent with this model, QS11 is a highly hydrophobic compound partly due to the biphenyl rings. In addition, four hydrophobic amino acids in the second ALPS region of ARFGAP1 are essential for the interaction of ARFGAP1 with lipid membrane and subsequent formation

of α-helix structures by non-structured ALPS motifs.

Scheme 2.1. Mode of inhibition of ARFGAP1 by QS11 QS11 binds to the non-structured ALPS motifs in ARFGAP1 and prevent the interaction of ARFGAP1 with lipid membranes, where active ARFs localize.

2.2.8 Synthesis of a small library of QS11 analogs To improve the potency and water solubility of QS11, we carried out further SAR studies. The structure of QS11 is shown in **Fig 2.14**. Previous SAR results demonstrate the critical role of the biphenyl substitution at the N9 position. Therefore, our initial plan was to vary the C2 and C6 substitutions with the intention to systematically modify the N9 substitution in the future. The route for synthesizing QS11 analogs is similar to what has been described previously (**Fig 2.15**).(123) Briefly, 2,6-dichloro-9H-purine (**1**) reacted with biphenyl-4-ylmethanol via Mitsunobu reaction to provide 9-[(1,1'-biphenyl)-4-ylmethyl]-2,6-dichloro-9H-purine (**2**). Amines (**R^1-NH$_2$**) were then added to 9-[(1,1'-biphenyl)-4-ylmethyl]-2,6-dichloro-9H-purine (**2**) in the presence of diisopropylethylamine in *t*-butanol to yield intermediate **3**. Finally, compound **3** was coupled with various aryloxy groups (**R^2-OH**) in the presence of tris(dibenzylideneacetone)dipalladium and di-*tert*-butyl(phenyl)phosphine to generate the products (**4**). Six amines and six phenol derivatives (**Fig. 2.16**) were chosen as the building blocks to probe the electronic and steric effects. 2-(2-aminoethylamino)ethanol (**B1**) was selected at the C6 position to also improve water solubility of the analogs. Using the described synthetic scheme and building blocks, I have synthesized twenty-two QS11 analogs and Dr. Zhiquan Song synthesized another nine analogs including B1C0, B1C1, B1C2, B1C5, B5C0, B5C1, B5C2, B5C3 and B5C5. The chemical structures of all the analogs are shown in **Fig 2.17**.
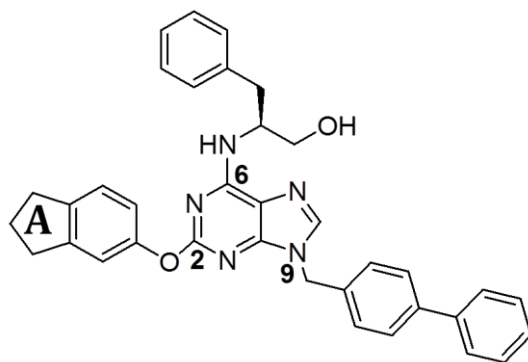
Figure 2.14. Chemical structure of QS11
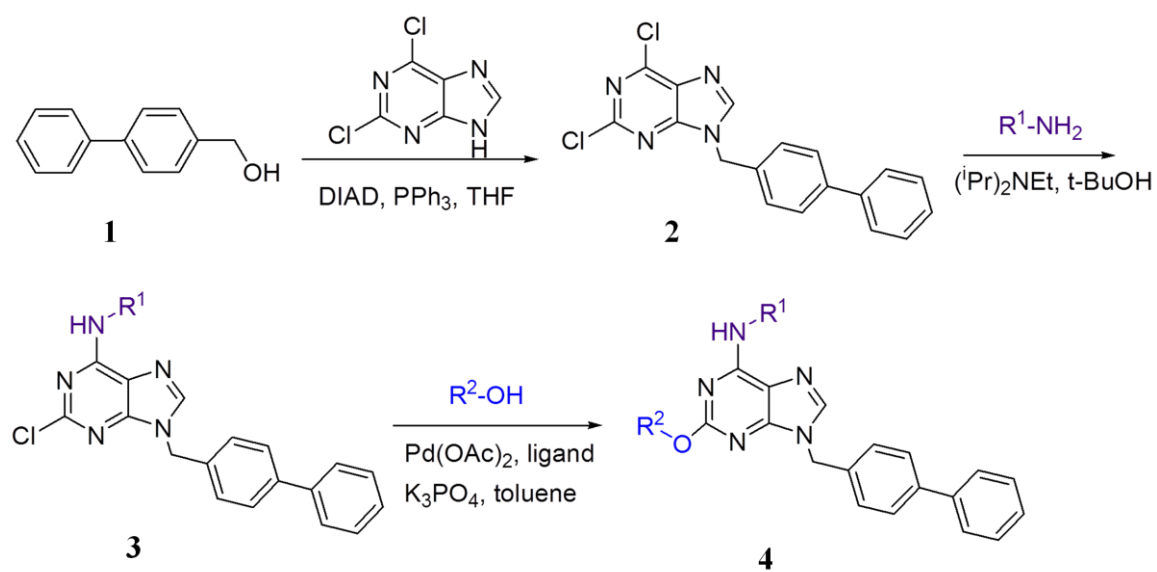
Figure 2.15. Synthetic schemes for the focused library of 2,6,9-trisubstituted purines

Amine building blocks:

| B0 | B1 | B2 | B3 | B4 | B5 |
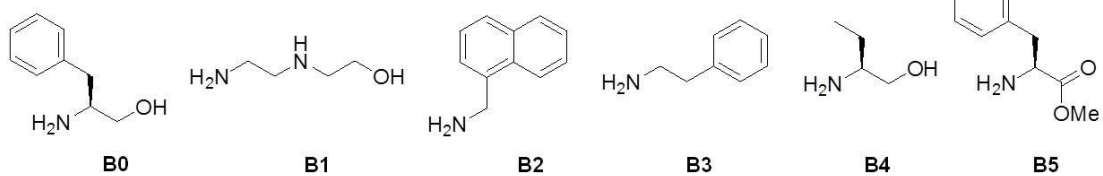
Phenol building blocks:

| C0 | C1 | C2 | C3 | C4 | C5 |
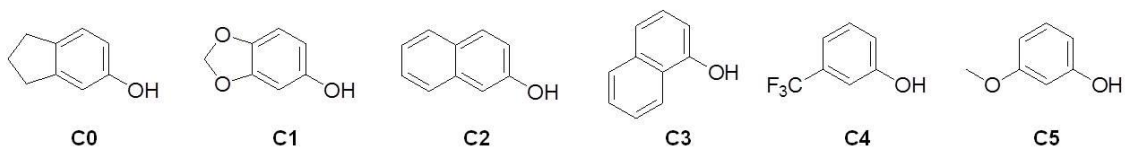
Figure 2.16. Building blocks selected for analog synthesis

Figure 2.17. Chemical structures of 31 analogs

QS11 Analogs	Remaining GAP activity (%)	K_d μM	Log P (predicted)
QS11	17.0	1.3 ± 0.3	7.9
QS11NC	88.9	n.d.	6.2
DMSO	100.0	Control	-1.5
B0C1	30.6	4.1 ± 0.9	6.8
B0C2	93.1	3.4 ± 0.8	8
B0C3	76.7	3.6 ± 0.4	8
B0C4	111.7	n.d.	7.9
B0C5	65.2	7.8 ± 2.0	6.9
B1C0	102.1	n.d.	5.8
B1C1	N/A	n.d.	4.6
B1C2	102.1	n.d.	5.9
B1C5	77.9	n.d.	4.7
B2C0	85	n.d.	9.2
B2C1	62.6	n.d.	8
B2C2	78.2	n.d.	9.3
B2C3	55.9	n.d.	9.3
B2C4	77.5	n.d.	9.2
B2C5	72	n.d.	8.1
B3C0	97.4	n.d.	8.4
B3C1	59.8	2.5 ± 0.9	7.3
B3C2	58.5	n.d.	8.5
B3C3	72.3	n.d.	8.5
B3C4	118	n.d.	8.5
B3C5	61.4	3.4 ± 0.4	7.4
B4C0	90.6	n.d.	6.7
B4C1	61.7	n.d.	5.6
B4C2	69.4	1.0 ± 0.2	6.8
B4C3	74.2	9.7 ± 1.7	6.8
B4C5	91.5	n.d.	5.7
B5C0	95.7	n.d.	8.1
B5C1	25.2	1.5 ± 0.3	7
B5C2	80.4	n.d.	8.2
B5C3	36.4	3.9 ± 1.2	8.2
B5C5	84.9	1.4 ± 0.2	7.1

Table 2.1 Inhibition effects, binding affinities, and clogP of analogs Note: For B1C0, B1C1, B1C2 and B1C5, log D values would be more useful to determine their Partition coefficient.

2.2.9 Inhibition studies of QS11 analogs The synthetic analogs were first evaluated in ARF-[γ^{32}P] GTP hydrolysis assays where their capacities to inhibit the catalytic activity of the full-length ARFGAP1 were tested. Myristoylated ARF1 was loaded with [γ^{32}P] GTP in the presence of EDTA and liposome. Then, MgCl$_2$ was added to quench the nucleotide exchange reaction. All analogs were first dissolved in DMSO to make a stock solution at 10 mM and then diluted into aqueous solution to make the final concentration at 20 μM. In a representative reaction, one QS11 analog was pre-incubated with ARFGAP1 (16 nM) at room temperature for 10 min and the resulting mixture was added to myristoylated ARF-[γ^{32}P] GTP in liposome to initiate the hydrolysis. As fixeded time, the reaction was stopped, free GTP and phosphate were separated and the remaining membrane-bound [γ^{32}P]ATP was measured by scintillation counting (**Table 2.1**).

Replacing the biphenyl group in **QS11** with a phenyl group (**QS11NC**) dramatically abolished the inhibition. This is consistent with the fact that the removal of one of the benzene groups of QS11 abolished the synergist effect of QS11 in the Wnt reporter assays.(123) Replacing the 5-methyl-2,3-dihydro-1H-indene moiety (**QS11**) with 5-methylbenzo[d][1,3]dioxole (**B0C1**) did not affect the inhibition effect (IC$_{50}$ of **B0C1** is 3.8 ± 2.4 μM in **Fig 2.18**). This suggests that replacement with carbons in the cyclopentane is tolerable. However, modification of C2 position with naphthalene ring (**B0C2 and B0C3**) is not favored. Interestingly, the (trifluoromethyl)benzene substitution (**B0C4**) at this position totally disrupted the activity of this molecule while the anisole modification (**B0C5**) still demonstrates certain inhibition. These results suggest that the ring **A** in C2 position is important for activity of this molecule.

43
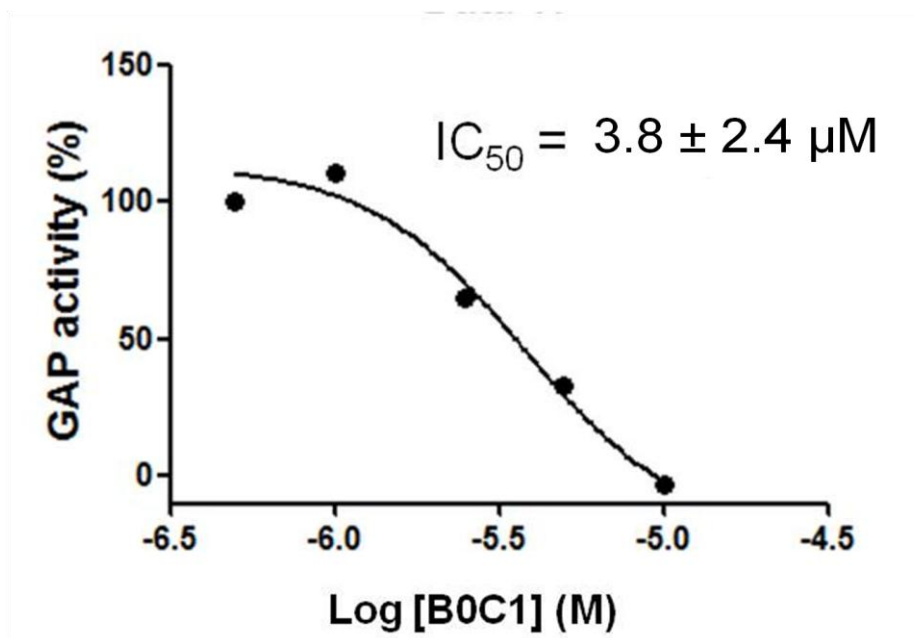
Figure 2.18 IC$_{50}$ curve of analog-B0C1

The water solubility of QS11 is a concern when the compound is used in aqueous solution. QS11 begins to precipitate beyond 10 μM in aqueous solution. It was shown that when K_d and IC$_{50}$/EC$_{50}$ of the compound is around low micromolar or high nanomolar range, in a number of biochemical and biophysical assays, the concentrations of small molecules need to go beyond 10 μM to get sufficient signal for accurate activity measurement.(131-133) It is well known that PEGylation can provide water solubility to hydrophobic drugs and proteins.(134-137) In order to improve the water solubility of QS11, PEG like structure, 2-(2-aminoethylamino)ethanol (**B1**) was utilized to modify the C6 position of QS11. This set of four analogs (**B1C0, B1C1, B1C2, and B1C5**) indeed showed a better solubility in assay buffer (50 mM Hepes pH 7.2, 120 mM KAc, 3 mM MgCl$_2$, 2 mM EDTA, 1 mM DTT). No precipitations were observed when the concentrations of the analogs were up to 50 μM, yet these four analogs lost the inhibition towards ARFGAP1 as tested in enzymatic assays (**Table 2.1**).

Substitution of the C6 position of QS11 with naphthalen-1-ylmethanamine (**B2C0**) significantly decreased the inhibition of the molecule (**Table 2.1**). The bulky naphthalene moiety is not favored at this position. Interestingly, the analog **B2C3**, with naphthalene groups on both C2 and C6 positions, showed moderate inhibition. It is not clear whether the moderate inhibition is due to the increased steric effects or aromatic effects provided by the substitutions at the C6 position of QS11.

The removal of the methoxy group in amine part (**B3C0**) dramatically decreased the inhibition effect (**Table 2.1**). This hydroxyl group is likely to be important to form a hydrogen bond with ARFGAP1 for its activity. This hypothesis was further confirmed by replacing the hydroxyl group with a methyl formate group in **B5C0**. This analog **B5C0** and hydroxyl-free analog **B3C0** showed similar decreased activity against ARFGAP1. Surprisingly, by replacing the cyclopentane moiety (**C0**) with 1,3-dioxolane (**C1**), the new analog **B5C1** almost rescued the inhibition of this molecule. The two oxygen atoms in **B5C1** are suspected to form hydrogen bonds with the ARFGAP1 which contribute to the inhibition.

The benzene group in the amine part is necessary for maintaining the inhibition of this molecule. After removal of this benzene group, all the analogs (**B4C0, B4C1, B4C2, B4C3,** and **B4C5**) showed dramatically decreased inhibition of ARFGAP1.

2.2.10 Binding studies of QS11 analogs The binding affinities, as measured by SPR, between ARFGAP1 and analogs were summarized in **Table 2.1**. The SPR analysis is carried out in a similar manner as described previously. Any analog with a saturation signal higher than 10 μM will be considered as non-detectable K_d (**n.d**).

QS11NC lacking one benzene ring in the biphenyl group did not bind to ARFGAP1. This is consistent with previous results that QS11NC did not inhibit the GAP activity in the *in vitro* GTP hydrolysis assays, did not increase ARF-GTP levels in NIH 3T3 cells and did not activate the Wnt signaling pathway.

Interactions between ARFGAP1 and the analogs are not sensitive to substitutions at the C2 positions, although the other modifications (**B0C1, B0C2, B0C3, and B0C5**) indeed decreased the binding affinity, except for (trifluoromethyl)benzene (**B0C4**). The substitution at the C2 position of QS11 with (trifluoromethyl)benzene (**B0C4**) abolished the interaction. This is consistent with the disrupted inhibition of this molecule. (**Table 4.1**) Substitutions at the C6 position of QS11 with either 2-(2-aminoethylamino)ethanol (**B1**) or naphthalen-1-ylmethanamine (**B2**) disrupted bindings interactions between QS11 analogs and ARFGAP1. These results are consistent with the fact that none of these analogs could effectively inhibit ARFGAP1 in activity assays. (**Table 2.1**) The removal of the hydroxyl group (**B3C0**) or the replacement of the hydroxyl group (**B5C0**) also disrupted the binding interactions between QS11 and ARFGAP1. These data suggest that the hydroxyl group is important for the interaction with ARFGAP1. After removing the benzene group in the amine part (**B4C0**), the analog lost its binding to ARFGAP1. However, with the substitution of a naphthalene group (**B4C2**) at the C2 position, the new analog rescued the binding affinity. The different binding affinities for **B4C2** and **B4C3** are likely due to different orientations of naphthalene. Consistent with the inhibition study, **B5C1** showed good interaction with ARFGAP1.

2.3 Experimental Section

2.3.1 Expression and purification of ARFs and ARFGAPs Rat ARFGAP1 and human myristoylated ARF1 are used in this work. Full-length ARFGAP1 and its R50K mutant are expressed in SF9 cells by Dr. Richard Premont (Duke Univesity) (125,138). The other constructs are expressed in bacterial systems.The expression constructs of [1-257]ARFGAP1, [1-257]ARFGAP1[L207D] and [1-415]ARFGAP1[L207D/V279D] are from Dr. Bruno Antonny (Institut de Pharmacologie Moleculaire et Cellulaire). (77,79) The expression constructs of [Δ17]ARF1 and [1-136]ARFGAP1 are from Dr. Jonathan Goldberg (Memorial Sloan-Kettering Cancer Center). (21) The single colonies of mysritoylated ARF1 are from Dr. Paul Randazzo (National Cancer Institute). (139,140) All the proteins were expressed and purified according to literature protocols.(21,77,125,139)

2.3.2 Small molecule pulldown assay and western blot The small molecule affinity matrix was prepared according to the literature. (123) Purified ARFGAP1 was added to the packed affinity matrix (30 μl), and bead buffer [50 mM TrisHCl (pH 7.4), 5 mM NaF, 250 mM NaCl, 5 mM EDTA, 5 mM EGTA, and 0.1% Nonidet P-40] was added up to a final volume of 600 μl. After rotating at 4 °C for 2 h, the mixture was centrifuged at 14,000 g for 1 min at 4 ℃, and the supernatant was removed. The affinity matrix was then washed (six times) with cold bead buffer and eluted by boiling with Laemmli sample buffer (60 μL) at 95 ℃ for 5 min. Samples were loaded and separated on a 4–20% Tris-glycine gel (Invitrogen). The proteins were detected by coomassie blue staining and western blot against anti- ARFGAP1 antibody (Santa Cruz).

2.3.3 Measurement of binding affinities by SPR BIACore 3000 instrument (BIACore, GE) was used in this study. The CM5 sensor chip was activated by running through a 1:1 mixture of N-hydroxysuccinimide (0.05 M) and 1-ethyl-3-(3-dimethylaminopropyl) carbodiimide (0.2 M) at 10 μl/min for 7 min. Purified full-length ARFGAP1, ARFGAP1[R50K], [1-136]ARFGAP1, [1-257]ARFGAP1, or [1-257]ARFGAP1[L207D] [100 μg/ml in 10 mM KAc (pH 5.0)] or [1-415]ARFGAP1[L207D/V279D] [100 μg/ml in 10 mM KAc (pH 4.0)] was then injected for 10 min at 10 μl/min to covalently immobilize it to the CM5 chip surface. The control channel was treated in the same way but without protein immobilized. Ethanolamine (1.0 M, pH 8.5) was injected for 7 min to block the unreacted surface. The CM5 chip surface was equilibrated in HBS-EP buffer (0.01 M Hepes, 0.15 M NaCl, 3 mM EDTA, and 0.005% surfactant P20, pH 7.4). QS11 was then injected for 3 min at increasing concentrations (0, 156, 312, 625, 1,250, 2,500, 5,000, 8,000 and 10,000 nM) in HBS-EP buffer with a flow rate of 20 μl/min, and dissociation of ARFGAP1-QS11 complexes was followed for 10 min. The surface was regenerated with 10 mM glycine (pH 2.5). Data from at least two independent titration experiments were averaged. Data in the control channel were subtracted from that in the corresponding protein channel. Data resulted from DMSO injection were further subtracted from those derived from QS11 injections. The data were analyzed by fitting into a one-site specific binding mode to calculate the binding affinities using Graphpad Prism 5.

2.3.4 Liposome Lipids in chloroform or in powder were purchased from Avanti Polar Lipids. A lipid film containing (mole percent [Note]) PC (35%), PE (19%), PS (5%), PI (10%), cholesterol (16%), and 1,2-DAG (15%) was prepared by evaporation under

argon steam for 1 h and followed by drying under vacuum for 1 h. The film was resuspended in buffer [50 mM Hepes (pH 7.5), 120 mM KAc, 3 mM MgCl$_2$, 2 mM EDTA and 1 mM DTT] and hydrated at for 0.5 h. (77,79) The mixtures were freezed and thawed in ethanol/dry ice and warm water batch five times, and then extrude through (pore size) 0.03 μm polycarbonate filters using a hand extruder (Avanti). (Note: mole percent is the ratio of the moles of a substance in a mixture to the moles of the mixture).

2.3.5 Radio active GTP hydrolysis assay Myristoylated ARF1 (800 nM) is activated in buffer [50 mM Hepes (pH 7.5), 120 mM KAc, 1 mM MgCl$_2$, 1 mM DTT, 2.4 μM GTP, 800 nM [γ^{32}P] GTP (specific activity = 6, 000-3, 000 Ci/mmol), 2 μM EDTA and 0.2 mM liposome] for 40 min at room temperature. Then, 2 mM MgCl$_2$ was added to stabilize myristoylated ARF-GTP. The so-formed myristoylated ARF-GTP is stable on ice for up to two days. The GTP hydrolysis was initiated by adding ARFGAP1, stopped by diluting with ice cold buffer [50 mM Hepes (pH 7.5), 120 mM KAc, 3 mM MgCl$_2$, 3 mM EDTA, 1 mM DTT), and separated by filtration through BA 85 with pore size at 0.45 μm (Millipore). The radioactivity of the membrane-bound [γ^{32}P] GTP was measured by a scintillation counter. For IC$_{50}$ measurement, ARFGAP1 was pretreated with QS11 or DMSO in buffer [50 mM Hepes (pH 7.5), 120 mM KAc, 3 mM MgCl$_2$, 3 mM EDTA, 1 mM DTT, 50 μg/ml BSA). After incubation at room temperature for 10 min, ARFGAP1 and QS11 mixture was added to myristoylated ARF-GTP at a 1:1 ratio to initiate the hydrolysis. The reactions were incubated at indicated time, stopped and analyzed as described above.

2.3.6 Secondary structure measurements by circular dichroism CD spectroscopy was performed on a Chirascan Spectropolarimeter Plus (Applied

Photophysics). The proteins were dialyzed against buffer [10 mM Tris pH 7.5, 150 mM KCl and 1 mM DTT] at 4 °C overnight. The experiments were performed at room temperature in a HELLMA quartz cell with an optical path length of 0.1 cm. Each spectrum was recorded from 200 to 260 nm with a bandwidth of 1 nm and a speed of 1.25 s per point. QS11 (10 μM) was added to a mixture of ARFGAP1 and liposome and the spectrum was recorded after incubation for 10 min. Control spectra of liposome or QS11 in buffer were subtracted from the protein spectra.

2.3.7 Golgi localization of ARFGAP1 in the presence of QS11 The procedures were similar as previously described (18). Briefly, GFP-[1-415]ARFGAP1 was transfected into NIH3T3 cells. The cells were cultured at 37 °C with 5% CO_2 for 24 h before QS11 (2 μM) or QS11NC (2 μM) were added. After another 24 h, the cells were fixed for confocal microscopy.

2.3.8 Chemical synthesis DIAD (2.58 ml, 26.25 mmol) was added dropwise to a mixture of biphenyl-4-ylmethanol (2.42 g, 26.25 mmol), 2,6-dichloro-9H-purine (2.36 g, 25 mmol) and PPh3 (3.36 g, 26.25 mmol) in THF (100 ml). The resulting mixture was heated to 75 °C (oil bath temperature) for overnight before it was cooled and diluted with CHCl3 (50 ml). The layers were separated and the organic fraction was washed with H_2O and brine, dried over Na_2SO_4, and concentrated under vacuum. The residue was purified by flash column chromatography over silica gel to give 9-[(1,1'-biphenyl)-4-ylmethyl]-2,6-dichloro-9H-purine (5.68 g, 16 mmol, 64%).

The commercially available amine-containing building block (0.62 mmol) was then added into 9-[(1,1'-biphenyl)-4-ylmethyl]-2,6-dichloro-9H-purine (200 mg, 0.56 mmol) in the presence of diisopropylethylamine (193 μl, 1.1 mmol) in *t*-butanol (2 ml) at

room temperature. After stirring at 80 ℃ overnight, the reaction mixture was cooled and diluted with CHCl$_3$ (10 ml). The layers were separated and the organic fraction was washed with H$_2$O and brine, dried over Na$_2$SO$_4$, and concentrated under vacuum. The residue was purified by flash column chromatography over silica gel to give compound **3**.

Next, compound **3** (0.05 mmol) was mixted with commercial available phenol derivatives (0.18 mmol) in the presence of tris(dibenzylideneacetone)dipalladium (2.3 mg, 0.002 mmol) and di-*tert*-butyl(phenyl)phosphine (2 mg, 0.0045 mmol) under reflux conditions for 2 h. The reaction mixture was diluted with CHCl$_3$ (100 ml) and the layers were separated. The organic layer was washed with H$_2$O and brine, dried over Na$_2$SO$_4$ and concentrated under vacuum. The residue was purified by flash column chromatography over silica gel to generate the final analog **4**.

2.3.9 Calculation of ClogP Chemdraw software was employed to estimate the ClogP value of each analog.

2.3.10 NMR and mass analysis Each analog was dissolved in deuterated chloroform and the proton NMR signal were determined with a Inova 400 MHz NMR spectrometer. The analogs were also analyzed with MALDI-TOF Mass Spectrometry with alpa-cyano-4-hydroxycinnamic acid as the matrix..

9-(biphenyl-4-ylmethyl)-2,6-dichloro-9H-purine (2): (5.68 g, 16 mmol, 64%). ^{1}H NMR (400 MHz, CDCl$_3$) δ 8.09 (s, 1H), 7.62-7.57 (m, 4H), 7.55-7.38 (m, 5H), 5.45 (s, 2H).

(S)-2-(9-(biphenyl-4-ylmethyl)-2-chloro-9H-purin-6-ylamino)-3-phenylpropan-1-ol (B0): (144.75 mg, 0.31 mmol, 55%). ^{1}H NMR (400 MHz, CDCl$_3$) δ 7.64-7.54 (m, 5H), 7.44-7.18 (m, 10H), 7.00-6.97 (m, 1H), 5.38-5.28 (m, 2H), 4.58 (br. s, 1H), 3.90-3.88 (m, 1H), 3.74-3.71 (m, 1H), 3.06-2.96 (m, 2H).

2-(2-(9-(biphenyl-4-ylmethyl)-2-chloro-9H-purin-6-ylamino)ethylamino)ethyl acetate (B1): (97.44 mg, 0.21 mmol, 36%). ^{1}H NMR (400 MHz, CDCl$_3$) δ 7.89-7.84 (m, 1H), 7.56-7.54 (m, 4H), 7.44-7.28 (m, 5H), 5.35 (s, 2H), 4.25 (s, 2H), 3.79 (s, 2H), 3.68-3.65 (m, 4H), 2.63 (s, 1H), 2.19-2.06 (m, 4H), 2.01 (m, 3H), 1.26 (m, 2H).

9-(biphenyl-4-ylmethyl)-2-chloro-N-(naphthalen-1-ylmethyl)-9H-purin-6-amine (B2): (261.25 mg, 0.55 mmol, 99%). ^{1}H NMR (400 MHz, CDCl$_3$) δ 8.08-8.07 (m, 1H), 7.85-7.82 (m, 2H), 7.56-7.27 (m, 14H), 6.62 (br. s, 1H), 5.28-5.22 (m, 2H).

9-(biphenyl-4-ylmethyl)-2-chloro-N-phenethyl-9H-purin-6-amine (B3): (237.06 mg, 0.54 mmol, 97%). ^{1}H NMR (400 MHz, CDCl$_3$) δ 7.59-7.55 (m, 5H), 7.46-7.42 (m, 2H), 7.38-7.22 (m, 9H), 6.01 (br. s, 1H), 5.35 (s, 2H), 3.91 (br. s, 1H), 3.01-2.97 (m, 2H).

(S)-2-(9-(biphenyl-4-ylmethyl)-2-chloro-9H-purin-6-ylamino)butan-1-ol (B4): (219.78 mg, 0.54 mmol, 96%). ^{1}H NMR (400 MHz, CDCl$_3$) δ 7.66-7.54 (m, 4H), 7.45-7.41 (m, 2H), 7.37-7.33 (m, 3H), 7.07 (br. s, 1H), 5.39-5.23 (m, 2H), 4.33 (br. s, 1H), 4.00-3.96(m, 1H), 3.75-3.71 (m, 1H), 1.76-1.62 (m, 2H), 1.01-0.97 (m, 3H).

(S)-methyl 2-(9-(biphenyl-4-ylmethyl)-2-chloro-9H-purin-6-ylamino)-3-phenylpropanoate (B5): (168.98 mg, 0.34 mmol, 60%). ^{1}H NMR (400 MHz, CDCl$_3$) δ

7.70 (s, 1H), 7.59-7.55 (m, 4H), 7.46-7.41 (m, 2H), 7.37-7.34 (m, 3H), 7.30-7.15 (m, 7H), 6.39 (br. s, 1H), 5.34 (s, 2H), 4.12-4.09 (m, 1H), 3.74 (s, 3H), 3.32-3.22 (m, 2H).

(S)-2-(2-(benzo[*d*][1,3]dioxol-5-yloxy)-9-(biphenyl-4-ylmethyl)-9H-purin-6-ylamino)-3-phenylpropan-1-ol (B0C1): (26.28 mg, 0.046 mmol, 92%). ^{1}H NMR (400 MHz, CDCl$_3$) δ 7.60-7.54 (m, 5H), 7.43 (t, *J* = 7.4 Hz, 2H), 7.38-7.32 (m, 3H), 7.11-7.22 (m, 3H), 7.01 (s, 1H), 6.90 (s, 1H), 6.81-6.83 (d, *J* = 8.0 Hz, 1H), 6.74 (s, 1H), 6.88 (dd, *J* = 8.0, 4.0 Hz, 1H), 5.95 (d, *J* = 20 Hz, 2H), 5.25 (t, *J* = 18 Hz, 2H), 4.31 (br. s, 1H), 3.78-3.59 (m, 2H), 2.96 (dd, *J* = 14.0, 6.0 Hz, 1H). MALDI-MS: *m/z* 572.2 (M + H)[+].

(S)-2-(9-(biphenyl-4-ylmethyl)-2-(naphthalen-2-yloxy)-9H-purin-6-ylamino)-3-phenylpropan-1-ol (B0C2): (25.98 mg, 0.045 mmol, 90%). ^{1}H NMR (400 MHz, CDCl$_3$) δ 7.87-7.80 (m, 3H), 7.67 (s, 1H), 7.59-7.33 (m, 13H), 7.11 (s, 1H), 7.00 (s, 1H), 6.82 (s, 2H), 6.68 (s, 2H), 5.32-5.23 (m, 2H), 4.68 (s, 1H), 4.13 (s, 1H), 3.64-3.52 (m, 2H), 2.91-2.61 (m, 2H). MALDI-MS: *m/z* 578.3 (M + H)[+].

(S)-2-(9-(biphenyl-4-ylmethyl)-2-(naphthalen-1-yloxy)-9H-purin-6-ylamino)-3-phenylpropan-1-ol (B0C3): (25.98 mg, 0.045 mmol, 90%). ^{1}H NMR (400 MHz, CDCl$_3$) δ 8.02-7.77 (m, 3H), 7.51-7.36 (m, 15H), 7.15 (s, 3H), 6.83 (s, 2H), 6.47 (s, 1H), 5.22 (s, 2H), 4.04 (br. s, 1H), 3.41 (m, 1H), 2.75 (s, 2H). MALDI-MS: *m/z* 578.3 (M + H)[+].

(S)-2-(9-(biphenyl-4-ylmethyl)-2-(3-(trifluoromethyl)phenoxy)-9H-purin-6-ylamino)-3-phenylpropan-1-ol (B0C4): (23.80 mg, 0.040 mmol, 80%). ^{1}H NMR (400 MHz, CDCl$_3$) δ 7.67 (s, 1H), 7.55-7.51 (m, 7H), 7.46-7.33 (m, 6H), 7.22-7.18 (m, 2H), 7.05 (s, 2H), 6.50 (s, 1H), 5.25 (d, *J* = 12.0 Hz, 2H), 4.32 (s, 1H), 3.75 (d, *J* = 12.0 Hz, 1H), 3.64 (dd, *J* = 12.0, 4.0 Hz, 1H), 2.94-2.92 (m, 3H), 2.63 (s, 0.71). MALDI-MS: *m/z* 596.2 (M + H)[+].

(S)-2-(9-(biphenyl-4-ylmethyl)-2-(3-methoxyphenoxy)-9H-purin-6-ylamino)-3-phenylpropan-1-ol (B0C5): (25.08 mg, 0.045 mmol, 90%). ^{1}H NMR (400 MHz, CDCl$_3$) δ 7.62-7.56 (m, 5H), 7.46-7.43 (m, 2H), 7.37-7.26 (m, 4H), 7.22-7.15 (m, 3H), 7.03 (s, 2H), 5.35-5.20 (m, 2H), 4.30 (br. s, 1H), 3.77-3.71 (m, 4H), 3.63-3.59 (m, 1H), 2.96 (dd, J = 12.0, 8.0 Hz, 1H), 2.89-2.84 (m, 1H). MALDI-MS: m/z 558.2 (M + H)$^+$.

2-(2-(9-(biphenyl-4-ylmethyl)-2-(2,3-dihydro-1H-inden-5-yloxy)-9H-purin-6-ylamino)ethylamino)ethanol (B1C0): (18.20 mg, 0.035 mmol, 70%). ^{1}H NMR (400 MHz, CDCl$_3$) δ 7.56-7.54 (m, 1H), 7.44-7.42 (m, 4H), 7.37-7.35 (m, 2H), 7.35-7.34 (m, 3H), 7.22-7.20 (m, 1H), 7.09-7.07 (m, 1H), 7.00-6.96 (m, 1H), 5.26-5.22 (m, 2H), 3.82-3.68 (m, 4H), 3.51-3.40 (m, 4H), 2.92 (s, 4H). MALDI-MS: m/z 521.3 (M + H)$^+$.

2-(2-(2-(benzo[d][1,3]dioxol-5-yloxy)-9-(biphenyl-4-ylmethyl)-9H-purin-6-ylamino)ethylamino)ethanol (B1C1): (17.29 mg, 0.033 mmol, 65%). ^{1}H NMR (400 MHz, CDCl$_3$) δ 7.68-7.67 (m, 1H), 7.57-7.55 (m, 4H), 7.46-7.42 (m, 2H), 7.37-7.35 (m, 3H), 6.78-6.73 (m, 2H), 6.66-6.58 (m, 1H), 6.01 (s, 2H), 5.25-5.22 (m, 2H), 3.80-3.67 (m, 5H), 3.54-3.44 (m, 4H), 2.16 (s, 2H), 2.02 (s, 2H). MALDI-MS: m/z 525.5 (M + H)$^+$.

2-(2-(9-(biphenyl-4-ylmethyl)-2-(naphthalen-2-yloxy)-9H-purin-6-ylamino)ethylamino)ethanol (B1C2): (18.03 mg, 0.034 mmol, 68%). ^{1}H NMR (400 MHz, CDCl$_3$) δ 7.85-7.80 (m, 3H), 7.70-7.63 (m, 2H), 7.56-7.26 (m, 12H), 5.25 (s, 2H), 3.99 (s, 1H), 3.77 (s, 1H), 3.64-3.44 (m, 4H), 3.27-3.08 (m, 2H), 2.02-1.98 (m, 4H).

2-(2-(9-(biphenyl-4-ylmethyl)-2-(3-methoxyphenoxy)-9H-purin-6-ylamino)ethylamino)ethanol (B1C5): (18.88 mg, 0.037 mmol, 73%). ^{1}H NMR (400 MHz, CDCl$_3$) δ 7.65-7.64 (m, 1H), 7.57-7.55 (m, 4H), 7.46-7.42 (m, 2H), 7.37-7.29 (m,

4H), 6.85-6.76 (m, 3H), 5.26-6.23 (m, 2H), 3.79-3.68 (m, 7H), 3.51-3.38 (m, 4H). MALDI-MS: *m/z* 511.2 (M + H)$^+$.

9-(biphenyl-4-ylmethyl)-2-(2,3-dihydro-1H-inden-5-yloxy)-N-(naphthalen-1-ylmethyl)-9H-purin-6-amine (B2C0): (27.52 mg, 0.048 mmol, 95%). ^{1}H NMR (400 MHz, CDCl$_3$) δ 8.02-8.00 (m, 1H), 7.85-7.77 (m, 2H), 7.56-7.27 (m, 15H), 7.18-7.09 (m, 2H), 7.03-7.01 (m, 1H), 6.21 (s, 1H), 5.28-5.09 (m, 4H), 2.89-2.85 (m, 4H), 2.09-2.04 (m, 2H). MALDI-MS: *m/z* 574.3 (M + H)$^+$.

2-(benzo[d][1,3]dioxol-5-yloxy)-9-(biphenyl-4-ylmethyl)-N-(naphthalen-1-ylmethyl)-9H-purin-6-amine (B2C1): (27.71 mg, 0.048 mmol, 96%). ^{1}H NMR (400 MHz, CDCl$_3$) δ 8.02-8.00 (m, 1H), 7.86-7.78 (m, 2H), 7.55-7.27 (m, 16H), 6.80-6.76 (m, 3H), 6.35 (s, 1H), 5.98-5.95 (m, 2H), 5.27-5.21 (m, 2H), 5.10 (s, 2H). MALDI-MS: *m/z* 578.2 (M + H)$^+$.

9-(biphenyl-4-ylmethyl)-N-(naphthalen-1-ylmethyl)-2-(naphthalen-2-yloxy)-9H-purin-6-amine (B2C2) (28.59 mg, 0.049 mmol, 98%).: ^{1}H NMR (400 MHz, CDCl$_3$) δ 7.96-7.94 (m, 1H), 7.85-7.69 (m, 6H), 7.55-7.20 (m, 17H), 6.42 (s, 1H), 5.18 (s, 2H), 5.05 (s, 2H). MALDI-MS: *m/z* 584.2 (M + H)$^+$.

9-(biphenyl-4-ylmethyl)-N-(naphthalen-1-ylmethyl)-2-(naphthalen-1-yloxy)-9H-purin-6-amine (B2C3): (28.59 mg, 0.049 mmol, 97%). ^{1}H NMR (400 MHz, CDCl$_3$) δ 8.09-8.07 (m, 1H), 7.91-7.73 (m, 5H), 7.52-7.34 (m, 16H), 7.20-7.15 (m, 4H), 6.22 (s, 1H), 5.15 (s, 2H), 4.93 (s, 2H). MALDI-MS: *m/z* 584.2 (M + H)$^+$.

9-(biphenyl-4-ylmethyl)-N-(naphthalen-1-ylmethyl)-2-(3-(trifluoromethyl)phenoxy)-9H-purin-6-amine (B2C4): (26.45 mg, 0.044 mmol, 87%). ^{1}H NMR (400 MHz, CDCl$_3$)

δ 8.01-7.98 (m, 1H), 7.88-7.80 (m, 2H), 7.56-7.26 (m, 17H), 6.26 (s, 1H), 5.23 (s, 2H), 5.08 (s, 2H). MALDI-MS: *m/z* 602.2 (M + H)$^+$.

9-(biphenyl-4-ylmethyl)-2-(3-methoxyphenoxy)-N-(naphthalen-1-ylmethyl)-9H-purin-6-amine (B2C5): (26.47 mg, 0.047 mmol, 93%). ^{1}H NMR (400 MHz, CDCl$_3$) δ 8.01-7.99 (m, 1H), 7.86-7.77 (m, 2H), 7.54-7.24 (m, 14H), 6.89-6.74 (m, 3H), 6.35 (s, 1H), 5.24 (s, 2H), 5.09 (s, 2H), 3.75 (s, 3H). MALDI-MS: *m/z* 564.2 (M + H)$^+$.

9-(biphenyl-4-ylmethyl)-2-(2,3-dihydro-1H-inden-5-yloxy)-N-phenethyl-9H-purin-6-amine (B3C0): (25.79 mg, 0.048 mmol, 96%). ^{1}H NMR (400 MHz, CDCl$_3$) δ 7.63 (s, 1H), 7.57-7.55 (m, 4H), 7.46-7.42 (m, 2H), 7.37-7.34 (m, 3H), 7.28-7.18 (m, 3H), 7.11-7.08 (m, 2H), 7.02-7.00 (m, 2H), 6.07 (br. s, 1H), 5.26 (s, 2H), 3.69 (br. s, 2H), 2.95-2.87 (m, 6H), 2.13-2.04 (m, 2H). MALDI-MS: *m/z* 538.3 (M + H)$^+$.

2-(benzo[d][1,3]dioxol-5-yloxy)-9-(biphenyl-4-ylmethyl)-N-phenethyl-9H-purin-6-amine (B3C1): (25.44 mg, 0.047 mmol, 93%). ^{1}H NMR (400 MHz, CDCl$_3$) δ 7.63 (s, 1H), 7.57-7.55 (m, 3H), 7.46-7.42 (m, 2H), 7.37-7.30 (m, 3H), 7.28-7.13 (m, 3H), 6.83-6.81 (m, 2H), 6.79-6.72 (m, 1H), 5.26 (m, 2H), 3.72 (br. s, 2H), 2.89 (s, 2H). MALDI-MS: *m/z* 542.2 (M + H)$^+$.

9-(biphenyl-4-ylmethyl)-2-(naphthalen-2-yloxy)-N-phenethyl-9H-purin-6-amine (B3C2): (26.27 mg, 0.048 mmol, 96%). ^{1}H NMR (400 MHz, CDCl$_3$) δ 7.90-7.81 (m, 3H), 7.70 (s, 1H), 7.64 (s, 1H), 7.55-7.32 (m, 12H), 7.12 (m, 3H), 6.91 (br. s, 2H), 5.25 (s, 2H), 3.64 (s, 2H), 2.82 (s, 2H). MALDI-MS: *m/z* 548.2 (M + H)$^+$.

9-(biphenyl-4-ylmethyl)-2-(naphthalen-1-yloxy)-N-phenethyl-9H-purin-6-amine (B3C3): (26.27 mg, 0.048 mmol, 96%). ^{1}H NMR (400 MHz, CDCl$_3$) δ 8.05-8.03 (m, 1H), 7.92-7.90 (m, 1H), 7.78-7.76 (m, 1H), 7.44-7.34 (m, 12H), 7.26-7.15 (m, 6H), 6.91 (s,

2H), 5.94 (br. s, 1H), 5.17 (s, 2H), 3.54 (s, 2H), 2.67 (s, 2H). MALDI-MS: *m/z* 548.2 (M + H)$^+$.

9-(biphenyl-4-ylmethyl)-N-phenethyl-2-(3-(trifluoromethyl)phenoxy)-9H-purin-6-amine (B3C4): (25.43 mg, 0.045 mmol, 90%). ^{1}H NMR (400 MHz, CDCl$_3$) δ 7.62-7.42 (m, 11H), 7.37-7.32 (m, 3H), 7.24-7.18 (m, 2H), 7.09 (br. s, 2H), 5.25 (s, 2H), 3.70 (s, 2H), 2.86 (s, 2H). MALDI-MS: *m/z* 566.2 (M + H)$^+$.

9-(biphenyl-4-ylmethyl)-2-(3-methoxyphenoxy)-N-phenethyl-9H-purin-6-amine (B3C5): (24.25 mg, 0.046 mmol, 92%). ^{1}H NMR (400 MHz, CDCl$_3$) δ 7.61-7.54 (m, 5H), 7.45-7.42 (m, 2H), 7.35-7.32 (m, 3H), 7.28-7.25 (m, 4H), 7.21-7.18 (m, 1H), 7.11 (br. s, 2H), 6.87-6.77 (m, 3H), 5.95 (br. s, 1H), 5.25 (s, 2H), 3.80 (s, 3H), 3.72-3.70 (m, 2H), 2.87 (s, 2H). MALDI-MS: *m/z* 528.2 (M + H)$^+$.

(S)-2-(9-(biphenyl-4-ylmethyl)-2-(2,3-dihydro-1H-inden-5-yloxy)-9H-purin-6-ylamino)butan-1-ol (B4C0): (22.74 mg, 0.045 mmol, 90%). ^{1}H NMR (400 MHz, CDCl$_3$) δ 7.58-7.53 (m, 4H), 7.43-7.31 (m, 5H), 7.21-7.19 (m, 1H), 7.05 (s, 1H), 6.97-6.95 (m, 1H), 6.21 (br. s, 1H), 5.21 (s, 2H), 4.03 (br. s, 1H), 3.76-3.64 (m, 3H), 2.91 (s, 4H), 2.11-2.09 (m, 2H), 1.62-1.58 (m, 2H), 0.94-0.88 (m, 3H). MALDI-MS: *m/z* 506.3 (M + H)$^+$.

(S)-2-(2-(benzo[d][1,3]dioxol-5-yloxy)-9-(biphenyl-4-ylmethyl)-9H-purin-6-ylamino)butan-1-ol (B4C1): (22.91 mg, 0.045 mmol, 91%). ^{1}H NMR (400 MHz, CDCl$_3$) δ 7.60-7.54 (m, 5H), 7.45-7.41 (m, 2H), 7.36-7.32 (m, 3H), 6.81-6.79 (m, 1H), 6.74 (m, 1H), 6.67-6.65 (m, 1H), 6.34 (br. s, 1H), 5.99 (s, 2H), 5.21 (s, 2H), 4.06 (br. s, 1H), 3.77-3.63 (m, 2H), 1.61 (m, 2H), 0.87-0.83 (m, 3H). MALDI-MS: *m/z* 510.2 (M + H)$^+$.

(S)-2-(9-(biphenyl-4-ylmethyl)-2-(naphthalen-2-yloxy)-9H-purin-6-ylamino)butan-1-ol (B4C2): (24.22 mg, 0.047 mmol, 93%). ^{1}H NMR (400 MHz, CDCl$_3$) δ 7.87-7.85 (m,

2H), 7.80-7.78 (m, 1H), 7.63-7.61 (m, 2H), 7.53-7.34 (m, 10H), 7.30-7.28 (m, 2H), 6.20 (br. s, 1H), 5.19 (s, 2H), 3.76 (br. s 1H), 3.62-3.58 (m, 2H), 1.69 (m, 2H), 0.91 (m, 3H). MALDI-MS: m/z 516.2 (M + H)$^+$.

(S)-2-(9-(biphenyl-4-ylmethyl)-2-(naphthalen-1-yloxy)-9H-purin-6-ylamino)butan-1-ol (B4C3): (24.73 mg, 0.048 mmol, 95%). ^{1}H NMR (400 MHz, CDCl$_3$) δ 7.36 (s, 1H), 7.56-7.54 (m, 4H), 7.45-7.42 (m, 2H), 7.35-7.26 (m, 4H), 6.83-6.77 (m, 3H), 6.24 (br. s, 1H), 5.23 (s, 2H), 4.04 (br. s, 1H), 3.78 (s, 5H), 3.66-3.61 (m, 2H), 2.63 (s, 1H), 1.63 (m, 2H), 0.93 (m, 3H). MALDI-MS: m/z 516.2 (M + H)$^+$.

(S)-2-(9-(biphenyl-4-ylmethyl)-2-(3-methoxyphenoxy)-9H-purin-6-ylamino)butan-1-ol (B4C5): (22.28 mg, 0.045 mmol, 90%). ^{1}H NMR (400 MHz, CDCl$_3$) δ 7.99-7.97 (m, 1H), 7.90-7.80 (m, 1H), 7.75-7.73 (m, 1H), 7.63-7.26 (m, 13H), 7.25-7.17 (m, 2H), 6.25 (br. s, 1H), 5.09 (s, 2H), 3.78-3.48 (m, 3H), 2.63 (s, 1H), 1.77 (m, 2H), 0.93 (m, 3H). MALDI-MS: m/z 496.2 (M + H)$^+$.

(S)-methyl 2-(9-(biphenyl-4-ylmethyl)-2-(2,3-dihydro-1H-inden-5-yloxy)-9H-purin-6-ylamino)-3-phenylpropanoate (B5C0): (23.80 mg, 0.040 mmol, 80%). ^{1}H NMR (400 MHz, CDCl$_3$) δ 7.65 (s, 1H), 7.57-7.55 (m, 4H), 7.46-7.45 (m, 2H), 7.44-7.43 (m, 3H), 7.24-7.22 (m, 4H), 7.08-7.05 (m, 3H), 6.99-6.97 (m, 1H), 6.26 (br. s, 1H), 5.27 (s, 2H), 5.09 (br. s, 1H), 3.64 (s, 3H), 3.15 (s, 2H), 2.94 (s, 4H), 2.15-2.09 (m, 2H). MALDI-MS: m/z 596.3 (M + H)$^+$.

(S)-methyl 2-(2-(benzo[d][1,3]dioxol-5-yloxy)-9-(biphenyl-4-ylmethyl)-9H-purin-6-ylamino)-3-phenylpropanoate (B5C1): (21.02 mg, 0.035 mmol, 78%). ^{1}H NMR (400 MHz, CDCl$_3$) δ 7.65 (s, 1H), 7.57-7.55 (m, 4H), 7.46-7.45 (m, 2H), 7.44-7.43 (m, 3H),

7.24-7.22 (m, 5H), 7.08 (s, 2H), 6.75-6.66 (m, 3H), 6.22 (br. s, 1H), 5.99 (m, 2H), 5.26 (s, 2H), 5.03 (br. s, 1H), 3.66 (s, 3H), 3.16 (s, 2H). MALDI-MS: *m/z* 600.2 (M + H)$^+$.

(S)-methyl 2-(9-(biphenyl-4-ylmethyl)-2-(naphthalen-2-yloxy)-9H-purin-6-ylamino)-3-phenylpropanoate (B5C2): (24.20 mg, 0.040 mmol, 80%). ^{1}H NMR (400 MHz, CDCl$_3$) δ 7.88-7.86 (m, 2H), 7.82-7.81 (m, 1H), 7.61-7.29 (m, 14H), 6.96-6.84 (m, 3H), 6.84 (s, 2H), 6.82 (m, 1H), 6.33 (br. s, 1H), 5.25 (s, 2H), 4.96 (s, 1H), 3.98 (s, 1H), 3.54 (s, 3H), 3.09 (s, 2H). MALDI-MS: *m/z* 606.2 (M + H)$^+$.

(S)-methyl 2-(9-(biphenyl-4-ylmethyl)-2-(naphthalen-1-yloxy)-9H-purin-6-ylamino)-3-phenylpropanoate (B5C3): (25.11 mg, 0.041 mmol, 83%). ^{1}H NMR (400 MHz, CDCl$_3$) δ 8.01-7.99 (m, 1H), 7.92-7.90 (m, 1H), 7.78-7.76 (m, 1H), 7.52-7.31 (m, 13H), 7.18-7.10 (m, 3H), 6.91 (s, 2H), 6.19 (br. s, 1H), 5.19 (s, 2H), 4.78 (s, 1H), 3.52 (s, 3H), 2.93 (s, 2H). MALDI-MS: *m/z* 606.2 (M + H)$^+$.

(S)-methyl 2-(9-(biphenyl-4-ylmethyl)-2-(3-methoxyphenoxy)-9H-purin-6-ylamino)-3-phenylpropanoate (B5C5): (23.99 mg, 0.041 mmol, 82%). ^{1}H NMR (400 MHz, CDCl$_3$) δ 7.55 (s, 1H), 7.46-7.44 (m, 4H), 7.37-7.34 (m, 2H), 7.32-7.28 (m, 8H), 7.07 (s, 2H), 6.83-6.79 (m, 3H), 6.24 (br. s, 1H), 5.26 (s, 2H), 5.03 (br. s, 1H), 3.79 (s, 3H), 3.65 (s, 3H), 3.15 (s, 2H). MALDI-MS: *m/z* 586.2 (M + H)$^+$.

2.4 Conclusion

Small GTPases ARFs and their effectors ARFGAPs and ARFGEFs have emerged to be therapeutic targets for many cancers and neurological diseases. (5,138,141,142) However, there are limited small molecule regulators of these families of proteins. In this study, we report the characterization of one small molecule ARFGAP inhibitor, QS11, and the molecular basis of its inhibition. QS11 non-competitively inhibits ARFGAP1 activity in ARF-GTP hydrolysis assay (IC$_{50}$ = 4.0 ± 0.5 μM). To our knowledge, this is the first small molecule ARFGAP inhibitor and demonstrates the feasibility of developing small molecules to target ARFGAPs. Interestingly, QS11 inhibits the GAP activity through regulating the unique ALPS motifs, particularly the second ALPS motif in ARFGAP1, instead of the GAP domain. This interesting mechanism provide novel insights into developing more potent and selective ARFGAP inhibitors. Toward that goal, we have synthesized and characterized 31 QS11 analogs. Several analogs showed promising binding affinities and potencies.

2.5 Future Plan

ARFGAP1 contains two ALPS motifs. It will be interesting to know how much each ALPS motif contributes to QS11's binding to ARFGAP1. Consequently, it would be helpful to measure the direct interactions between each ALPS motif and QS11. The information on the interaction between [1-415]ARFGAP1[V279D] and QS11 will also be useful. Since [1-415]ARFGAP1[V279D] maintains the GAP activity of ARFGAP1(77), QS11 could be tested to inhibit its GAP activity. To our knowledge, ALPS motifs are present only in ARFGAP1 among ARFGAPs.(76) However, the Bar domain in ASAP1 plays similar roles as the ALPS motifs in ARFGAP1.(72,81) Is QS11 a specific inhibitor for ARFGAP1, or does it also inhibit other ARFGAPs? It would be very likely to investigate whether QS11 could interact with the Bar domain in ASAP1 and inhibit its GAP activity. ARFGAP1 is also regulated by COPI systems (29,36,126) and interacts with several SNARE proteins and coatomer in a GAP-independent manner.(21,29,36,64,68,85,87,122) Since QS11 does not interact with the catalytic GAP domain, we will test whether these interactions are affected by QS11. In addition, coatomer enhances GAP activity of ARFGAP1(21,68,122,127) while a peptide derived from p24 is shown to inhibit GAP activity in a coatomer-dependent manner.(122) It would also be helpfulto test whether QS11 affects coatomer-dependent GAP activity.

None of 31 QS11 analogs showed improved activity against ARFGAP1. One possibility is that the regions we modified are not the most crucial ones for QS11-ARFGAP1 interactions. Given the critical roles of the biphenyl substitution at the N9 position for activity, we will systematically modify this position to generate more potent ARFGAP inhibitors. Considering that the hydrophobic residues (tryptophan, tyrosine

and phenylalanine) in the ALPS motifs are responsible for their interaction with lipid membranes, we might be able to increase the binding affinity through both hydrophobic interactions and hydrogen bonds by modifying the substitution at the N9 position.

Chapter 3.

High Throughput Fluorescence Polarization Assay for the Enzymatic Activity of ARFGAP[1]

3.1 Introduction

High throughput screening (HTS) has emerged as an integral part of the pharmaceutical industry and academic laboratories for basic discovery and drug development.(143-145) Using robotics, liquid handling devices, sensitive detectors and informatics software, HTS provides an efficient method to investigate large numbers of synthetic compounds or genes in miniaturized assays to identify those capable of modulating a biological target of interest or a particular biomolecular pathway.(146-148) Originally, HTS was primarily utilized by pharmaceutical industry to generate hit compounds for further development. Recently, there are growing numbers of academic researchers who use HTS to identify chemical probes (tool compounds) for basic research.(149-151)

ARFGAP family proteins have 31 members in human.(20) Despite their crucial roles in cell physiologies and human pathologies, no effective small molecule regulators have been reported. The zinc figure motif that is responsible for the catalytic activity of ARFGAPs is highly conserved among ARFGAPs(20,117,118) while each subfamily of ARFGAPs also has distinct functional structures.(20) This provides us a tremendous

---

[1] Part of this chapter is taken directly from *J Biomol Screen*. **2011** Aug; 16(7):717-23.

opportunity to develop both pan inhibitors targeting the GAP domain and selective inhibitors targeting distinct functional structures of ARFGAPs through HTS. However, there is no assay of ARFGAP activity that is amenable for high-throughput screening.

Conventional ARFGAP activity assays have relied on utilization of radiolabeled GTP analogs [α^{32}P] GTP and [γ^{32}P] GTP that behave similarly to the native GTP and can be easily detected(152,153). These methods require separation of GTP from GDP either through thin layer chromatography or a filter-binding approach, which makes them time-consuming and only suitable for terminal measurements. Recently, fluorescent guanine nucleotide derivatives N-methyl-3'-O-anthranoyl (MANT) and BODIPY have been developed(154,155), allowing for G protein assays with greater sensitivity than previous fluorescence assays that relied on detection of changes in intrinsic tryptophan fluorescence. A number of studies have been reported on use of these fluorescent GTP derivatives with low molecular Ras-like G proteins with good sensitivities.(156-159) However, these reagents have not been applied to ARF activity assays. Clearly, a high throughput ARFGAP assay that can be used for development of small molecule regulators is urgently needed.

In our efforts to dissect ARFGAP-regulated cell signaling, a novel fluorescence polarization-based ARFGAP assay has been developed. The Z' factor of the assay is 0.75 in 384-well format. When applied to a pilot screen of the Prestwick library of around 1,000 compounds, the assay demonstrated high reproducibility, reasonable hit rates, and suitability for automation. This represents the first assay of ARFGAP enzymatic activity that is not based on radiolabeled GTP analogs and can be used for large scale screening to generate ARFGAP-selective small molecule inhibitors.

64

3.2 Results and Discussion

3.2.1 Development of a high throughput fluorescence polarization assay for the enzymatic activity of ARFGAP Fluorescence polarization assay(160) has been successfully used to identify small molecule inhibitors of protein-protein interactions. Polarization is a measure of the change in the molecular movement of a labeled species and is defined as the ratio of the difference between the vertical and horizontal components of the emitted light over their sum. Because polarization is a dimensionless value, it is independent of the emitted light or the concentration of the fluorophore. These features make the FP assay suitable for screening compound libraries in a high throughput format to identify small molecule inhibitors.

Recently, the BellBrook Labs have developed a homogenous, fluorescence polarization-based Transcreener Assay for GDP (www.bellbrooklabs.com). Using the same strategy, we have validated a novel fluorescence polarization-based ARFGAP assay with the GAP domain (residues 6-136) of rat ARFGAP1 and human ARF1 lacking its first 17 residues (**Fig 3.1**). The expression constructs were kindly provided by Dr. Jonathan Goldberg (Memorial Sloan-Kettering Cancer Center) and both proteins were expressed and purified using published protocols as described in Chapter two. The purified GAP domain efficiently catalyzed the conversion of ARF1-GTP to ARF1-GDP based on the differential mobility of the two nucleotide-bound forms during native gel electrophoresis (**Fig. 3.2**), demonstrating that both ARFGAP1 and ARF1 are functional. In the fluorescence polarization assay, the GAP activity is measured using a commercially available assay kit (Transcreener assay) based on fluorescence polarization detection of GDP that is generated by the GTP hydrolysis of ARF1. When the fluorescent

tracer binds to the antibody, the fluorescence polarization in mP (milli-polarization) is high. When the tracer is in free form in the solution, the fluorescence polarization is low. As shown in **Fig. 3.3**, the GTP hydrolysis of ARF1 that is catalyzed by ARFGAP1 can be effectively monitored through this method. The fluorescence polarization in mP changed from 250 at the start of the reaction to around 80 when in 4 h (**Fig. 3.3**). Such a big change in mP value will make the assay suitable for screening of small molecule collections.
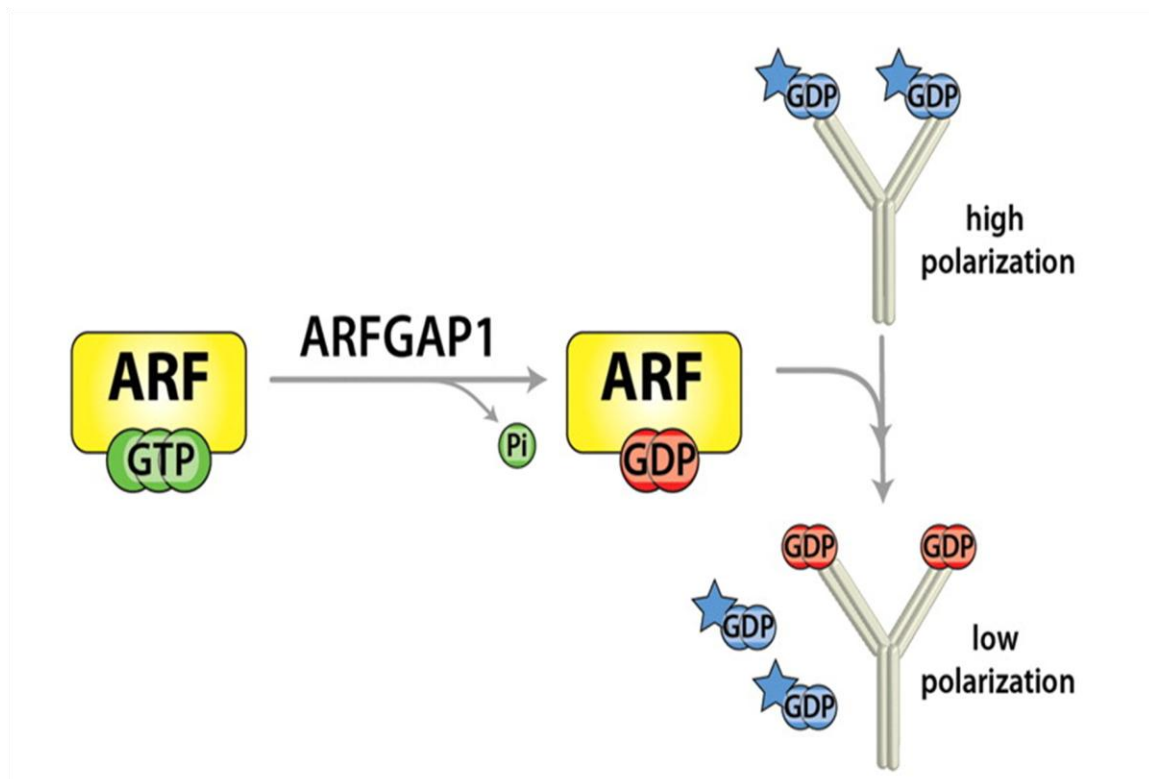
Figure 3.1. Schematic illustration of the assay. The guanosine diphosphate (GDP) that is derived from the guanosine triphosphate (GTP) hydrolysis displaces the fluorescent tracer that binds to antibody against GDP, leading to mP (milli-polarization) decrease.
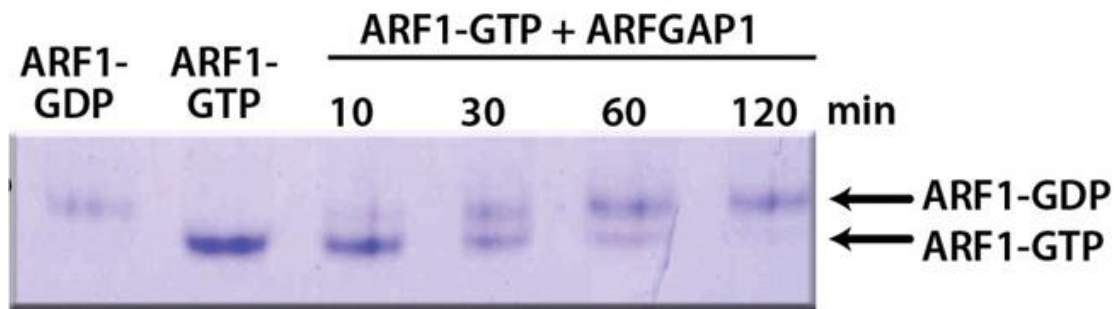
Figure 3.2. GTPase-activating protein (GAP) domain of ARFGAP1 effectively catalyzes the conversion of ARF1-GTP to ARF1-GDP. GAP domain (3.2 μM) was added to ARF1-GTP (16.5 μM) for the indicated times prior to native gel electrophoresis of the samples.
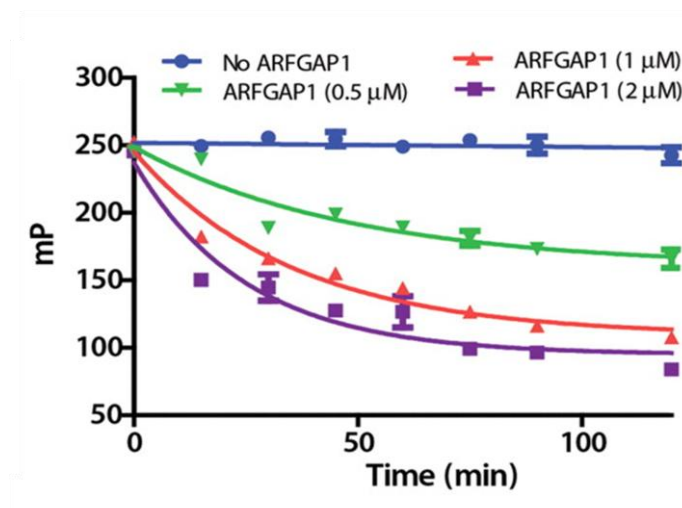
Figure 3.3. Time course reaction of ARF-GTP hydrolysis in FP assay. GAP domain of rat ARFGAP1 (0.5, 1, or 2 μM) was added to ARF1-GTP (2 μM) for the indicated times, and the GDP generated from the GAP reaction was detected through fluorescence polarization according to the manufacturer's instructions. For comparison, the reactions without adding ARFGAP1 were also carried out.

67

To ensure that the assay conditions are applicable for inhibitor development, the kinetics of the ARFGAP1-catalyzed hydrolysis of ARF1-GTP was measured. The amount of hydrolyzed GTP was measured for different concentrations of ARF1-GTP (**Fig. 3.4**) by using radiolabeled [γ32P]GTP. The plot of the initial velocity versus ARF1 concentration was fitted to the Michaelis-Menton equation, and the Km was estimated as 73.4 μM, consistent with the literature value when truncated ARF1 was used. These data collectively suggest that this FP-based assay is suitable for identifying small-molecule inhibitors of ARFGAPs.
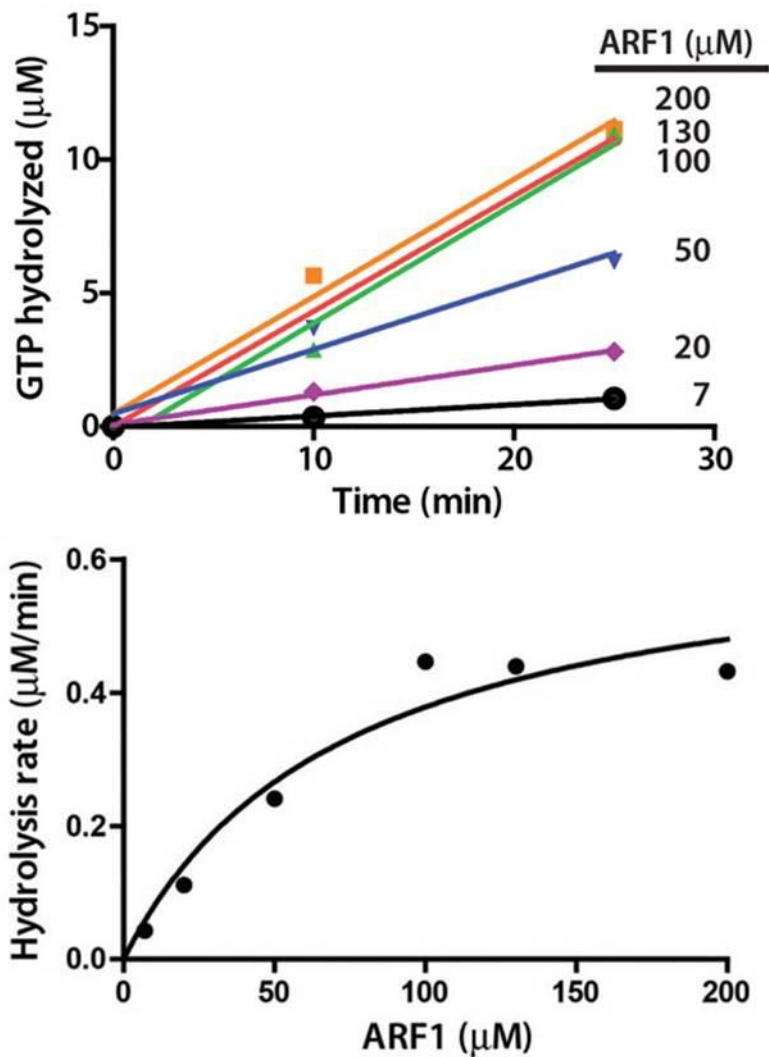
Figure 3.4. The ARFGAP1-catalyzed GTP hydrolysis with different concentrations of ARF1-GTP The plot of the hydrolysis rate versus the ARF1 concentration

69

To correlate the mP changes with percentage of GTP hydrolysis, we generated a standard curve using defined GTP/GDP ratio (**Fig. 3.5**). Under the same conditions, the GTP hydrolysis can be effectively detected up to 15% conversion, suggesting that the assay is ideal for performing ARFGAP assays under initial rate conditions. The amount of enzymes used in the assay significantly changed the rate of hydrolysis, with higher concentration of ARFGAP1 and ARF1 leading to more rapid mP change (data not shown). This feature makes it feasible to complete the assay in a time window that is sufficient for sample and plate handling by the screening facility while still achieve maximal signal-to-background signal. Finally, the ARF1-GTP was purified through a desalting column and was used in the assay; similar kinetics profile was observed (data not shown) indicating that the free GTP does not have significant impacts on the assay.
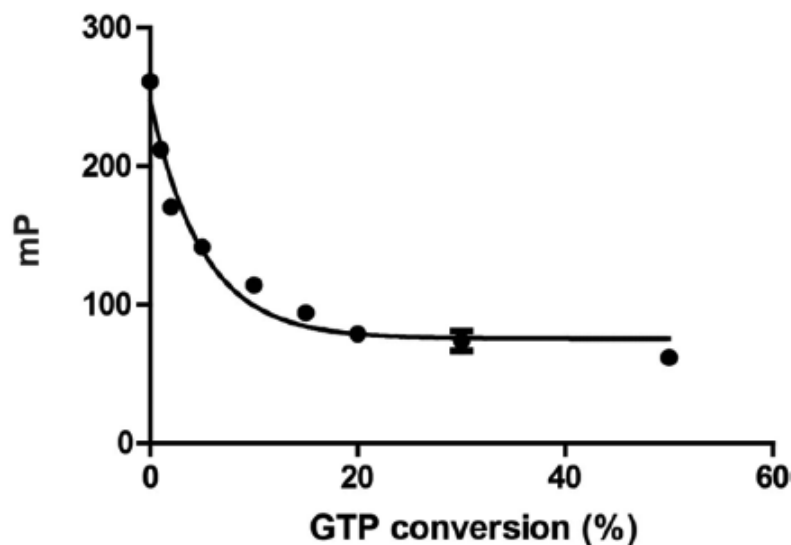
Figure. 3.5. Standard curve for guanosine triphosphate (GTP) hydrolysis. The guanosine diphosphate (GDP) detection reagent was added to GTP/GDP standards prepared by mixing different amounts of GDP and GTP. The % GTP conversion = [μM GDP/ (μM GDP + μM GTP)] * 100. The total concentration of GDP and GTP is 2 μM.

3.2.2 Scope of the fluorescence polarization assay At least 31 ARFGAPs are encoded in the human genome, among which approximately 17 have GAP enzymatic

activity(161). To test whether the newly developed fluorescence polarization assay can also be applied to measure the GAP activities of other ARFGAPs, two distinct ARFGAPs (ASAP1 and SMAP2) have also been purified (**Fig. 3.6**) using literature protocols. As shown in Fig. 3B, the GAP activity of both ASAP1 and SMAP2 to catalyze the hydrolysis of ARF1-GTP can be effectively monitored (**Fig. 3.7**). The kinetics profiles for ASAP1 and SMAP2 under the same concentrations are different, suggesting that their catalytic capacity is different. Taken together, these results suggest that the newly developed fluorescence polarization assay can be used to measure the GAP activity of different ARFGAPs.
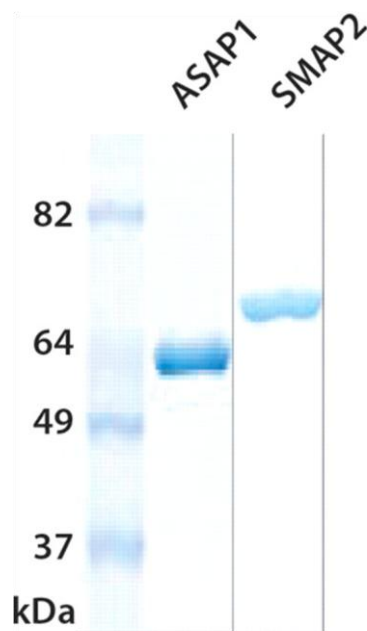
Figure 3.6. Highly purified human His$_6$-[325-724]ASAP1 and human GST-[1-163]SMAP2-His$_6$ as assessed by sodium dodecyl sulfate polyacrylamide gel electrophoresis (SDS-PAGE) analysis
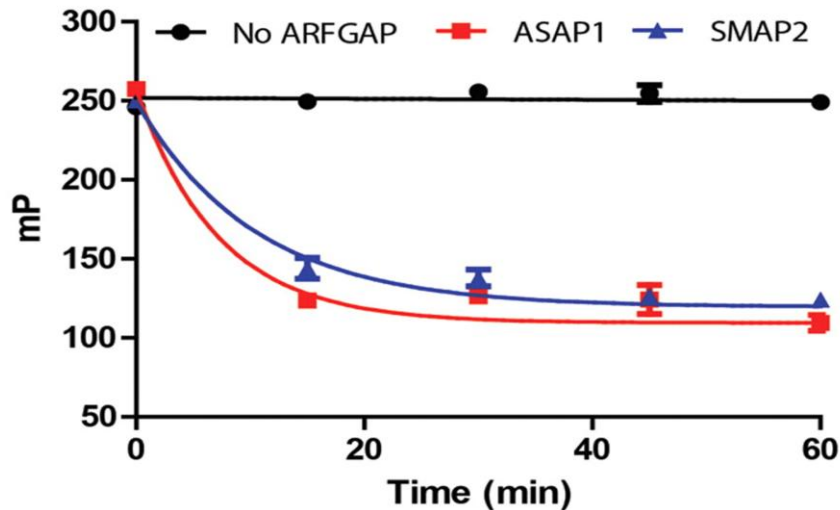
Figure 3.7. Fluorescence polarization assay monitoring the GTPase-activating protein (GAP) activity of SMAP2 and ASAP1. Either ASAP1 (0.2 μM) or SMAP2 (1 μM) was added to ARF1-GTP (2 μM) for the indicated times, and the guanosine diphosphate (GDP) generated from the GAP reaction was detected through fluorescence polarization

3.2.3 Assay development towards high throughput screening In the design and validation of high throughput screening (HTS) assays, an assessment of the screening data variability, by measures such as standard deviation (SD) and Z' factor, is critical in determining whether an assay can identify hits with confidence(162). To measure the Z' factor value in our assay, 24 parallel experiments in which the ARF1-GTP was incubated with either the GAP domain of rat ARFGAP1 (positive control) or the reaction assay buffer (negative control) at room temperature for 2 h was carried out and the flurorescence polarization was recorded (**Fig. 3.8**). The calculated Z' factor is 0.75, indicating that the quality of the assay is good. We also tested the effect of DMSO on the change of fluorescence polarization in the reaction (**Fig. 3.9**). The assay is robust and tolerates up to 10% DMSO in 384-well plates.

72
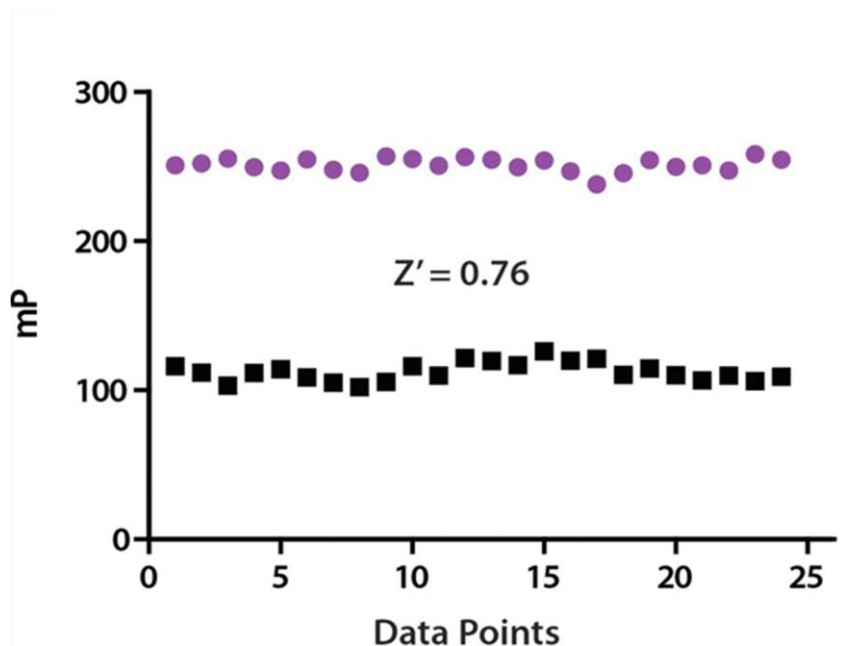
Figure 3.8. Assay development toward high-throughput screen. Measuring the Z′ factor of the assay. Either GTPase-activating protein (GAP) domain of rat ARFGAP1 (1 μM, circle dots) or the assay buffer (square dots) was added to ARF1-GTP (2 μM) for 2 h, and the guanosine diphosphate (GDP) generated from the GAP reaction was detected through fluorescence polarization. Each condition was repeated 23 times.
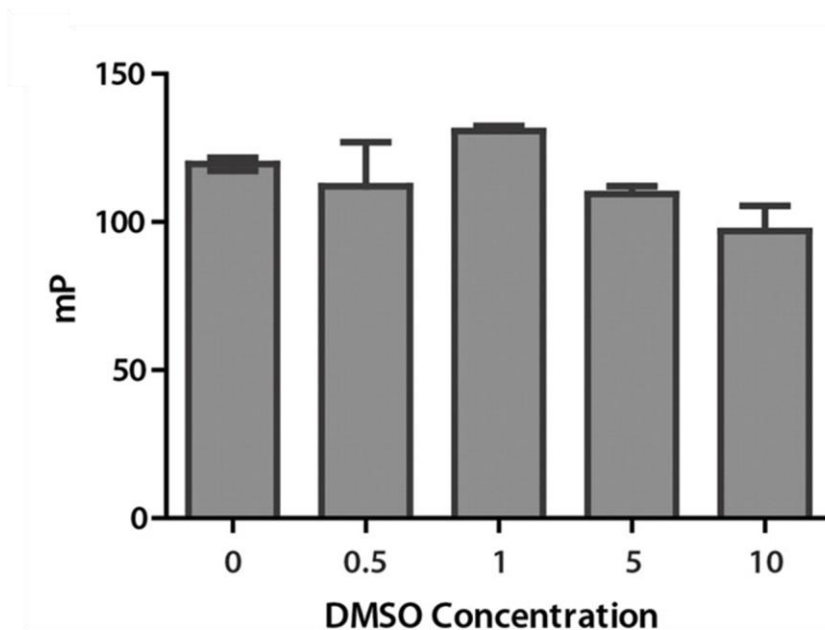
Figure 3.9. DMSO effect on the assay. The GAP assay as described in Figure 1D was carried out in the presence of DMSO at the indicated concentrations. Error bars are SD.

3.2.4 Screen of the Prestwick and LOPAC1280 Collection To further demonstrate the utility of this assay, we screened the Prestwick collection of 960 compounds for ARFGAP regulators in 384-well format at the NIMH Psycoactive Drug Screening Center directed by Dr. Bryan Roth. The screen was carried out in triplicates and the mean GTP hydrolysis was controlled at around 10% under the screen conditions so that both activators and inhibitors can be identified. The mean of the triplicates of each well is plotted (**Fig. 3.10 A**). The coefficient of variation (CV) was 4% and the hit (more than 3 SD from the mean of the plate) rate was about 0.4%. One compound, BM11 (**Fig. 3.10 B**), showed the most potent inhibition of the ARFGAP activity and the IC_{50} was measured as 1.2 μM.
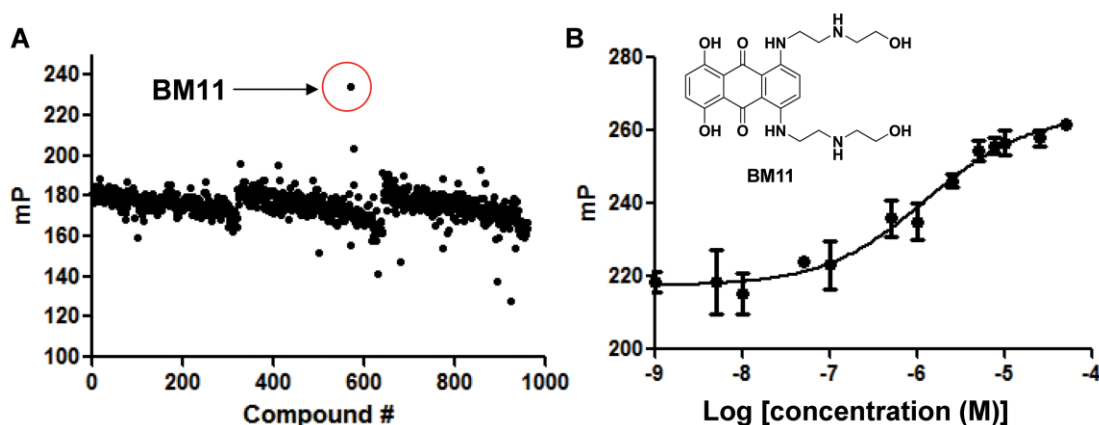
Figure 3.10. Pilot screen of the Prestwick library. A. The fluorescence polarization assay was used to screen the Prestwick collection in 384-well format for small molecule ARFGAP regulators. One compound, BM11, showed more than 50% inhibition of the GAP activity. **B.** Chemical structure of BM11; The IC_{50} of BM11 was measured as 1.2 μM through dose-dependent response experiment.

In addition, we screened the LOPAC1280 collection of 1280 pharmacologically active compounds in the Center for Integrative Chemical Biology and Drug Discovery. The screen was carried out in duplicates, and the mean of the duplicates of each well is plotted (**Fig. 3.11 A**). In each assay plate, DMSO was used as the negative control (low signal in mP), whereas blank assay buffer was used in the reaction to function as the

positive control (high signal in mP). The average Z′ factor was 0.73 when both intra- and interplate variations were considered. The hit rate was 0.31% for compounds (10 μM) exhibiting more than 3 standard deviations from the mean of the plate in the fluorescence polarization reading. The correlation coefficient for the parallel runs was 0.98 (**Fig. 3.11 B**), further demonstrating that the assay exhibits excellent characteristics for a high-throughput screen.
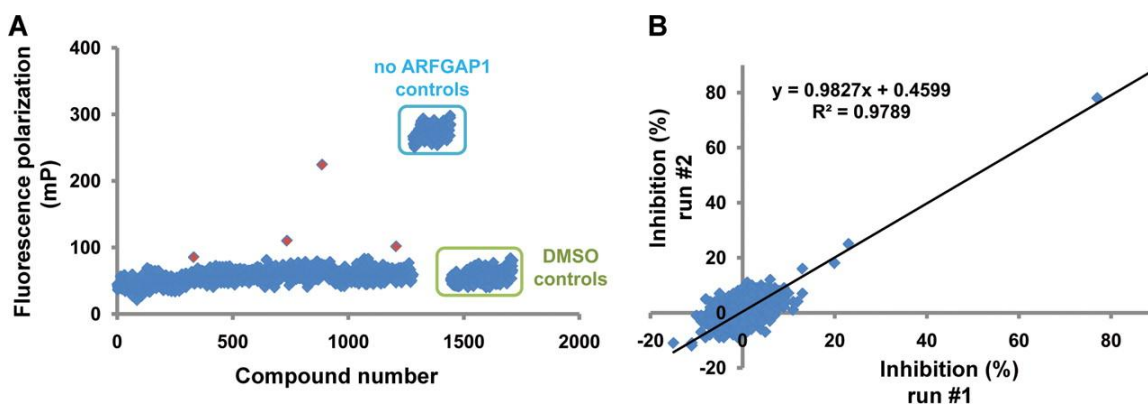
Figure 3.11. Pilot screen of the LOPAC1280 library. (A) Scatter plot of fluorescence polarization changes after incubation of ARF1 and ARFGAP1 with individual compounds of the LOPAC1280 collection. (B) The correlation coefficient for two parallel screens of the LO PAC 1280 library was 0.98.

3.2.5 Screen of 5, 000 kinase inhibitors To further demonstrate the utility of this assay to identify ARFGAP regulators in the 384-well format, we screened the collection of 5, 000 kinase inhibitors at CICBDD with the help of Drs William Janzen and Emily Hull-Ryde (**Fig 3.12**). The screen was carried out in singlet. In each assay plate, DMSO was used as the negative control (low signal in mP), whereas the assay buffer instead of the GAP domain of ARFGAP1 was used in the reaction to function as the positive control (high signal in mP). The screening results indicated that only two compounds showed more than 50% inhibition. If considering a cutoff of 16% inhibition of the GAP activity of the GAP domain, we were able to obtain 32 hit compounds. The hit rate is

75

about 0.64%. 12 concentrations of these hit compounds were used for dose-response studies which covered just a whole 384 well plate.
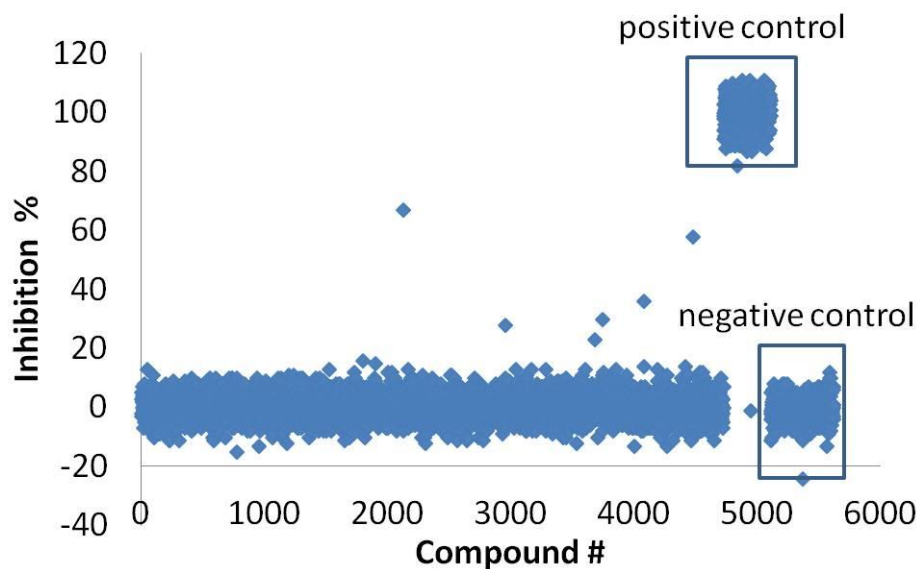
Figure 3.12. Screen of 5, 000 kinase inhibitors. Normalized inhibition of reactions of ARF1 and ARFGAP1 with individual compounds of 5, 000 kinase inhibitors.

To validate hit compounds we started with BM11, which showed potent inhibition in both the screens against the Preswick library and LOPAC library. This chemical structure is shown in **Fig 3.10 B**. This molecule showed dose-dependent inhibition in FP assays (**Fig 3.10 B**). In MBA-MD-231 cells, it inhibited GAP activity and led to accumulation of ARF-GTP levels (data not shown). However in radio active GTP hydrolysis assays this molecule did not inhibit GAP activity (data not shown). In ITC assays and SPR assays, this molecule also did not bind to the GAP domain (data not shown). We later realize that false positive response of BM11 is due to the spectral overlap of BM11 and Alexa 633 in the FP assay.

Only three hits from the 5, 000 kinase inhibitors showed dose-response curve in the follow-up validations (**Fig 3.13**). We picked these three hits for further characterization. However, none of them inhibited GAP activity in radio active GTP

76

hydrolysis assays (**Fig 3.14**). In ITC binding assays, these hit compounds did not bind to GAP domains (data not shown). We concluded that these three compounds are false positive hits. We briefly looked into the potential reasons for these false positive results. Compound E13 is not soluble when making the 100 µM stock solution for dose-response studies. The precipitation still present when further diluted to 1 µM. This precipitation could alter the fluorescence signals in the screening assays leading to the apparent "inhibition". The reasons for false inhibition by compounds I3 and L3 remain unclear.
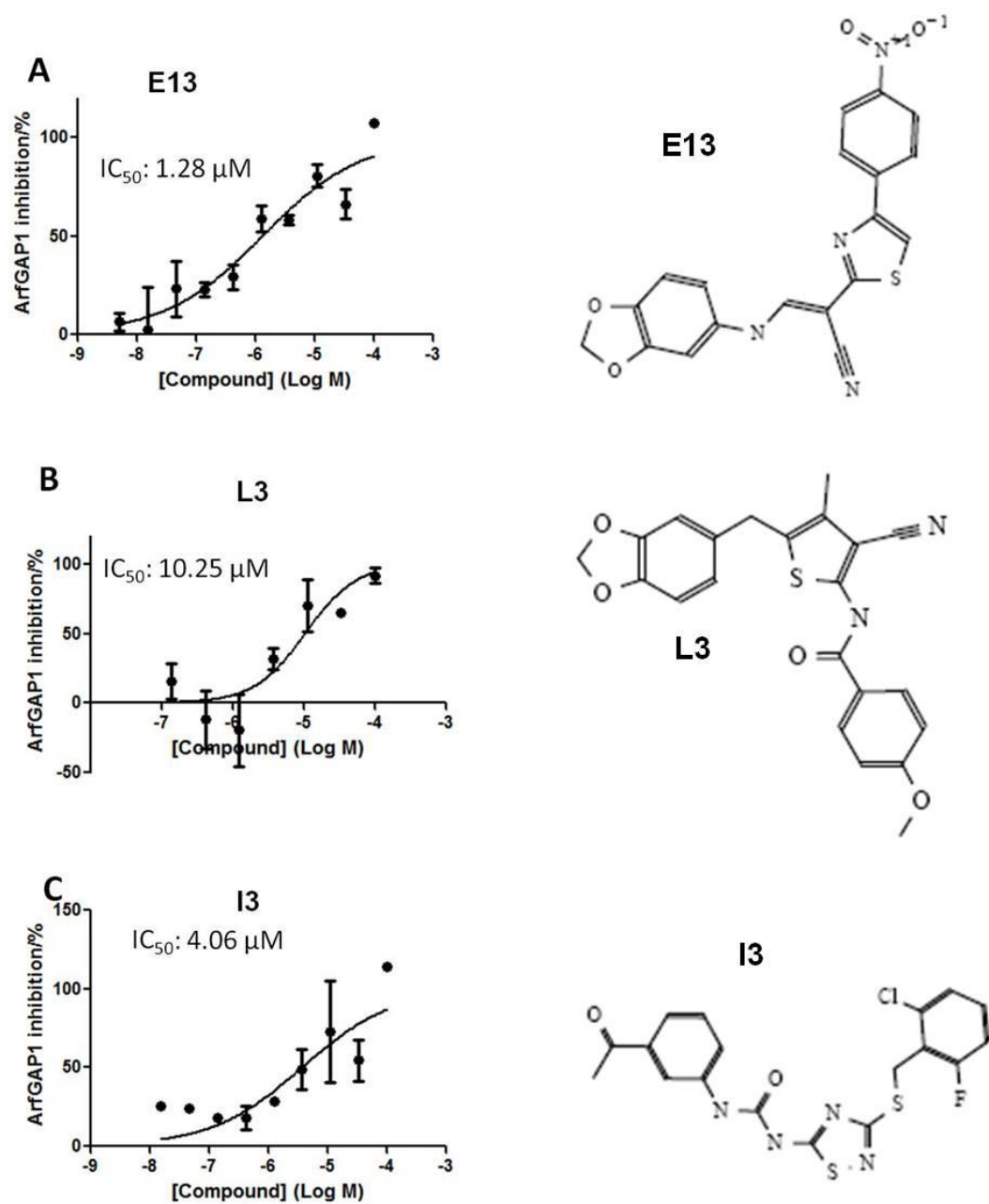
Figure 3.13. Chemical structures and IC$_{50}$ of E13, I3 and L3. The IC$_{50}$ were measured as 1.3 µM, 4.1 µM and 10.3 µM through dose-dependent response experiment.
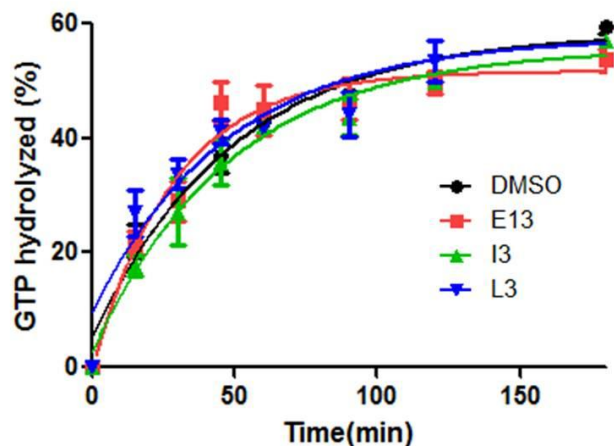
Figure 3.14. Inhibition effecs of E13, I3, L3 and DMSO on GAP activity of ARF-GTP hydrolysis.

3.2.6 Preparation ARF1, GAP domain and ASAP1 for screening in the molecular screening center at the Scripps Research Institute To discover ARFGAP inhibitors that directly interact with the GAP domain, we are collaborating with the Scripps Molecular Screening Center to screen a diverse library of 360,000 compounds. The ARFGAPs that will be used in the screen include [1-136]ARFGAP1 and [325-724]ASAP1. In collaboration with a technician, Mr. Pavan Denduluri, in the lab, we have prepared the first batch of 288.7 mg of ARF-GTP protein, 68.4 mg of the GAP domain of ARFGAP1 and 60.2 mg of [325-724]ASAP1. Using these purified proteins, the screening center has completed the validation of FP assay in 384-and 1536-well formats.

3.3 Experimental Section

3.3.1 Expression and purification of ARF1 and ARFGAPs Three different ARFGAPs including rat ARFGAP1, human ASAP1, and human stromal membrane-associated GTPase-activating protein 2 (SMAP2), are used in this work. The expression constructs for the GAP domain of rat ARFGAP1 (His$_6$-ARFGAP1[1-126])(118), His$_6$-ASAP1[325-724](163), and GST-SMAP2[1-163]-His$_6$(164) are obtained from Drs. Jonathan Goldberg (Memorial Sloan-Kettering Cancer Center), Paul Randazzo (National Cancer Institute), and Masanobu Satake (Tohoku University), respectively. The soluble ARF1, with the N-terminal 17 amino acid residues deleted, was used as the ARF for the assay development. The expression construct was also obtained from Dr. Jonathan Goldberg. All the four proteins were expressed and purified according to literature protocols.

3.3.2 Native gel assay The native gel assay was carried out according to the literature protocol(118). Briefly, The purified ARF1 (1.7 mM, 4 µL) was loaded with GTP (5 mM, 4 µL) by incubating the protein with GTP in the loading buffer (25 mM HEPES, 150 mM NaCl, 1 mM MgCl$_2$, 5 mM EDTA, 2 mM DTT, pH 7.5) at room temperature for 40 min. A solution of MgCl$_2$ (2 M) was then added to a final concentration of 20 mM. The so-formed ARF-GTP was stored at 4 $^{\circ}$C prior to use. To carry out the native gel assay, ARF-GTP (170 µM, 1.9 µL) and ARFGAP1 (15 µM, 4.3 µL) were incubated in the assay buffer (25 mM HEPES, 150 mM NaCl, 20 mM MgCl$_2$, 5 mM EDTA, 2 mM DTT, pH 7.5) for indicated times at room temperature. The mixtures were then loaded into GE homogeneous 20% polyacryamide gel (GE Healthcare Life

Sciences) and the ARF1-GTP was separated from the ARF1-GDP on the gel subjected to electrophoresis at 4 $^{\circ}$C and visualized through Coomassie blue staining.

3.3.3 Fluorescence polarization assay A solution of the GAP domain of rat ARFGAP1 (5 µM, 4 µL) in the buffer (25 mM HEPES, 150 mM NaCl, 20 mM MgCl$_2$, 5 mM EDTA, 2 mM DTT, pH 7.5) was added to a 384-well plate that contains ARF1-GTP (2.5 µM, 16 µL), which was generated as described in the native gel assay. The reaction mixture was incubated at room temperature for varying times. The enzymatic reaction was terminated by adding the stop and detection buffer (10 µL, Bellbrook labs, contains 20 mM HEPES, 40 mM EDTA, 0.02% Brij-35, 4 nM GDP Alexa 633 tracer, and 14 µg/mg GDP antibody). The fluorescence polarization was measured 20 min after adding the detection buffer on a BMG labtech PHERAstar plus instrument with an excitation wavelength of 590 nm and an emission wavelength of 675 nm. A well that contains free tracer (30 µL) was set as 20 mP and used as an internal standard. Each reaction was carried out in triplicates and GraphPad Prism 5 was used to analyze the data.

3.3.4 Enzyme kinetics [Δ17]ARF1 (400 µm) is loaded with GTP in buffer [25 mM HEPES, pH 7.5, 150 mM NaCl, 1 mM MgCl$_2$, 5 mM EDTA, 2 mM DTT, 2.4 µM GTP, [γ32P] GTP] for 40 min at room temperature. A solution of MgCl$_2$ (2 M) was then added to a final concentration of 20 mM. The ARF-GTP solution was then diluted into desired concentration for kinetic reactions. The GTP hydrolysis was initiated by adding GAP domain of ARFGAP1 to a series of [Δ17]ARF1 solutions.

3.3.5 Screening of the Prestwick chemical library The small molecule compounds from the Prestwick chemical library were dissolved in DMSO to form a stock solution with the concentration of each compound at 1 mM. The stock solution was

further diluted with the ARFGAP assay buffer to generate the working solution with the concentration of each compound at 100 μM. To carry out the screen, the working solution of compounds (2 μL) was added to the GAP domain of rat ARFGAP1 (5 μM, 4 μL) in the assay buffer (10 μL). The plate was incubated at room temperature for 10 min, and then ARF1-GTP (10 μM, 4 μL) was added to initiate the reaction. After 2 h, the enzymatic reaction was stopped by adding the stop and detection buffer (10 μL), and the fluorescence polarization was read as above described. Each reaction was carried out in triplicates.

3.3.6 Screening of the LOPAC1280 chemical library The small-molecule compounds from the LOPAC1280 (Sigma-Aldrich) were dissolved in DMSO to form stock solutions (1 mM). The stock solutions were further diluted with ARFGAP assay buffer to generate working solutions (100 μM). The 384 plate (Corning) used in screening of the Prestwick Chemical Library is not adapted into the screening facilities in the CICBDD center. To use a low volume 384 well plate (Perkin Elmer) fitted in the screening robot, we optimized the concentrations and volumes of the reaction. To carry out the screen, working solutions of compounds (2 μL) were added to the GAP domain of rat ARFGAP1 (6.7 μM, 3 μL). The plate was incubated at room temperature for 10 min, and ARF1-GTP (13.3 μM, 3 μL) was subsequently added to initiate the reaction. After 2 h, the enzymatic reaction was stopped by adding the stop and detection buffer (8 μL), and the fluorescence polarization was read as described above. Each reaction was carried out in duplicate.

3.3.7 Screening of 5, 000 Kinase Inhibitors The screening of 5, 000 Kinase inhibitors were carried out the same way as the screening of LOPAC1280 Chemical Library.

3.3.8 Validation of hit compounds in radio active GTP hydrolysis assays The radioactivity-based GTP hydrolysis assay was carried out similarly as described in Chapter Two.

3.3.9 ITC binding assays Microcalorimetric measurements of QS11 and hits binding to the GAP domain of ARFGAP1 were performed on a VP-ITC isothermal titration calorimeter (Microcal, Northampton, MA, USA). QS11 (10 μM) dissolved in 25 mM HEPES, pH 7.5 and 150 mM NaCl was filled into the microcalorimetric cell (volume, 1.3 mL) and titrated with 30 X 8 μL injections of 200 μM the GAP domain at 240 s intervals from a 250 mL injection syringe at room temperature. The solutions were thoroughly degassed before the titration and the cell contents were stirred constantly at 300 rpm. As a control, the GAP domain was also titrated into buffer under the same conditions and the heat of dilution was subtracted. The heat that was generated from each injection was plotted versus time. and analyzed with the MicroCAL Origin software.

3.3.10 SPR Analysis The SPR analysis was carried out as described in Chapter Two.

3.4 Conclusion

In summary, we have developed a robust high-throughput screen that will be useful to identify small molecule ARFGAP modulators. Compared to traditional ARFGAP assays based on radiolabeled GTP analogs, this methodology uses fluorescence polarization to monitor GTP hydrolysis of ARF-GTP and handling radioactive, hazardous waste is avoided. Nonetheless, reliance on fluorescence polarization is not without potential limitations. For example, compounds that directly interfere with fluorescence polarization could be misinterpreted as potential leads. Perhaps more relevant, any compound that affected the affinity of (1) the antibody to bind the fluorescent tracer or (2) the ARF GTPase to bind guanine nucleotides might also be misinterpreted as a potential modulator. Consequently, secondary assays such as measuring the direct binding of compounds with ARFGAPs have to be developed to confirm the ARFGAP inhibition in the fluorescence polarization assay. In conclusion, this newly developed assay is ideal for measuring ARFGAP activity in large numbers of samples and should be particularly useful for the HTS of compound libraries to identify small-molecule modulators of ARFGAPs.

3.5 Future Plan

We are currently collaborating with the Scripps Molecular Screening Center to discover small molecule inhibitors of both ARFGAP1 and ASAP1. Once the hits are discovered from the screen, single dose of these new hit compounds will be first confirmed in $[\gamma^{32}P]$ GTP hydrolysis assays. Those hit compounds showing potent inhibition (>50% inhibition) compared to the DMSO control will be then verified in dose-response studies in $[\gamma^{32}P]$ GTP hydrolysis assays. The confirmed hit compounds will be further evaluated in ITC and SPR binding assays. The most potent hit compounds will be tested in cell-based ARF-GTP pull down experiments. The best hit compounds will be then optimized through SAR studies and tested for selectivity among ARFGAPs. The effects of the inhibitors on ARFGAP-related cellular processes, such as cell migration, will also be tested.

ARFGAPs require membrane components to function efficiently in the endogenous system. In *in vitro* environment, various lipids have been used to mimic the membrane structures. It would be interesting to investigate whether the ARFGAP activity in the presence of liposome can be measured in this FP assay. We will first test whether the assay can be used to efficiently measure the hydrolysis of GTP that bounds to the myristoylated ARF1 in the presence of full-length ARFGAP1 and phosphatidylcholine. Once validated, more complex lipid conditions would be used to optimize the GAP activity of ARFGAP1 and other ARFGAPs.

Chapter 4.

Generation of Novel Myristoylated ARFs by Metabolic Interference

This work is a collaboration project with Drs. Zhiquan Song and Yanbao Yu. Dr. Song synthesized six myristic acid analogs and expressed and purified four myristoylated ARF1. He also demonstrated that the incorporation of a keto functional group would enable its labeling by a fluorescent dye. I expressed and purified the first four myristoylated ARF1s, and characterized the modified ARF1s by measuring their capacities of GTP-loading and hydrolysis catalyzed by ARFGAP1. The mass spectra for the modified ARF1s were obtained by Dr. Yanbao Yu.

4.1 Introduction

Myristoylation and palmitoylation of proteins play important roles including localizing proteins to various cellular membranes and sub-membrane domains and facilitating protein-protein interactions.[165] Myristoylation is the irreversible covalent attachment of myristic acid to an N-terminal glycine in a target protein, catalyzed by the enzyme N-myristoyl transferase (NMT).[166] Although myristoylation is an irreversible modification, the duration of myristoylated proteins on membranes can be dynamically regulated by ligand binding.[167-171] For examples, GTP binding to ARF could induce the conformation change of ARF and allow the exposure of the myristol motif and lead to membrane localization of ARF[169].

The regulation of NMT activity is not well understood and it was shown that endogenous inhibitors NMT inhibitor protein 71 (NIP71) regulate NMT activity in *in vitro* NMT assays.(172-174) In addition, the glycolytic enzyme enolase is able to inhibit N-myristoylation *in vitro*.(175) Phosphorylation of NMT1 also regulates the activity of the enzyme and affects the efficiency.(176,177) For example, the N-terminal domain of NMT1 interacts with the Lyn tyrosine kinase in a phosphorylation-dependant manner.(176) However, how phosphorylation crosstalks with myristoylation has not been well understood.

Myristoylation is implicated in many diseases. Increased expression of NMT has been found in colon, gallbladder, breast and brain cancers.(178-181) Inefficient myristoylation of the SHOC2 protein has been linked to the development of the Noonan-like syndrome with loose anagen hair in twenty-five patients.(182) In addition, some bacterial strains inject bacterial proteins into the cytoplasm of the host cell.(183-185) Myristoylation of these bacterial proteins by host cells would facilitate the bacteria virulence.(184,185) Consequently, targeting these proteins may present an effective strategy to prevent bacteria infection .

Most studies of myristoylated proteins relied on the [^{3}H]-myristic acid.(186) However, the method of using radioactive [^{3}H]-myristic acid has low sensitivity and the detection takes one to three months. To shorten the experimental time, [^{125}I]-iodomyristate has also been synthesized and utilized so that the experiment can be finished within days.(187,188) However, the handling of the hazardous high-energy ^{125}I radioisotope has caused health concerns. In order to avoid the use of radioactive materials, several chemical bio-orthogonal tools have been developed.(186,189,190) These tools

use "click chemistry" to identify novel myristoylated proteins in faster and more sensitive manners. However, these tools require preparations of both azide and alkyne reagents and they are used for affinity purification and identification of lipid modified proteins.

We are interested in developing novel and convenient methods to identify and charaterize both myristoylated proteins and their interacting proteins through metabolic interference. The small GTPase ARF1 is used as a model system because it is myristoyalted under endogenous conditions and we have substantial experience in characterizing ARFs and ARFGAPs.

4.2 Results and Discussion

4.2.1 Modified myristic acid To explore whether modified myristic acids could serve as chemical probes for protein myristoylation, we synthesized a series of myristic acid analogs (**Table 4.1**). The modifications are designed for specific, potential functional applications. For example, the keto modification could be used for labeling proteins modified by this lipid with hydrazine-containing fluorophore. Proteins modified with the three perfluorinated lipids can be digested by proteases and the resulting peptides conjugated with perfluorinated group could be enriched by fluorous affinity resin for detection of low abundant myristoylation proteins through MS analysis. Furthermore, the selenium (Se)-modified lipid could be cleaved selectively by oxidation, thus the activity and localization of the corresponding ARF1 could be regulated. Finally, the diazirine-containing myristic acid analog will generate reactive carbine upon light illumination, thus providing a new method to identify interacting proteins of myristoylated proteins.
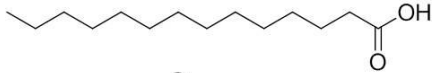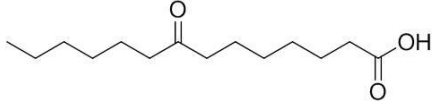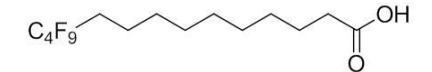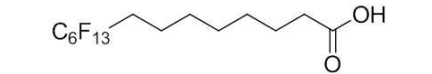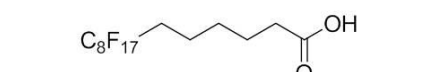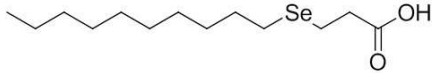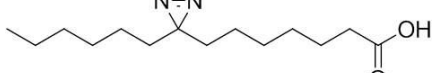
modification	chemical structure	Name	modified ARF1
myr		Myris ARF1	20775.78
keto		Keto ARF1	20789.76
C_4F_9		C_4F_9 ARF1	20937.69
C_6F_{13}		C_6F_{13} ARF1	21009.66
C_8F_{17}		C_8F_{17} ARF1	21226.74
selenium		Se ARF1	20841.68
diazo		Diazo ARF1	20801.77

Table 4.1. Chemical structures of designed myristic acids.

Myristoylation of recombinant ARF1 is achieved by coexpression of ARF1 with N-myristoyltransferase (NMT) in *E. coli* because bacteria lack transferase activity. The colonies with full-length ARF1 were obtained from Dr. Paul Randazzo as described in Chapter Two. NMT catalyzes the transfer of exogenous myristic acids to the glycine residue at the N-terminal of ARF1. BL21 (DE3) bacteria were cultured in the presence of different myristic acid analogs before IPTG induction. The myristoylated ARF1 were then purified according to the literature protocols.(140)

4.2.2 Characterization of novel ARFs with modified myristic acids To confirm that the modified myristic acids were successfully incorporated into ARF1, we first analyzed the proteins by mass spectrometry. A representative mass spectrum for keto-ARF1 was shown in **Fig. 4.1**. To further confirm that the modification is at the right position, both the unmodified and keto-modified myristoylated ARF1 proteins were

digested by trypsin and the resulting peptides were analyzed by liquid chromatography-tandem mass spectrometry (LC-MS/MS) (**Fig 4.2**). The N-terminal peptide **GNIFANLFK** indicated that a keto group is specifically labeled on the glycine at the N-terminus of the ARF1 (**Fig 4.2**).
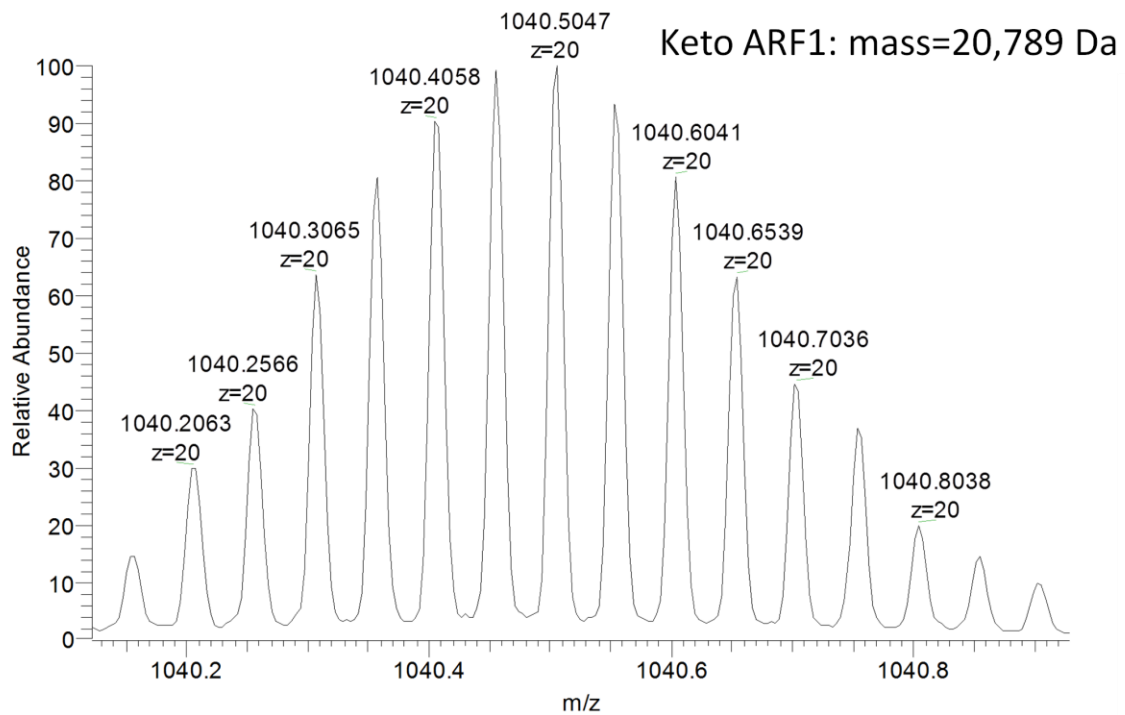
Figure 4.1. Mass spectra of full length Keto-ARF1.
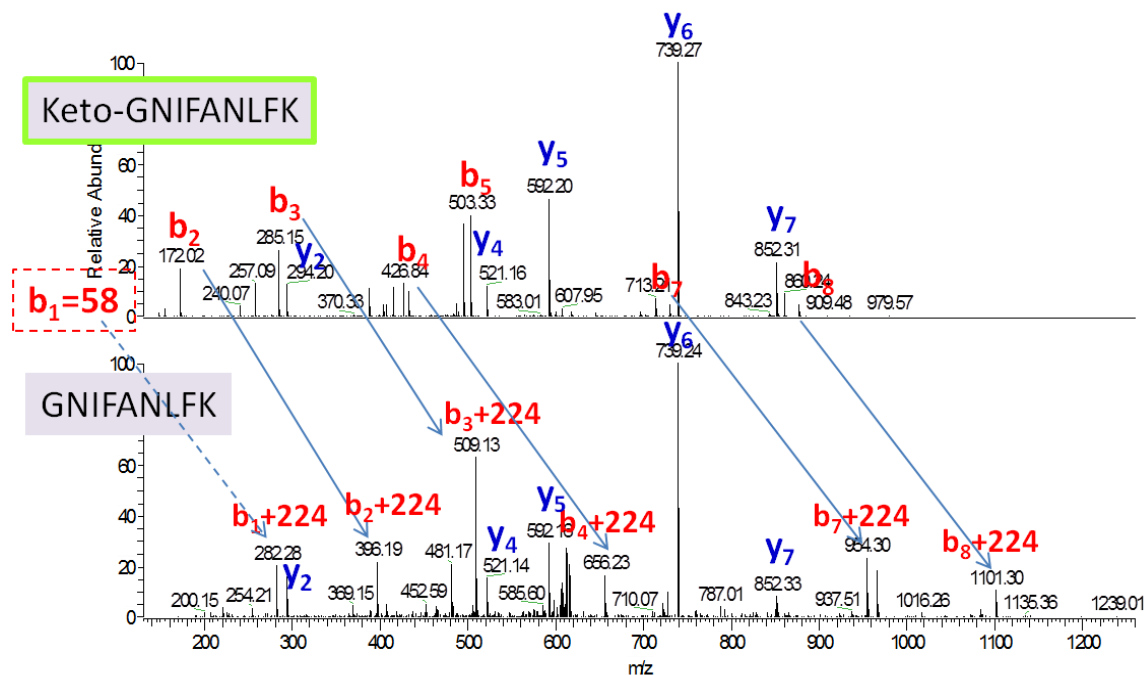
Figure 4.2. **Mass spectra of full-length myristoylated ARF1.** Unmodified and keto-modified myristoylated ARF1 proteins were digested by trypsin and the resulting peptides were analyzed by liquid chromatography-tandem mass spectrometry (LC-MS/MS).

Myristoylation controls ARF functions in membrane binding, vesicle coat protein recruitment, nucleotide exchange, interactions with guanine nucleotide exchange factors and interactions with PLD. Therefore, it is important to determine whether these modified myristic acids changed the activities of ARF1. Accordingly, we measured the guanine nucleotide exchange rate of modified ARF1 proteins and the GTP hydrolysis rate of the resulting GTP-bound ARF1 in an intrinsic fluorescence assay. As shown in **Fig 4.3**, all six modified myristoylated ARF1 showed similar guanine nucleotide exchange rate as that of the native myristoylated ARF1 indicating that the modifications on myristic acid did not affect the interaction between ARF1 and GTP. Furthermore, these nucleotide exchange reactions were carried out in the presence of liposome. Given that the

92

interaction between the lipid membrane and ARF increases nucleotide exchange rate,(119,191) this result also suggested that the interactions between myristoylated ARF1 and membrane are not significantly disrupted by modifications on the myristic acid. In addition, five modified myristoylated ARF1 showed similar GTP hydrolysis rate in the presence of ARFGAP1 indicating that these five modifications did not affect the interactions between ARF1 and ARFGAP1 (**Fig 4.4**). Interestingly, keto myristoylated ARF1 showed a 3-fold faster hydrolysis rate within the linear range of the GTP hydrolysis (**Fig 4.4**). One possible reason is that the keto group forms additional hydrogen bonds with ARFGAP1 resulting in a tighter interaction between ARF1 and ARFGAP1. Overall, these six myristoylated ARF1 proteins maintain the activities of unmodified myristoylated ARF1 in interacting with GTP, ARFGAP and lipid membranes.
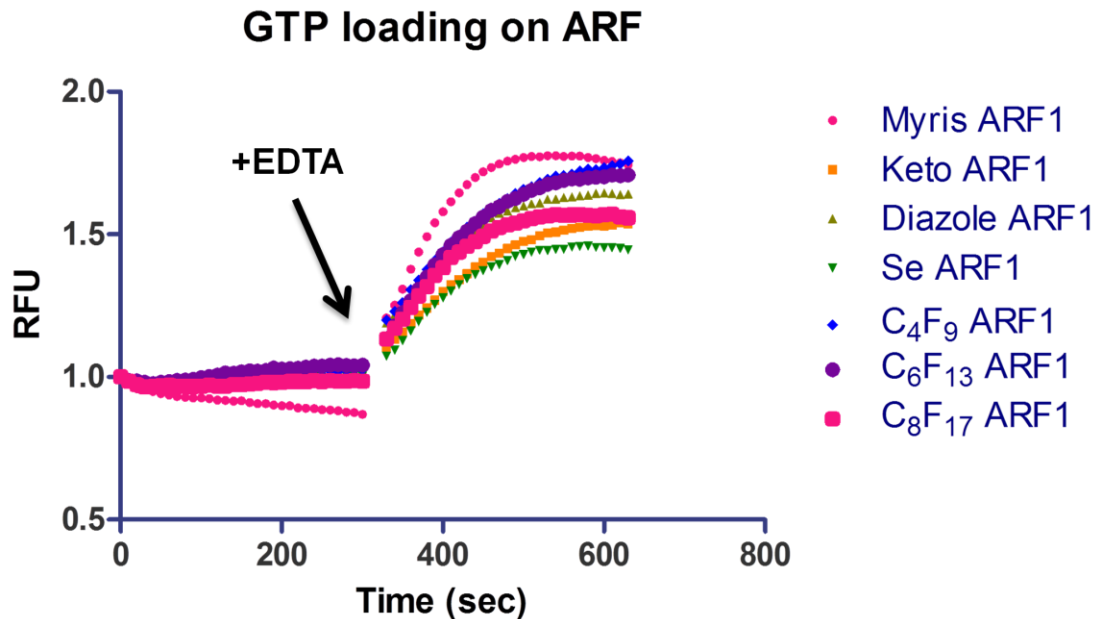
Figure 4.3. GTP exchange assays of ARFs. ARF1 was added to a final concentration of 500 nM in liposome. GTP solution was added to a final concentration of 40 μM. EDTA was subsequently added to the final concentration of 2 mM (free Mg^{2+} concentration is 1 μM) to initiate the GTP loading.
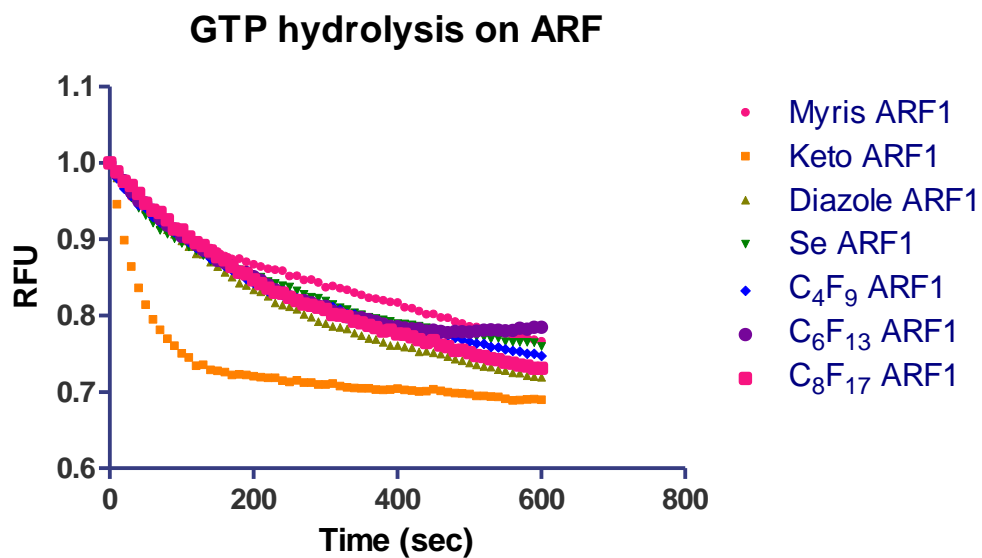
Figure 4.4. GTP hydrolysis on ARFs catalyzed by ARFGAP1. GTP hydrolysis was initiated by adding ARFGAP1 into the cuvette to reach a final concentration of 50 nM and the fluorescence was recorded continuously for 10 min.

4.2.3 Fluorophore labeling assays   To demonstrate the potential functional applications of modified myristoylated ARF1 proteins, purified keto-myristoylated ARF1 or native myristoylated ARF1 were incubated with fluorescein-hydrazide. The samples were separated by SDS-PAGE and detected with both coomassie blue staining and fluorescence scanning (**Fig. 4.5**). In coomassie blue staining, there are two close proteins bands shown in the keto myristoylated ARF treated with fluorescein-hydrazide. Compared to the untreated keto myristoylated ARF1, the upper band is likely to be the fluorescien-labeled myristoylated ARF1. This result is further confirmed by fluorescence scanning. Fluorescien-labeled myristoylated ARF1 is present in the samples with keto myristoylated ARF1 treated with fluorescein-hydrazide, making it possible to use keto myristic acid for identification of known or novel myristoylated proteins in mammalian cells.
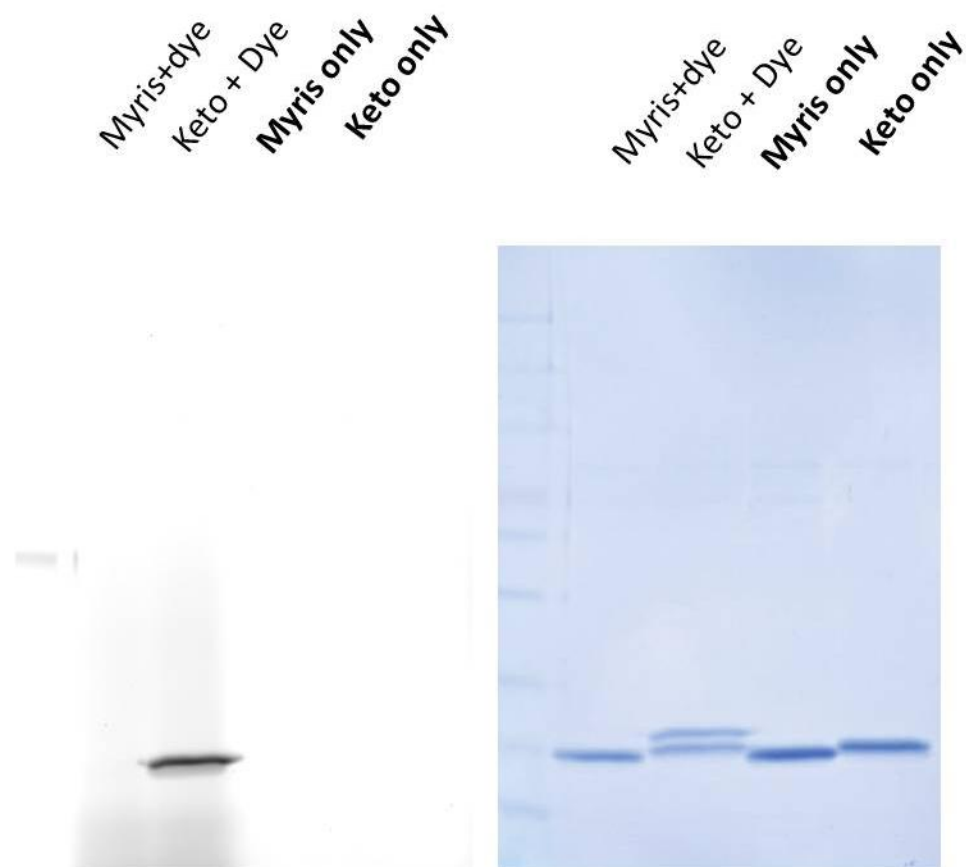
Figure 4.5. Selective fluorescein labeling of purified keto-ARF Purified myris-ARF or keto-ARF was dialyzed against phosphate buffered saline (PBS). The protein was either incubated with 1 mM fluorescein-hydrazide (Molecular Probe) (pre-dissolved in DMF) or DMF in PBS for 16 h at -20 ℃, respectively. Excess dyes were removed by dialysis in PBS buffer. The samples were then denatured, separated by SDS-PAGE and detected by both coomassie blue staining and fluorescent scanning.

4.3 Experimental Section

4.3.1 Expression and purification of modified myristoylated ARFs The single colonies of myristoylated ARF1 that contain NMT are from Dr. Paul Randazzo (National Cancer Institute). In analogy to the expression and purification of myrisoylated ARF1, we generated the modified ARF1s.(140) Briefly, a single colony from the transformation was cultured for 9 h at 37 ℃. This culture was used to inoculate 2 L of pre-warmed medium (1:100 dilution of culture) in two 2 L baffled flasks. The cells were grown at 37 ℃ with vigorous agitation till OD_{600} reaches ~ 0.6, at which time, modified myristic acid was added to the culture at a final concentration of 50 μM and the incubation was continued for another 20 min. Afterwards, IPTG was added to a final concentration of 1 mM. The cultures were cooled to 25 ℃ and agitation was continued at 25 ℃ for 12-16 h. The cells were harvested by centrifugation at 4000x rpm for 20 min (Beckman JA10 rotor, 5000 rpm), and the pellets were stored at -80 ℃.The purification methods of myristoylated ARF1 are similar to the ones described in Chapter 2.

The concentration of purified myristoylated ARF1 was determined by a dye reagent (Bio-Rad) at UV absorbance at 595 nm. The typical yield of myristoylated ARF1 is 1 mg from 2 L cell culture.

4.3.2 GTP loading and GTP hydrolysis in intrinsic fluorescence assay Liposome was prepared in a similar way as described in Chapter Two. GTP exchange reaction and GAP-catalyzed GTP hydrolysis were monitored in a cuvette containing buffer (300 μL) (50 mM Hepes pH 7.2, 120 mM KAc, 1 mM $MgCl_2$, 1 mM DTT) and liposome (0.2 mM) in a fluorometer. Tryptophan fluorescence of ARF1 was measured at the emission wavelength of 340 nm (bandwidth 14 nm) and the fluorophore was excited

at 297.5 nm (bandwidth 3 nm). The basal fluorescence was recorded for 5 min before ARF1 was added to a final concentration of 500 nM. After 5 min, GTP solution was added to a final concentration of 40 μM and fluorescence was recorded for another 5 min. EDTA was subsequently added to the final concentration of 2 mM (free Mg^{2+} concentration is 1 μM) to initiate the GTP loading and the fluorescence was recorded for 10 min. The GTP loading was stopped by adding $MgCl_2$ solution to a final concentration of 3 mM and the fluorescence was recorded for 10 min. GTP hydrolysis was initiated by adding ARFGAP1 to the cuvette to a final concentration of 50 nM and the fluorescence was recorded for 30 min. The fluorescence value was normalized by subtraction of the basal fluorescence value from buffer and liposome. In the GTP loading experiment, the fluorescence of different ARF-GDP was normazlied as 1.0 after subtractions of buffer and liposome. In the GTP hydrolysis experiment, the relative fluorescence of different ARF1-GTP was set as 1.0.

4.3.3 *In Vitro* fluorescence labeling Purified myris-ARF1 or keto-ARF1 was dialyzed against phosphate buffered saline (PBS) overnight (3 x 2 L) at -20 ^{o}C. The protein was either incubated with 1 mM fluorescein-hydrazide (Molecular Probe) (pre-dissolved in DMF) or DMF in PBS for 16 h at -20 ℃, respectively. Excess dyes were removed by dialysis in PBS buffer. The samples were then denatured, separated by SDS-PAGE and detected by both coomassie blue staining and fluorescent scanning with a Typhoon 9400 scanner (GE Healthcare).

4.3.4 Sample preparation for mass spectra Purified ARF proteins (1 mg/ml) were dialyzed in H_2O for 8 h at room temperature. The samples were then injected into LTQ-Orbitrap XL mass spectrometer for LC-MS analysis.

4.4 Conclusion

New chemical tools are needed to help us better understand protein myristoylation. Here, we describe the strategy of generating novel myristic acid analogs which can be efficiently incorporated into ARF1. These modified myristoylated ARF1 proteins maintain functions of endogenous myristoylated ARF1 such as nucleotide exchange and catalysis of GTP hydrolysis. More importantly, the ARF proteins gain novel functions through these designed modifications. We are exploring different functions of these modified myristoylated proteins.

4.5 Future Plan

The purified keto-ARF1 are efficiently labeled with a fluorescent dye, raising the question whether the proteins in live cells can be modified and labeled. We will explore different conditions to feed cultured mammalian cells with keto-modified myristic acid derivative and label the cell lysate with fluorescent dye. The myristoylated proteins in the cells can thus be identified. Once validated, this method could be further extended to explore the dynamic myristoylation of proteins under various extracellular stimulations. For perfluoroalkyl-modified ARF1 proteins, we will explore conditions that can enrich and detect fluorous peptides from the digested fluorous-ARF1 through fluorous solid phase extraction followed by MS analysis. Such enrichment of a subset of peptides is essential to identify low-abundant proteins. Regarding the Se-ARF1, we will continue to search for a mild oxidation reagent that could cleave the Se-C bond without disrupting the structure of Se-ARF1. We are also interested in demonstrating the novel functions of diazo-ARF1. It will be interesting to see whether this novel protein can be used to identify ARF1-interacting proteins through light-induced crosslinking.

Appendix
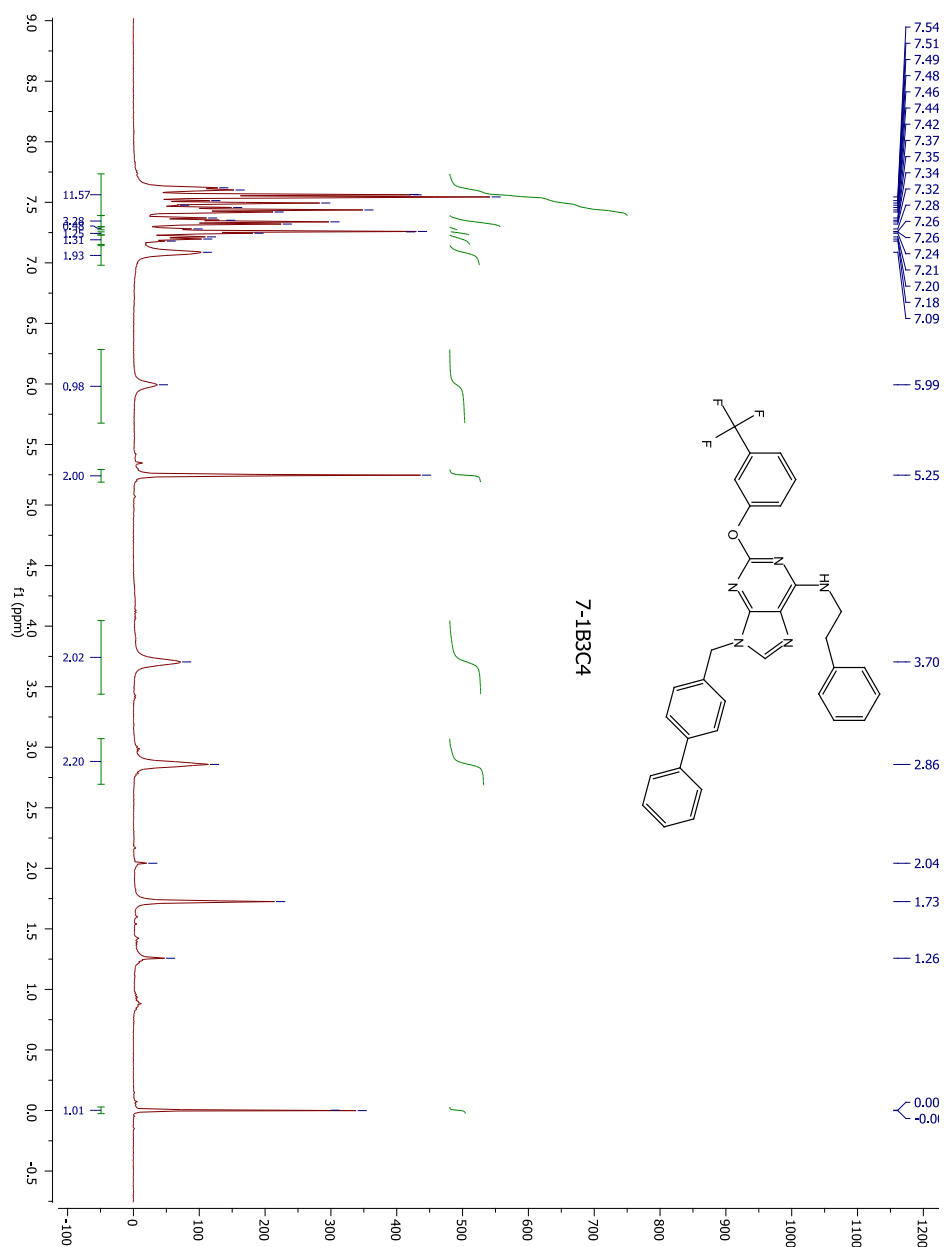
Appendix A ^{1}H NMR (CDCl3) of B3C4 in as an example of QS11 analogs
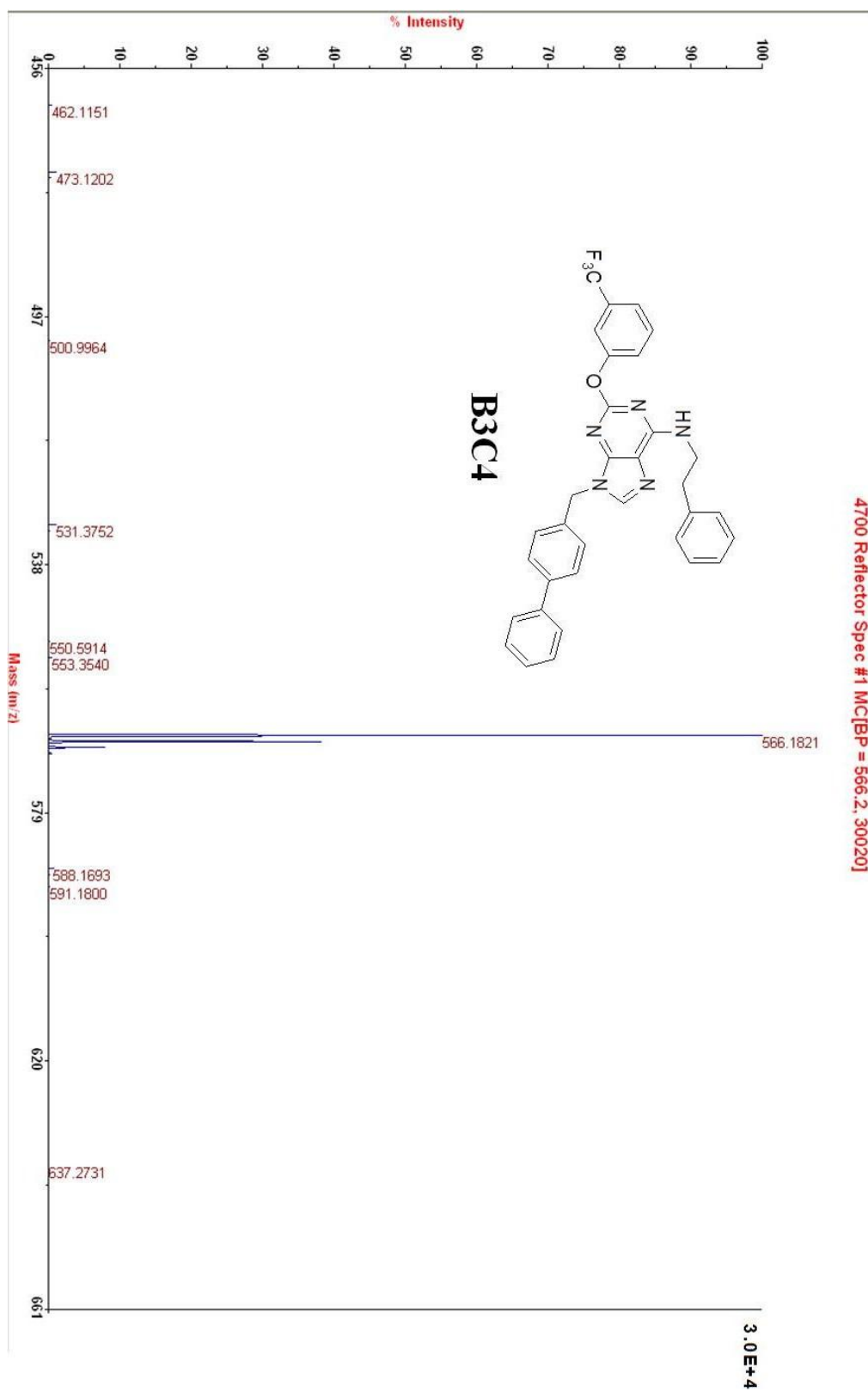
Appendix B Mass spectrum of of B3C4 as an example of QS11 analogs

References

1. Gillingham, A. K., and Munro, S. (2007) *Annu Rev Cell Dev Biol* **23**, 579-611

2. East, M. P., and Kahn, R. A. (2011) *Semin Cell Dev Biol* **22**, 3-9

3. Amor, J. C., Harrison, D. H., Kahn, R. A., and Ringe, D. (1994) *Nature* **372**, 704-708

4. Chavrier, P., and Ménétrey, J. (2010) *Structure* **18**, 1552-1558

5. Donaldson, J. G., and Jackson, C. L. (2011) *Nat Rev Mol Cell Biol* **12**, 362-375

6. D'Souza-Schorey, C., and Chavrier, P. (2006) *Nat Rev Mol Cell Biol* **7**, 347-358

7. Randazzo, P. A., Yang, Y. C., Rulka, C., and Kahn, R. A. (1993) *J Biol Chem* **268**, 9555-9563

8. Randazzo, P. A., and Kahn, R. A. (1994) *J Biol Chem* **269**, 10758-10763

9. Randazzo, P. A., Weiss, O., and Kahn, R. A. (1995) *Methods Enzymol* **257**, 128-135

10. Randazzo, P. A., Terui, T., Sturch, S., Fales, H. M., Ferrige, A. G., and Kahn, R. A. (1995) *J Biol Chem* **270**, 14809-14815

11. Serafini, T., Orci, L., Amherdt, M., Brunner, M., Kahn, R. A., and Rothman, J. E. (1991) *Cell* **67**, 239-253

12. Norman, J. C., Jones, D., Barry, S. T., Holt, M. R., Cockcroft, S., and Critchley, D. R. (1998) *J Cell Biol* **143**, 1981-1995

13. Mizuno-Yamasaki, E., Rivera-Molina, F., and Novick, P. (2012) *Annu Rev Biochem*

14. D'Souza-Schorey, C., and Stahl, P. D. (1995) *Exp Cell Res* **221**, 153-159

15. Cukierman, E., Huber, I., Rotman, M., and Cassel, D. (1995) *Science* **270**, 1999-2002

16. D'Souza-Schorey, C., Li, G., Colombo, M. I., and Stahl, P. D. (1995) *Science* **267**, 1175-1178

17. Hashimoto, S., Onodera, Y., Hashimoto, A., Tanaka, M., Hamaguchi, M., Yamada, A., and Sabe, H. (2004) *Proc Natl Acad Sci U S A* **101**, 6647-6652

18. Hashimoto, S., Hirose, M., Hashimoto, A., Morishige, M., Yamada, A., Hosaka, H., Akagi, K., Ogawa, E., Oneyama, C., Agatsuma, T., Okada, M., Kobayashi, H.,

Wada, H., Nakano, H., Ikegami, T., Nakagawa, A., and Sabe, H. (2006) *Proc Natl Acad Sci U S A* **103**, 7036-7041

19. Sabe, H., Hashimoto, S., Morishige, M., Ogawa, E., Hashimoto, A., Nam, J. M., Miura, K., Yano, H., and Onodera, Y. (2009) *Traffic* **10**, 982-993

20. Kahn, R. A., Bruford, E., Inoue, H., Logsdon, J. M., Nie, Z., Premont, R. T., Randazzo, P. A., Satake, M., Theibert, A. B., Zapp, M. L., and Cassel, D. (2008) *J Cell Biol* **182**, 1039-1044

21. Goldberg, J. (1999) *Cell* **96**, 893-902

22. Makler, V., Cukierman, E., Rotman, M., Admon, A., and Cassel, D. (1995) *J Biol Chem* **270**, 5232-5237

23. Flanagan-Steet, H., Johnson, S., Smith, R. D., Bangiyeva, J., Lupashin, V., and Steet, R. (2011) *Exp Cell Res* **317**, 2342-2352

24. Sata, M., Donaldson, J. G., Moss, J., and Vaughan, M. (1998) *Proc Natl Acad Sci U S A* **95**, 4204-4208

25. Tsai, S. C., Adamik, R., Haun, R. S., Moss, J., and Vaughan, M. (1993) *J Biol Chem* **268**, 10820-10825

26. Zhao, X., Lasell, T. K., and Melançon, P. (2002) *Mol Biol Cell* **13**, 119-133

27. Muller, T., Stein, U., Poletti, A., Garzia, L., Rothley, M., Plaumann, D., Thiele, W., Bauer, M., Galasso, A., Schlag, P., Pankratz, M., Zollo, M., and Sleeman, J. P. (2010) *Oncogene* **29**, 2393-2403

28. Krugmann, S., Williams, R., Stephens, L., and Hawkins, P. T. (2004) *Curr Biol* **14**, 1380-1384

29. Lee, S. Y., Yang, J. S., Hong, W., Premont, R. T., and Hsu, V. W. (2005) *J Cell Biol* **168**, 281-290

30. Randazzo, P. A., Inoue, H., and Bharti, S. (2007) *Biol Cell* **99**, 583-600

31. Spang, A., Shiba, Y., and Randazzo, P. A. (2010) *FEBS Lett* **584**, 2646-2651

32. Wong, T. A., Fairn, G. D., Poon, P. P., Shmulevitz, M., McMaster, C. R., Singer, R. A., and Johnston, G. C. (2005) *Proc Natl Acad Sci U S A* **102**, 12777-12782

33. Inoue, H., and Randazzo, P. A. (2007) *Traffic* **8**, 1465-1475

34. Nie, Z., Fei, J., Premont, R. T., and Randazzo, P. A. (2005) *J Cell Sci* **118**, 3555-3566

35. Aoe, T., Cukierman, E., Lee, A., Cassel, D., Peters, P. J., and Hsu, V. W. (1997) *EMBO J* **16**, 7305-7316

36. Lanoix, J., Ouwendijk, J., Stark, A., Szafer, E., Cassel, D., Dejgaard, K., Weiss, M., and Nilsson, T. (2001) *J Cell Biol* **155**, 1199-1212

37. Watson, P. J., Frigerio, G., Collins, B. M., Duden, R., and Owen, D. J. (2004) *Traffic* **5**, 79-88

38. Hirst, J., Motley, A., Harasaki, K., Peak Chew, S. Y., and Robinson, M. S. (2003) *Mol Biol Cell* **14**, 625-641

39. Szafer, E., Rotman, M., and Cassel, D. (2001) *J Biol Chem* **276**, 47834-47839

40. Dai, J., Li, J., Bos, E., Porcionatto, M., Premont, R. T., Bourgoin, S., Peters, P. J., and Hsu, V. W. (2004) *Dev Cell* **7**, 771-776

41. Li, J., Ballif, B. A., Powelka, A. M., Dai, J., Gygi, S. P., and Hsu, V. W. (2005) *Dev Cell* **9**, 663-673

42. Natsume, W., Tanabe, K., Kon, S., Yoshida, N., Watanabe, T., Torii, T., and Satake, M. (2006) *Mol Biol Cell* **17**, 2592-2603

43. Tanabe, K., Torii, T., Natsume, W., Braesch-Andersen, S., Watanabe, T., and Satake, M. (2005) *Mol Biol Cell* **16**, 1617-1628

44. Kowanetz, K., Husnjak, K., Höller, D., Kowanetz, M., Soubeyran, P., Hirsch, D., Schmidt, M. H., Pavelic, K., De Camilli, P., Randazzo, P. A., and Dikic, I. (2004) *Mol Biol Cell* **15**, 3155-3166

45. Oshiro, T., Koyama, S., Sugiyama, S., Kondo, A., Onodera, Y., Asahara, T., Sabe, H., and Kikuchi, A. (2002) *J Biol Chem* **277**, 38618-38626

46. Ikeda, M., Ishida, O., Hinoi, T., Kishida, S., and Kikuchi, A. (1998) *J Biol Chem* **273**, 814-821

47. Hashimoto, S., Hashimoto, A., Yamada, A., Kojima, C., Yamamoto, H., Tsutsumi, T., Higashi, M., Mizoguchi, A., Yagi, R., and Sabe, H. (2004) *J Biol Chem* **279**, 37677-37684

48. Bickford, L. C., Mossessova, E., and Goldberg, J. (2004) *Curr Opin Struct Biol* **14**, 147-153

49. Haendeler, J., Yin, G., Hojo, Y., Saito, Y., Melaragno, M., Yan, C., Sharma, V. K., Heller, M., Aebersold, R., and Berk, B. C. (2003) *J Biol Chem* **278**, 49936-49944

50. Ye, K., Aghdasi, B., Luo, H. R., Moriarity, J. L., Wu, F. Y., Hong, J. J., Hurt, K. J., Bae, S. S., Suh, P. G., and Snyder, S. H. (2002) *Nature* **415**, 541-544

51. Ye, K., Hurt, K. J., Wu, F. Y., Fang, M., Luo, H. R., Hong, J. J., Blackshaw, S., Ferris, C. D., and Snyder, S. H. (2000) *Cell* **103**, 919-930

52. Rong, R., Ahn, J. Y., Huang, H., Nagata, E., Kalman, D., Kapp, J. A., Tu, J., Worley, P. F., Snyder, S. H., and Ye, K. (2003) *Nat Neurosci* **6**, 1153-1161

53. Zhao, Z. S., Manser, E., Loo, T. H., and Lim, L. (2000) *Mol Cell Biol* **20**, 6354-6363

54. Premont, R. T., Claing, A., Vitale, N., Freeman, J. L., Pitcher, J. A., Patton, W. A., Moss, J., Vaughan, M., and Lefkowitz, R. J. (1998) *Proc Natl Acad Sci U S A* **95**, 14082-14087

55. Premont, R. T., Claing, A., Vitale, N., Perry, S. J., and Lefkowitz, R. J. (2000) *J Biol Chem* **275**, 22373-22380

56. Tang, X., Feng, Y., and Ye, K. (2007) *Cell Death Differ* **14**, 368-377

57. Ahn, J. Y., Rong, R., Kroll, T. G., Van Meir, E. G., Snyder, S. H., and Ye, K. (2004) *J Biol Chem* **279**, 16441-16451

58. Hu, Y., Liu, Z., and Ye, K. (2005) *Proc Natl Acad Sci U S A* **102**, 16853-16858

59. Yang, J. S., Lee, S. Y., Gao, M., Bourgoin, S., Randazzo, P. A., Premont, R. T., and Hsu, V. W. (2002) *J Cell Biol* **159**, 69-78

60. Liu, Y., Loijens, J. C., Martin, K. H., Karginov, A. V., and Parsons, J. T. (2002) *Mol Biol Cell* **13**, 2147-2156

61. Hashimoto, S., Hashimoto, A., Yamada, A., Onodera, Y., and Sabe, H. (2005) *Methods Enzymol* **404**, 216-231

62. Onodera, Y., Hashimoto, S., Hashimoto, A., Morishige, M., Mazaki, Y., Yamada, A., Ogawa, E., Adachi, M., Sakurai, T., Manabe, T., Wada, H., Matsuura, N., and Sabe, H. (2005) *EMBO J* **24**, 963-973

63. Yamamoto-Furusho, J. K., Barnich, N., Xavier, R., Hisamatsu, T., and Podolsky, D. K. (2006) *J Biol Chem* **281**, 36060-36070

64. Béthune, J., Kol, M., Hoffmann, J., Reckmann, I., Brügger, B., and Wieland, F. (2006) *Mol Cell Biol* **26**, 8011-8021

65. Liu, W., Duden, R., Phair, R. D., and Lippincott-Schwartz, J. (2005) *J Cell Biol* **168**, 1053-1063

66. Presley, J. F., Ward, T. H., Pfeifer, A. C., Siggia, E. D., Phair, R. D., and Lippincott-Schwartz, J. (2002) *Nature* **417**, 187-193

67. Antonny, B., Bigay, J., Casella, J. F., Drin, G., Mesmin, B., and Gounon, P. (2005) *Biochem Soc Trans* **33**, 619-622

68. Luo, R., and Randazzo, P. A. (2008) *J Biol Chem* **283**, 21965-21977

69. Bradley, R. R., and Terajima, M. (2005) *Virus Res* **114**, 104-112

70. Meurer, S., Pioch, S., Wagner, K., Müller-Esterl, W., and Gross, S. (2004) *J Biol Chem* **279**, 49346-49354

71. Kartberg, F., Asp, L., Dejgaard, S. Y., Smedh, M., Fernandez-Rodriguez, J., Nilsson, T., and Presley, J. F. (2010) *J Biol Chem* **285**, 36709-36720

72. Nie, Z., Hirsch, D. S., Luo, R., Jian, X., Stauffer, S., Cremesti, A., Andrade, J., Lebowitz, J., Marino, M., Ahvazi, B., Hinshaw, J. E., and Randazzo, P. A. (2006) *Curr Biol* **16**, 130-139

73. Spang, A. (2002) *Curr Opin Cell Biol* **14**, 423-427

74. Weiss, M., and Nilsson, T. (2003) *Traffic* **4**, 65-73

75. Bigay, J., Casella, J. F., Drin, G., Mesmin, B., and Antonny, B. (2005) *EMBO J* **24**, 2244-2253

76. Drin, G., Casella, J. F., Gautier, R., Boehmer, T., Schwartz, T. U., and Antonny, B. (2007) *Nat Struct Mol Biol* **14**, 138-146

77. Mesmin, B., Drin, G., Levi, S., Rawet, M., Cassel, D., Bigay, J., and Antonny, B. (2007) *Biochemistry* **46**, 1779-1790

78. Yang, J. S., Lee, S. Y., Spanò, S., Gad, H., Zhang, L., Nie, Z., Bonazzi, M., Corda, D., Luini, A., and Hsu, V. W. (2005) *EMBO J* **24**, 4133-4143

79. Bigay, J., Gounon, P., Robineau, S., and Antonny, B. (2003) *Nature* **426**, 563-566

80. Manneville, J. B., Casella, J. F., Ambroggio, E., Gounon, P., Bertherat, J., Bassereau, P., Cartaud, J., Antonny, B., and Goud, B. (2008) *Proc Natl Acad Sci U S A* **105**, 16946-16951

81. Jian, X., Brown, P., Schuck, P., Gruschus, J. M., Balbo, A., Hinshaw, J. E., and Randazzo, P. A. (2009) *J Biol Chem* **284**, 1652-1663

82. Venkateswarlu, K., Brandom, K. G., and Lawrence, J. L. (2004) *J Biol Chem* **279**, 6205-6208

83. Zhang, C. J., Bowzard, J. B., Anido, A., and Kahn, R. A. (2003) *Yeast* **20**, 315-330

84. Zhang, C. J., Cavenagh, M. M., and Kahn, R. A. (1998) *J Biol Chem* **273**, 19792-19796

85. Rein, U., Andag, U., Duden, R., Schmitt, H. D., and Spang, A. (2002) *J Cell Biol* **157**, 395-404

86. Schindler, C., Rodriguez, F., Poon, P. P., Singer, R. A., Johnston, G. C., and Spang, A. (2009) *Traffic* **10**, 1362-1375

87. Schindler, C., and Spang, A. (2007) *Mol Biol Cell* **18**, 2852-2863

88. Blondeau, F., Ritter, B., Allaire, P. D., Wasiak, S., Girard, M., Hussain, N. K., Angers, A., Legendre-Guillemin, V., Roy, L., Boismenu, D., Kearney, R. E., Bell, A. W., Bergeron, J. J., and McPherson, P. S. (2004) *Proc Natl Acad Sci U S A* **101**, 3833-3838

89. Borner, G. H., Harbour, M., Hester, S., Lilley, K. S., and Robinson, M. S. (2006) *J Cell Biol* **175**, 571-578

90. Gilchrist, A., Au, C. E., Hiding, J., Bell, A. W., Fernandez-Rodriguez, J., Lesimple, S., Nagaya, H., Roy, L., Gosline, S. J., Hallett, M., Paiement, J., Kearney, R. E., Nilsson, T., and Bergeron, J. J. (2006) *Cell* **127**, 1265-1281

91. Girard, M., Allaire, P. D., McPherson, P. S., and Blondeau, F. (2005) *Mol Cell Proteomics* **4**, 1145-1154

92. Randazzo, P. A., and Hirsch, D. S. (2004) *Cell Signal* **16**, 401-413

93. Kam, J. L., Miura, K., Jackson, T. R., Gruschus, J., Roller, P., Stauffer, S., Clark, J., Aneja, R., and Randazzo, P. A. (2000) *J Biol Chem* **275**, 9653-9663

94. Terui, T., Kahn, R. A., and Randazzo, P. A. (1994) *J Biol Chem* **269**, 28130-28135

95. Salazar, G., Craige, B., Wainer, B. H., Guo, J., De Camilli, P., and Faundez, V. (2005) *Mol Biol Cell* **16**, 3692-3704

96. Kruljac-Letunic, A., Moelleken, J., Kallin, A., Wieland, F., and Blaukat, A. (2003) *J Biol Chem* **278**, 29560-29570

97. Ehlers, J. P., Worley, L., Onken, M. D., and Harbour, J. W. (2005) *Clin Cancer Res* **11**, 3609-3613

98. Buffart, T. E., Coffa, J., Hermsen, M. A., Carvalho, B., van der Sijp, J. R., Ylstra, B., Pals, G., Schouten, J. P., and Meijer, G. A. (2005) *Cell Oncol* **27**, 57-65

99. Lin, D., Watahiki, A., Bayani, J., Zhang, F., Liu, L., Ling, V., Sadar, M. D., English, J., Fazli, L., So, A., Gout, P. W., Gleave, M., Squire, J. A., and Wang, Y. Z. (2008) *Cancer Res* **68**, 4352-4359

100. Müller, T., Stein, U., Poletti, A., Garzia, L., Rothley, M., Plaumann, D., Thiele, W., Bauer, M., Galasso, A., Schlag, P., Pankratz, M., Zollo, M., and Sleeman, J. P. (2010) *Oncogene* **29**, 2393-2403

101. Giorgini, F., and Muchowski, P. J. (2005) *Genome Biol* **6**, 210

102. Goehler, H., Lalowski, M., Stelzl, U., Waelter, S., Stroedicke, M., Worm, U., Droege, A., Lindenberg, K. S., Knoblich, M., Haenig, C., Herbst, M., Suopanki, J., Scherzinger, E., Abraham, C., Bauer, B., Hasenbank, R., Fritzsche, A., Ludewig, A. H., Büssow, K., Buessow, K., Coleman, S. H., Gutekunst, C. A., Landwehrmeyer, B. G., Lehrach, H., and Wanker, E. E. (2004) *Mol Cell* **15**, 853-865

103. Audebert, S., Navarro, C., Nourry, C., Chasserot-Golaz, S., Lécine, P., Bellaiche, Y., Dupont, J. L., Premont, R. T., Sempéré, C., Strub, J. M., Van Dorsselaer, A., Vitale, N., and Borg, J. P. (2004) *Curr Biol* **14**, 987-995

104. Kim, S., Lee, S. H., and Park, D. (2001) *J Biol Chem* **276**, 10581-10584

105. Blagoveshchenskaya, A. D., Thomas, L., Feliciangeli, S. F., Hung, C. H., and Thomas, G. (2002) *Cell* **111**, 853-866

106. Borrmann, C., Stricker, R., and Reiser, G. (2011) *Neurochem Int* **59**, 936-944

107. Reiser, G., and Bernstein, H. G. (2002) *Neuroreport* **13**, 2417-2419

108. Reiser, G., and Bernstein, H. G. (2004) *Neuroreport* **15**, 147-148

109. Taherkhani, H., Hajilooi, M., Fallah, M., Khyabanchi, O., and Haidari, M. (2009) *Int J Immunogenet* **36**, 345-349

110. von Rahden, B. H., Brücher, B. L., Langner, C., Siewert, J. R., Stein, H. J., and Sarbia, M. (2006) *Br J Surg* **93**, 1424-1432

111. Wassink, T. H., Piven, J., Vieland, V. J., Jenkins, L., Frantz, R., Bartlett, C. W., Goedken, R., Childress, D., Spence, M. A., Smith, M., and Sheffield, V. C. (2005) *Am J Med Genet B Neuropsychiatr Genet* **136B**, 36-44

112. Rittinger, K., Walker, P. A., Eccleston, J. F., Smerdon, S. J., and Gamblin, S. J. (1997) *Nature* **389**, 758-762

113. Scheffzek, K., Ahmadian, M. R., Kabsch, W., Wiesmüller, L., Lautwein, A., Schmitz, F., and Wittinghofer, A. (1997) *Science* **277**, 333-338

114. Scheffzek, K., Ahmadian, M. R., Wiesmüller, L., Kabsch, W., Stege, P., Schmitz, F., and Wittinghofer, A. (1998) *EMBO J* **17**, 4313-4327

115. Scheffzek, K., Ahmadian, M. R., and Wittinghofer, A. (1998) *Trends Biochem Sci* **23**, 257-262

116. Mandiyan, V., Andreev, J., Schlessinger, J., and Hubbard, S. R. (1999) *EMBO J* **18**, 6890-6898

117. Ismail, S. A., Vetter, I. R., Sot, B., and Wittinghofer, A. (2010) *Cell* **141**, 812-821

118. Goldberg, J. (1999) *Cell* **96**, 893-902

119. Antonny, B., Huber, I., Paris, S., Chabre, M., and Cassel, D. (1997) *J Biol Chem* **272**, 30848-30851

120. Ambroggio, E., Sorre, B., Bassereau, P., Goud, B., Manneville, J. B., and Antonny, B. (2010) *EMBO J* **29**, 292-303

121. Nie, Z., and Randazzo, P. A. (2006) *J Cell Sci* **119**, 1203-1211

122. Goldberg, J. (2000) *Cell* **100**, 671-679

123. Zhang, Q., Major, M. B., Takanashi, S., Camp, N. D., Nishiya, N., Peters, E. C., Ginsberg, M. H., Jian, X., Randazzo, P. A., Schultz, P. G., Moon, R. T., and Ding, S. (2007) *Proc Natl Acad Sci U S A* **104**, 7444-7448

124. Rawet, M., Levi-Tal, S., Szafer-Glusman, E., Parnis, A., and Cassel, D. (2010) *Biochem Biophys Res Commun* **394**, 553-557

125. Premont, R. T., and Vitale, N. (2001) *Methods Enzymol* **329**, 335-343

126. Shiba, Y., Luo, R., Hinshaw, J. E., Szul, T., Hayashi, R., Sztul, E., Nagashima, K., Baxa, U., and Randazzo, P. A. (2011) *Cell Logist* **1**, 139-154

127. Szafer, E., Pick, E., Rotman, M., Zuck, S., Huber, I., and Cassel, D. (2000) *J Biol Chem* **275**, 23615-23619

128. Balch, W. E., Kahn, R. A., and Schwaninger, R. (1992) *J Biol Chem* **267**, 13053-13061

129. Levi, S., Rawet, M., Kliouchnikov, L., Parnis, A., and Cassel, D. (2008) *J Biol Chem* **283**, 8564-8572

130. Parnis, A., Rawet, M., Regev, L., Barkan, B., Rotman, M., Gaitner, M., and Cassel, D. (2006) *J Biol Chem* **281**, 3785-3792

131. Bjelić, S., and Jelesarov, I. (2008) *J Mol Recognit* **21**, 289-312

132. Fedorov, O., Marsden, B., Pogacic, V., Rellos, P., Müller, S., Bullock, A. N., Schwaller, J., Sundström, M., and Knapp, S. (2007) *Proc Natl Acad Sci U S A* **104**, 20523-20528

133. Lea, W. A., and Simeonov, A. (2012) *PLoS One* **7**, e36219

134. Bharate, G. Y., Fang, J., Nakamura, H., Qin, H., Shinkai, S., and Maeda, H. (2011) *J Drug Target* **19**, 954-966

135. Fang, J., Qin, H., Seki, T., Nakamura, H., Tsukigawa, K., Shin, T., and Maeda, H. (2011) *J Pharmacol Exp Ther* **339**, 779-789

136. Li, H., Fronczek, F. R., and Vicente, M. G. (2011) *Tetrahedron Lett* **52**, 6675-6678

137. Shin, H. C., Cho, H., Lai, T. C., Kozak, K. R., Kolesar, J. M., and Kwon, G. S. (2012) *J Control Release*

138. Vitale, N., Patton, W. A., Moss, J., Vaughan, M., Lefkowitz, R. J., and Premont, R. T. (2000) *J Biol Chem* **275**, 13901-13906

139. Ha, V. L., Thomas, G. M., Stauffer, S., and Randazzo, P. A. (2005) *Methods Enzymol* **404**, 164-174

140. Randazzo, P. A., and Fales, H. M. (2002) *Methods Mol Biol* **189**, 169-179

141. Lappano, R., and Maggiolini, M. (2011) *Nat Rev Drug Discov* **10**, 47-60

142. Neubig, R. R., and Siderovski, D. P. (2002) *Nat Rev Drug Discov* **1**, 187-197

143. Bender, A., Bojanic, D., Davies, J. W., Crisman, T. J., Mikhailov, D., Scheiber, J., Jenkins, J. L., Deng, Z., Hill, W. A., Popov, M., Jacoby, E., and Glick, M. (2008) *Curr Opin Drug Discov Devel* **11**, 327-337

144. Macarron, R., Banks, M. N., Bojanic, D., Burns, D. J., Cirovic, D. A., Garyantes, T., Green, D. V., Hertzberg, R. P., Janzen, W. P., Paslay, J. W., Schopfer, U., and Sittampalam, G. S. (2011) *Nat Rev Drug Discov* **10**, 188-195

145. van Ommen, G. J. (2002) *J Inherit Metab Dis* **25**, 183-188

146. Duffy, K. J., Shaw, A. N., Delorme, E., Dillon, S. B., Erickson-Miller, C., Giampa, L., Huang, Y., Keenan, R. M., Lamb, P., Liu, N., Miller, S. G., Price, A. T., Rosen, J., Smith, H., Wiggall, K. J., Zhang, L., and Luengo, J. I. (2002) *J Med Chem* **45**, 3573-3575

147. Duffy, K. J., Price, A. T., Delorme, E., Dillon, S. B., Duquenne, C., Erickson-Miller, C., Giampa, L., Huang, Y., Keenan, R. M., Lamb, P., Liu, N., Miller, S. G.,

Rosen, J., Shaw, A. N., Smith, H., Wiggall, K. J., Zhang, L., and Luengo, J. I. (2002) *J Med Chem* **45**, 3576-3578

148. Gao, M., Nettles, R. E., Belema, M., Snyder, L. B., Nguyen, V. N., Fridell, R. A., Serrano-Wu, M. H., Langley, D. R., Sun, J. H., O'Boyle, D. R., Lemm, J. A., Wang, C., Knipe, J. O., Chien, C., Colonno, R. J., Grasela, D. M., Meanwell, N. A., and Hamann, L. G. (2010) *Nature* **465**, 96-100

149. Frye, S. V. (2010) *Nat Chem Biol* **6**, 159-161

150. Kaiser, J. (2008) *Science* **321**, 764-766

151. Silber, B. M. (2010) *Sci Transl Med* **2**, 30cm16

152. Makler, V., Cukierman, E., Rotman, M., Admon, A., and Cassel, D. (1995) *J Biol Chem* **270**, 5232-5237

153. Luo, R., Ahvazi, B., Amariei, D., Shroder, D., Burrola, B., Losert, W., and Randazzo, P. A. (2007) *Biochem J* **402**, 439-447

154. McEwen, D. P., Gee, K. R., Kang, H. C., and Neubig, R. R. (2001) *Anal Biochem* **291**, 109-117

155. Hiratsuka, T. (1983) *Biochim Biophys Acta* **742**, 496-508

156. Jameson, E. E., Roof, R. A., Whorton, M. R., Mosberg, H. I., Sunahara, R. K., Neubig, R. R., and Kennedy, R. T. (2005) *J Biol Chem* **280**, 7712-7719

157. Willard, F. S., Kimple, A. J., Johnston, C. A., and Siderovski, D. P. (2005) *Anal Biochem* **340**, 341-351

158. Korlach, J., Baird, D. W., Heikal, A. A., Gee, K. R., Hoffman, G. R., and Webb, W. W. (2004) *Proc Natl Acad Sci U S A* **101**, 2800-2805

159. Murakoshi, H., Iino, R., Kobayashi, T., Fujiwara, T., Ohshima, C., Yoshimura, A., and Kusumi, A. (2004) *Proc Natl Acad Sci U S A* **101**, 7317-7322

160. Huss, K. L., Blonigen, P. E., and Campbell, R. M. (2007) *J Biomol Screen* **12**, 578-584

161. Gillingham, A. K., and Munro, S. (2007) *Annu Rev Cell Dev Biol* **23**, 579-611

162. Zhang, J. H., Chung, T. D., and Oldenburg, K. R. (1999) *J Biomol Screen* **4**, 67-73

163. Luo, R., Jacques, K., Ahvazi, B., Stauffer, S., Premont, R. T., and Randazzo, P. A. (2005) *Curr Biol* **15**, 2164-2169

164. Tanabe, K., Kon, S., Ichijo, N., Funaki, T., Natsume, W., Watanabe, T., and Satake, M. (2008) *Methods Enzymol* **438**, 155-170

165. Resh, M. D. (1999) *Biochim Biophys Acta* **1451**, 1-16

166. Farazi, T. A., Waksman, G., and Gordon, J. I. (2001) *J Biol Chem* **276**, 39501-39504

167. Ames, J. B., Tanaka, T., Stryer, L., and Ikura, M. (1996) *Curr Opin Struct Biol* **6**, 432-438

168. Hantschel, O., Nagar, B., Guettler, S., Kretzschmar, J., Dorey, K., Kuriyan, J., and Superti-Furga, G. (2003) *Cell* **112**, 845-857

169. Goldberg, J. (1998) *Cell* **95**, 237-248

170. Matsubara, M., Nakatsu, T., Kato, H., and Taniguchi, H. (2004) *EMBO J* **23**, 712-718

171. McLaughlin, S., and Aderem, A. (1995) *Trends Biochem Sci* **20**, 272-276

172. van der Vusse, G. J., van Bilsen, M., Glatz, J. F., Hasselbaink, D. M., and Luiken, J. J. (2002) *Mol Cell Biochem* **239**, 9-15

173. Colombo, S., Longhi, R., Alcaro, S., Ortuso, F., Sprocati, T., Flora, A., and Borgese, N. (2005) *J Cell Biol* **168**, 735-745

174. King, M. J., and Sharma, R. K. (1993) *Biochem J* **291 (Pt 2)**, 635-639

175. Shrivastav, A., Pasha, M. K., Selvakumar, P., Gowda, S., Olson, D. J., Ross, A. R., Dimmock, J. R., and Sharma, R. K. (2003) *Cancer Res* **63**, 7975-7978

176. Rajala, R. V., Datla, R. S., Carlsen, S. A., Anderson, D. H., Qi, Z., Wang, J. H., and Sharma, R. K. (2001) *Biochem Biophys Res Commun* **288**, 233-239

177. Cross, F. R., Garber, E. A., Pellman, D., and Hanafusa, H. (1984) *Mol Cell Biol* **4**, 1834-1842

178. Rajala, R. V., Radhi, J. M., Kakkar, R., Datla, R. S., and Sharma, R. K. (2000) *Cancer* **88**, 1992-1999

179. Shrivastav, A., Varma, S., Senger, A., Khandelwal, R. L., Carlsen, S., and Sharma, R. K. (2009) *J Pathol* **218**, 391-398

180. Lu, Y., Selvakumar, P., Ali, K., Shrivastav, A., Bajaj, G., Resch, L., Griebel, R., Fourney, D., Meguro, K., and Sharma, R. K. (2005) *Neurochem Res* **30**, 9-13

181. Selvakumar, P., Lakshmikuttyamma, A., Shrivastav, A., Das, S. B., Dimmock, J. R., and Sharma, R. K. (2007) *Prog Lipid Res* **46**, 1-36

182. Cordeddu, V., Di Schiavi, E., Pennacchio, L. A., Ma'ayan, A., Sarkozy, A., Fodale, V., Cecchetti, S., Cardinale, A., Martin, J., Schackwitz, W., Lipzen, A., Zampino, G., Mazzanti, L., Digilio, M. C., Martinelli, S., Flex, E., Lepri, F., Bartholdi, D., Kutsche, K., Ferrero, G. B., Anichini, C., Selicorni, A., Rossi, C., Tenconi, R., Zenker, M., Merlo, D., Dallapiccola, B., Iyengar, R., Bazzicalupo, P., Gelb, B. D., and Tartaglia, M. (2009) *Nat Genet* **41**, 1022-1026

183. Hill, B. T., and Skowronski, J. (2005) *J Virol* **79**, 1133-1141

184. Nimchuk, Z., Marois, E., Kjemtrup, S., Leister, R. T., Katagiri, F., and Dangl, J. L. (2000) *Cell* **101**, 353-363

185. Ménard, R., Sansonetti, P., and Parsot, C. (1994) *EMBO J* **13**, 5293-5302

186. Martin, D. D., Vilas, G. L., Prescher, J. A., Rajaiah, G., Falck, J. R., Bertozzi, C. R., and Berthiaume, L. G. (2008) *FASEB J* **22**, 797-806

187. Deichaite, I., Berthiaume, L., Peseckis, S. M., Patton, W. F., and Resh, M. D. (1993) *J Biol Chem* **268**, 13738-13747

188. Kostiuk, M. A., Keller, B. O., and Berthiaume, L. G. (2010) *FASEB J* **24**, 1914-1924

189. Martin, B. R., and Cravatt, B. F. (2009) *Nat Methods* **6**, 135-138

190. Hang, H. C., Geutjes, E. J., Grotenbreg, G., Pollington, A. M., Bijlmakers, M. J., and Ploegh, H. L. (2007) *J Am Chem Soc* **129**, 2744-2745

191. Randazzo, P. A., Miura, K., and Jackson, T. R. (2001) *Methods Enzymol* **329**, 343-354